Electronic Supporting Information:

An anion-binding fluorinated alcohol isophthalamide isostere

*Nathalie Busschaert, Javier Jaramillo-Garcia, Mark E. Light, Julie Herniman, G. John Langley and Philip A. Gale**

Chemistry, University of Southampton, Southampton, SO17 1BJ, UK, e-mail: philip.gale@soton.ac.uk

S1. OVERVIEW OF COMPOUNDS

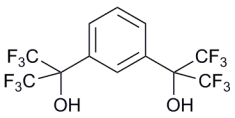

1

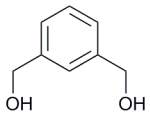

2

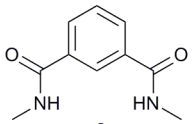

3

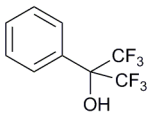

4

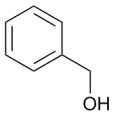

5

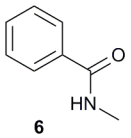

6

S2. SYNTHESIS

^{1}H NMR (300 MHz), ^{19}F{^{1}H} NMR (282 MHz) and ^{13}C{^{1}H} NMR (75 MHz) spectra were determined on a Bruker AV300 spectrometer, whilst ^{1}H NMR (400 MHz) and ^{13}C{^{1}H} NMR (100 MHz) spectra were determined on a Bruker DPX400 spectrometer. Chemical shifts (δ) are reported in parts per million (ppm) and calibrated to the appropriate residual protio solvent peak, *i.e.* δ = 2.50 (^{1}H) and 39.52 ppm (^{13}C) for DMSO-d_6, δ = 7.26 (^{1}H) and 77.16 ppm (^{13}C) for $CDCl_3$ and δ = 1.94 (^{1}H) and 1.32 ppm (^{13}C) for CD_3CN. The following abbreviations are used for spin multiplicity: s = singlet, d = doublet, dd = doublet of doublets, t = tri-plet, q = quartet, m = multiplet, br = broad. Infrared (IR) spectra were recorded on a Matterson Satellite (ATR) and are reported in wavenumbers (cm^{-1}). Low resolution mass spectra (LRMS) were recorded on a Walters ZMD single quadrupole spectrometer. High resolution mass spectra (HRMS) were recorded on a Bruker Apex III or Bruker maXis ESI spectrometer. All mass spectra are reported as *m/z* (relative intensity). Melting points were determined using open capillary tubes on a Barnstead Electrothermal 9100 or Gallenkamp melting point apparatus and were not corrected. Receptors **1** and **4** were purchased from *Apollo Scientific Ltd*, receptors **2** and **5** were purchased from *Alfa Aesar* and receptors **3** and **6** were prepared according to modified literature procedures.[1,2]

***N*^{1},*N*^{3}-dimethylisophthalamide (3).** A solution of methylamine (4.53 mL of a 2 M solution in tetra-hydrofuran, 9.06 mmol) was added dropwise to isophthaloyldichloride (0.8 g, 3.94 mmol) in CH_2Cl_2 (40 mL), and the reaction was stirred for 10-15 minutes at room temperature. The volume was reduced

to 10 mL on a rotary evaporator, and the resultant precipitate was filtered off and washed repeatedly with CH_2Cl_2 and petroleum ether. The crude product was then redissolved in *n*-butanol and extracted with a saturated aqueous $NaHCO_3$ solution to afford compound **3** as a white solid after drying under high vacuum (0.32 g, 1.66 mmol). Yield: 42%; Mp: 188-190°C (lit. 169-171 °C); ^{1}H NMR (300 MHz, DMSO-d_6) δ ppm 2.80 (d, *J*=4.4 Hz, 6 H), 7.54 (t, *J*=7.8 Hz, 1 H), 7.94 (dd, *J*=7.7, 1.46 Hz, 2 H), 8.29 (s, 1 H), 8.53 (br. s, 2 H); ^{13}C{^{1}H} NMR (75 MHz, DMSO-d_6) δ ppm 26.3, 126.0, 128.3, 129.4, 134.7, 166.2; IR (solid): ν= 3340, 1640, 1540 cm^{-1}; LRMS (ESI-): *m/z*= 191.1 [M-H]$^-$; HRMS (ES) for $C_{10}H_{12}O_2N_2Na$ [M+Na]$^+$: *m/z*= 215.0791 (calcd), 215.0795 (found). Characterisation in good agreement with literature values.[1]

***N*-methylbenzamide (6).** Benzoylchloride (0.70 mL, 6.0 mmol) was treated with aqueous methylamine (large excess) in the presence of triethylamine (2.10 mL, 15 mmol) in diethyl ether (14 mL) and the resulting mixture was stirred overnight at room temperature. The organic phase was separated and the aqueous phase was further extracted with diethyl ether. The combined organic layers were concentrated to obtain compound **6** as a white solid which was further purified by recrystallisation from diethyl ether and dried under high vacuum (0.26 g, 1.92 mmol). Yield: 32%; Mp: 72-74°C (lit. 79.5-80.5 °C); ^{1}H NMR (300 MHz, DMSO-d_6) δ ppm 3.02 (d, *J*=4.8 Hz, 3 H), 6.21 (br. s., 1 H), 7.46 (m, 3 H), 7.77 (d, *J*=6.9 Hz, 2 H); ^{13}C{^{1}H} NMR (75 MHz, $CDCl_3$) δ ppm 26.8, 126.8, 128.5, 131.3, 134.6, 168.2; IR (solid): ν= 3330, 1640, 1550 cm^{-1}; LRMS (ESI-): *m/z*= 134.1 [M-H]$^-$; HRMS (ES) for C_8H_9NONa [M+Na]$^+$: *m/z*= 158.0576 (calcd), 158.0574 (found). Characterisation in good agreement with literature values.[2]

S3. NMR BINDING STUDIES

S3.1. Experimental procedure of binding studies

NMR titrations were performed by addition of aliquots of the putative anionic guest as the tetrabutylammonium (TBA) or tetraethylammonium (TEA) salt (0.15 M), in a solution of the receptor (0.01 M) in CD_3CN, to a 0.01 M solution of the receptor in CD_3CN. Both salt and receptor were dried under high vacuum prior to use. ^{1}H NMR spectra were recorded on a Bruker AV300 spectrometer and calibrated to the residual protio solvent peak in CD_3CN (δ = 1.94 ppm). In most cases a change in the

chemical shift of the OH or the NH protons was observed, as well as a shift in the *ortho*-CH proton of the aromatic ring. Where possible, the WinEQNMR2 computer program[3] was used to curve-fit the data and to obtain binding constants (using a 1:1 model). Stack plots and fit plots can be found in figures S1-S54, whereas an overview of the obtained binding constants can be found in Table 1 and Table 2.

Table S1. Association constants (logK_a) for the binding of compounds **1-6** to various anions (as TBA salts) in CD_3CN at 298 K following the OH or NH signal. All results were fitted to a 1:1 model.

Anion	**1**	**2**	**3**	**4**	**5**	**6**
F^-[a]	-[b]	n.d.[d]	n.d.[d]	-[c]	n.d.[d]	n.d.[d]
Cl^-	2.48	n.d.[d]	2.74	1.92	1.38	1.56
Br^-	1.66	1.04	1.98	1.16	<1	1.16
NO_3^-	1.28	<1	1.21	<1	<1	<1
$H_2PO_4^-$	n.d.[d]	n.d.[d]	2.50	n.d.[d]	n.d.[d]	1.27
HCO_3^-[e]	-[c]	n.d.[d]	2.52	-[c]	n.d.[d]	1.30
OAc^-	n.d.[d]	n.d.[d]	2.92	n.d.[d]	n.d.[d]	1.29
OBz^-	>4	n.d.[d]	2.87	n.d.[e]	n.d.[d]	1.38
SO_4^{2-}	>4	n.d.[d]	-[f]	n.d.[d]	n.d.[d]	1.96

[a] Added as the trihydrate (TBAF·$3H_2O$); [b] Most likely deprotonation of both hydroxyl groups occurs upon addition of anion; [c] Data suggests that deprotonation of the receptor occurs upon addition of anion (most likely *mono* deprotonation); [d] Unable to determine association constant due to peak broadening, peak overlap and/or small changes in chemical shift; [e] Added as TEA salt; [f] Data could not be fitted to a 1:1 or 2:1 model, but suggests strong interaction.

Table S2. Association constants (logK_a) for the binding of compounds **1-6** to various anions (as TBA salts) in CD_3CN at 298 K following the *ortho* CH signal. All results were fitted to a 1:1 model.

Anion	**1**	**2**	**3**	**4**	**5**	**6**
F^-[a]	-[b]	3.35	>4	-[c]	n.d.[d]	2.23
Cl^-	3.35	n.d.[d]	2.79	2.03	n.d.[d]	1.51
Br^-	1.87	n.d.[d]	1.98	n.d.[d]	n.d.[d]	1.12
NO_3^-	1.76	n.d.[d]	1.20	n.d.[d]	n.d.[d]	n.d.[d]
$H_2PO_4^-$	2.82	1.82	2.60	2.38	n.d.[d]	1.27
HCO_3^-[e]	-[c]	1.74	2.52	-[c]	n.d.[d]	1.26
OAc^-	>4	2.46	2.92	3.49	n.d.[d]	1.29
OBz^-	>4	2.19	2.84	n.d.[d]	n.d.[d]	1.65
SO_4^{2-}	>4	3.16	-[f]	3.26	n.d.[d]	2.00

[a] Added as the trihydrate (TBAF·$3H_2O$); [b] Most likely deprotonation of both hydroxyl groups occurs upon addition of anion; [c] Data suggests that deprotonation of the receptor occurs upon addition of anion (most likely *mono*deprotonation); [d] Unable to determine association constant due to peak overlap and/or small changes in chemical shift; [e] Added as TEA salt; [f] Data could not be fitted to a 1:1 or 2:1 model, but suggests strong interaction.

Job plot analyses were performed in a separate experiment. 10 NMR tubes were filled with 0.5 mL of a CD_3CN solution containing 0.01 M of an anion-receptor mixture in different ratios (0.1, 0.2, 0.3, 0.4, 0.5, 0.6, 0.7, 0.8, 0.9 and 1 molar fraction of the receptor). Both salt (TBA or TEA salts of various anions) and receptor were dried under high vacuum prior to use. ^{1}H NMR spectra were recorded on a Bruker AV300 spectrometer and calibrated to the residual protio solvent peak in CD_3CN (δ = 2.50 ppm). Job plots were obtained by plotting the molar fraction of the receptor as a function of the relative change in chemical shift.

S3.2. Overview of ^{1}H NMR titrations

*S3.2.1. Interactions of compound **1** with various anions*

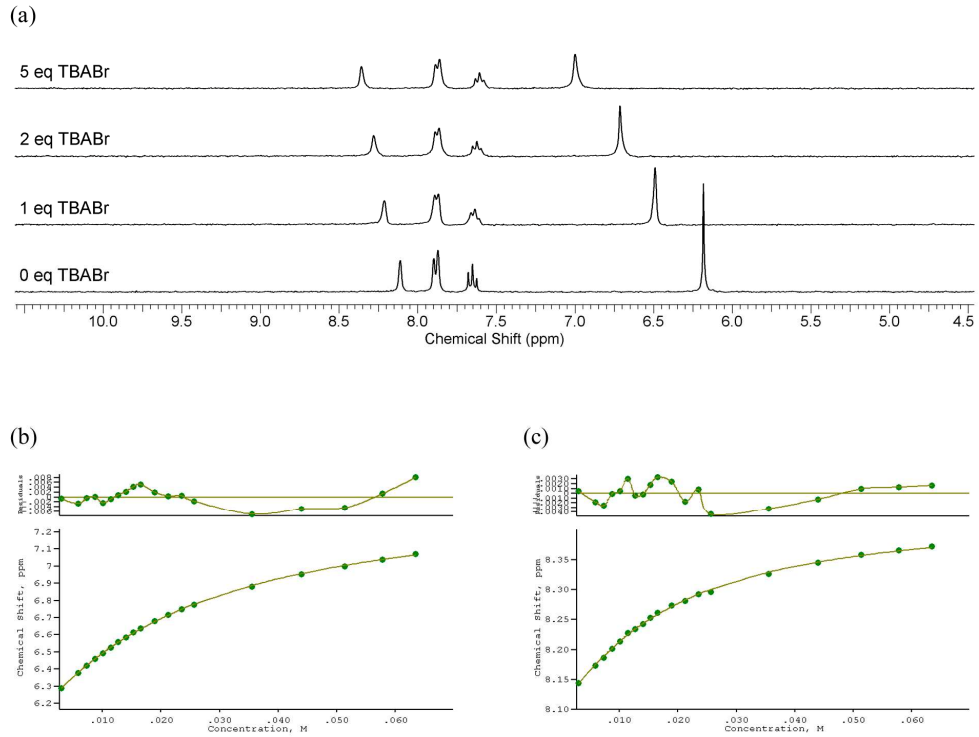

Figure S1. ^{1}H NMR titration of compound **1** with TBABr in CD_3CN at 298 K. Fit plots show chemical shift (ppm) versus anion concentration (M). (a) Stack plot. (b) Fit plot for OH proton at δ = 6.16 ppm. K_a = 46 M^{-1} (error 3%). (c) Fit plot for CH proton at δ = 8.11 ppm. K_a = 74 M^{-1} (error 4%).

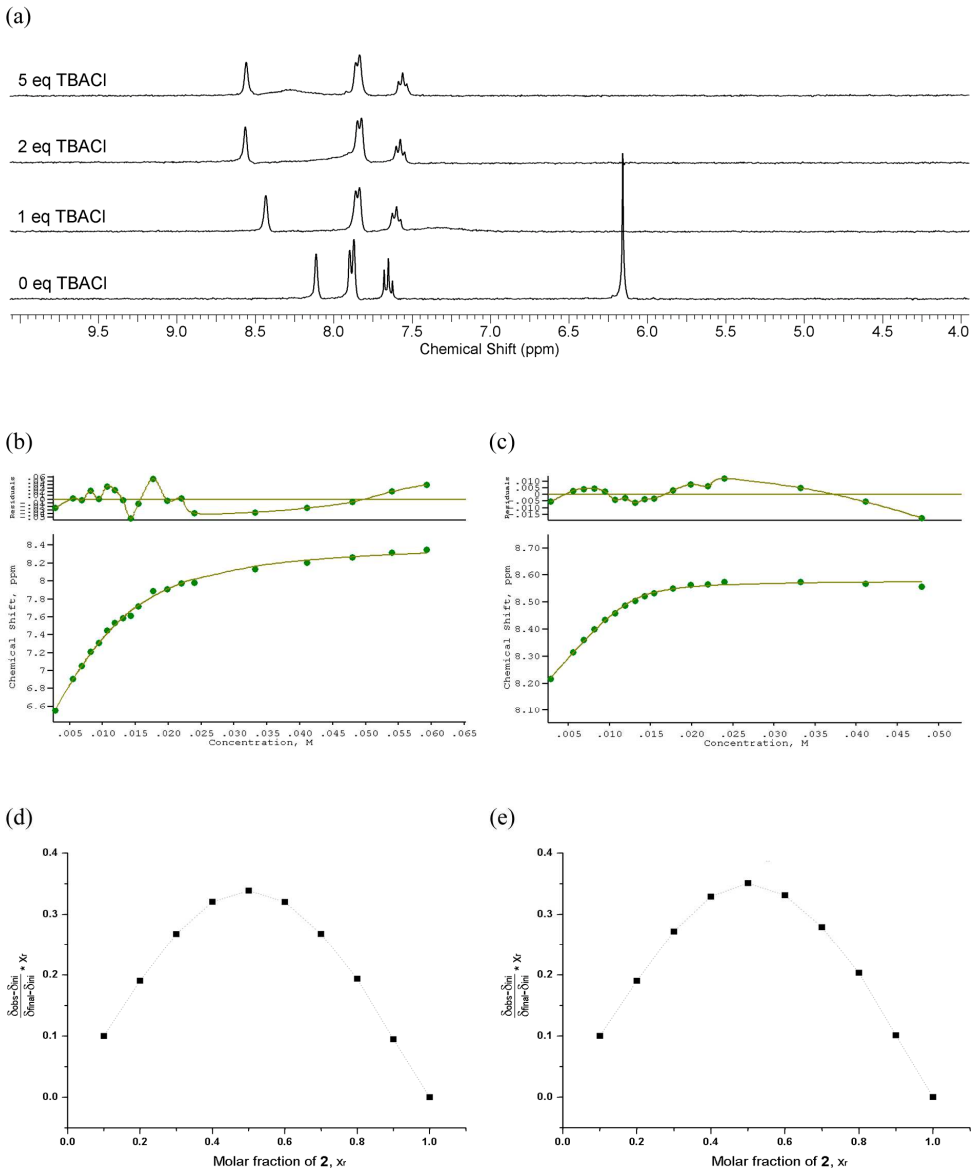

Figure S2. ^{1}H NMR titration of compound **1** with TBACl in CD_3CN at 298 K. Fit plots show chemical shift (ppm) versus anion concentration (M). (a) Stack plot. (b) Fit plot for OH proton at δ = 6.16 ppm. K_a = 306 M^{-1} (error 8%). (c) Fit plot for CH proton at δ = 8.11 ppm. K_a = 2218 M^{-1} (error 17%). (d) Job plot for OH proton at δ = 6.16 ppm. (e) Job plot for CH proton at δ = 8.11 ppm.

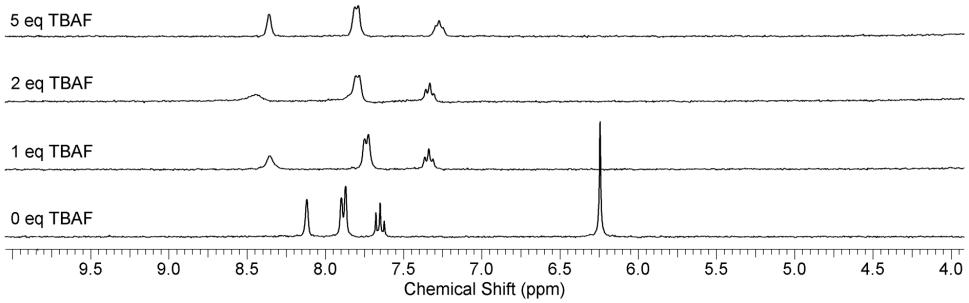

Figure S3. Stack plot of the ^{1}H NMR titration of compound **1** with TBAF·3H_2O in CD_3CN at 298 K. Deprotonation of receptor occurred (see section S3.3).

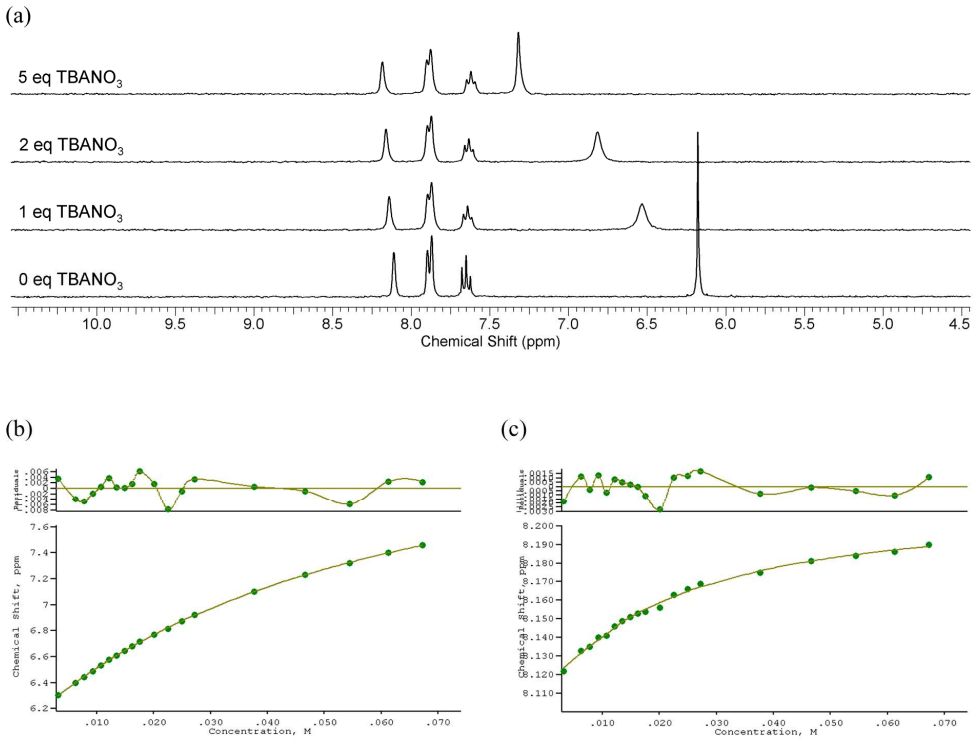

Figure S4. ^{1}H NMR titration of compound **1** with $TBANO_3$ in CD_3CN at 298 K. Fit plots show chemical shift (ppm) versus anion concentration (M). (a) Stack plot. (b) Fit plot for OH proton at δ = 6.16 ppm. K_a = 19.2 M^{-1} (error 3%). (c) Fit plot for CH proton at δ = 8.11 ppm. K_a = 58.2 M^{-1} (error 5%).

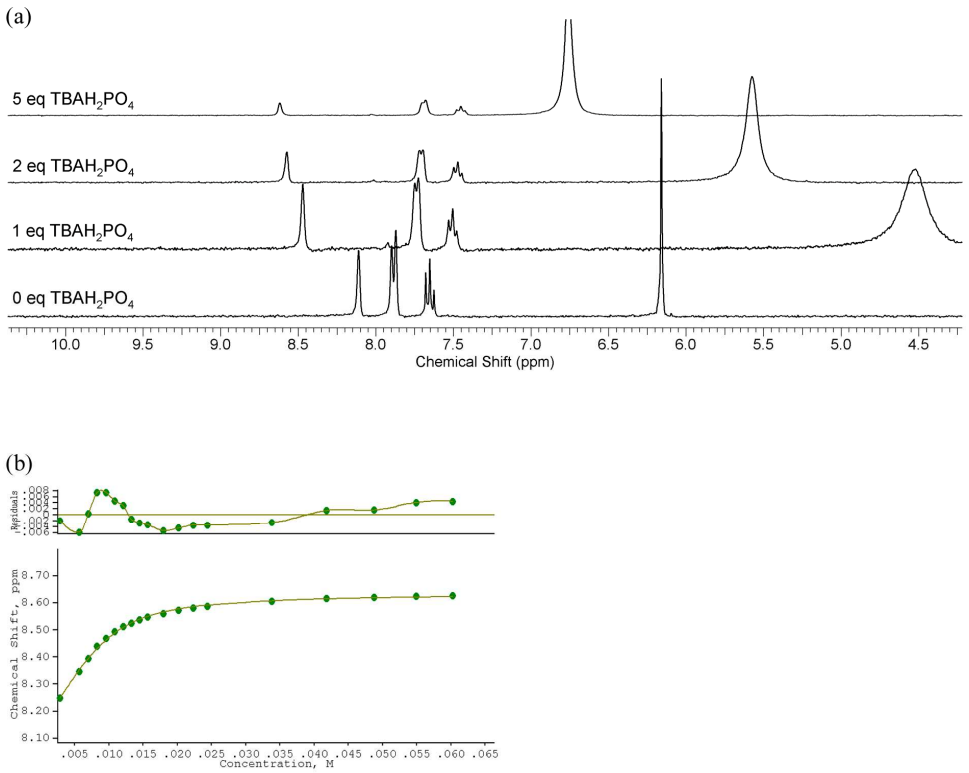

Figure S5. ^{1}H NMR titration of compound **1** with $TBAH_2PO_4$ in CD_3CN at 298 K. Fit plots show chemical shift (ppm) versus anion concentration (M). (a) Stack plot. (b) Fit plot for CH proton at δ = 8.11 ppm. K_a = 664 M^{-1} (error 5%).

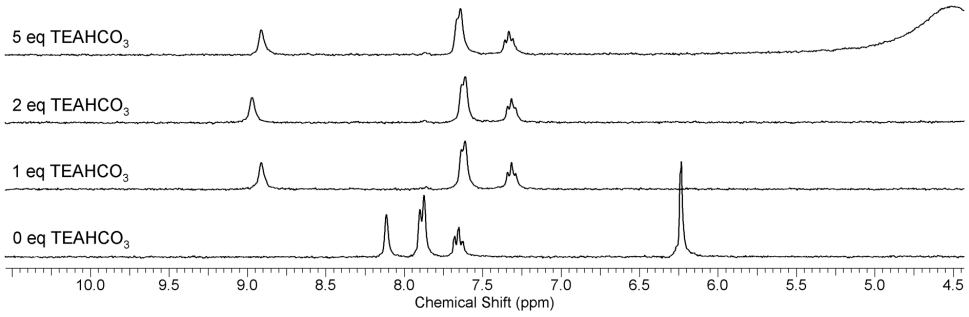

Figure S6. Stack plot of the ^{1}H NMR titration of compound **1** with $TEAHCO_3$ in CD_3CN at 298 K. Deprotonation of receptor occurred (see section S3.3).

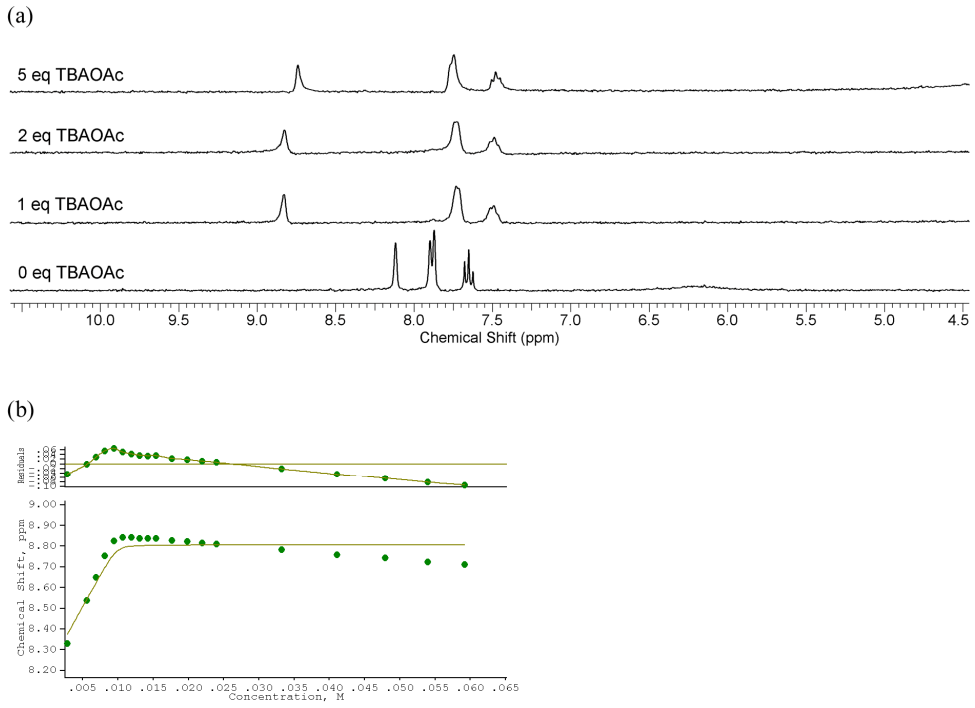

Figure S7. ^{1}H NMR titration of compound **1** with TBAOAc in CD_3CN at 298 K. Fit plots show chemical shift (ppm) versus anion concentration (M). (a) Stack plot. (b) Fit plot for CH proton at δ = 8.11 ppm. $K_a > 10^4$ M^{-1}.

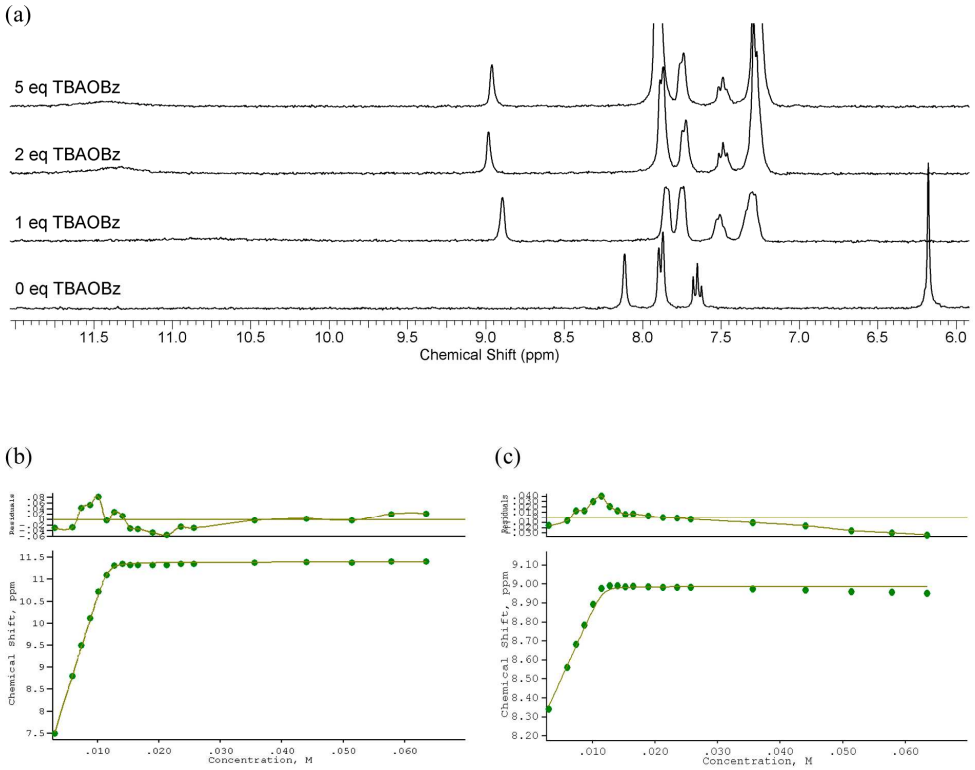

Figure S8. ^{1}H NMR titration of compound **1** with TBAOBz in CD_3CN at 298 K. Fit plots show chemical shift (ppm) versus anion concentration (M). (a) Stack plot. (b) Fit plot for OH proton at δ = 6.16 ppm. $K_a > 10^4$ M^{-1}. (c) Fit plot for CH proton at δ = 8.11 ppm. $K_a > 10^4$ M^{-1}.

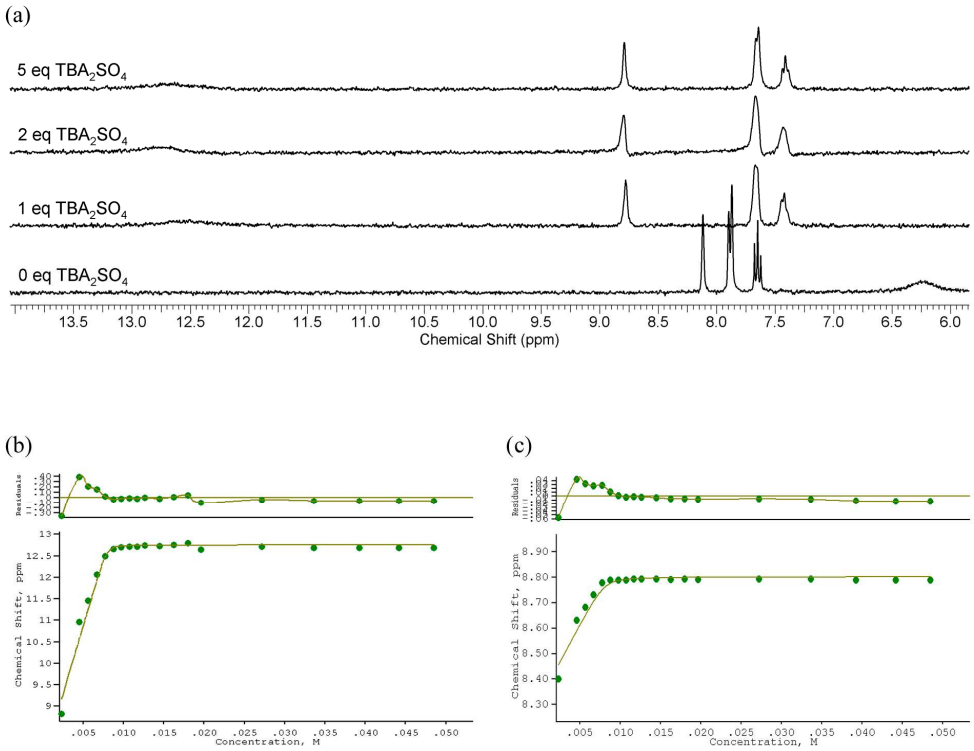

Figure S9. ^{1}H NMR titration of compound **1** with TBA_2SO_4 in CD_3CN at 298 K. Fit plots show chemical shift (ppm) versus anion concentration (M). (a) Stack plot. (b) Fit plot for OH proton at δ = 6.16 ppm. $K_a > 10^4$ M^{-1}. (c) Fit plot for CH proton at δ = 8.11 ppm. $K_a > 10^4$ M^{-1}.

*S3.2.2. Interactions of compound **2** with various anions*

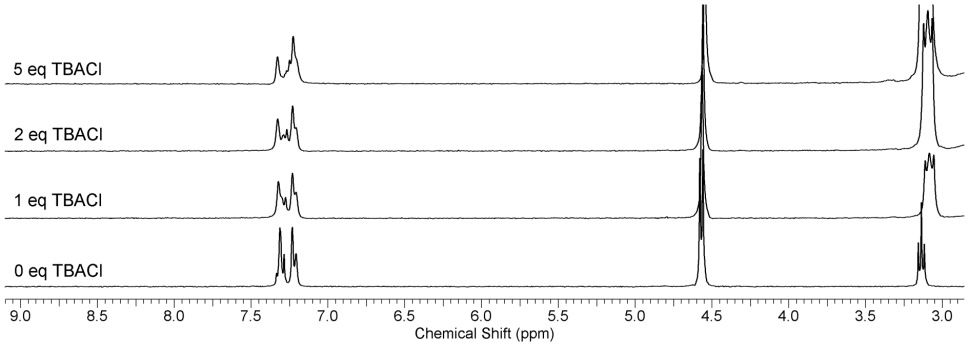

Figure S10. Stack plot of the ^{1}H NMR titration of compound **2** with TBACl in CD_3CN at 298 K. Change in chemical shift is too small to allow accurate calculation of the association constant.

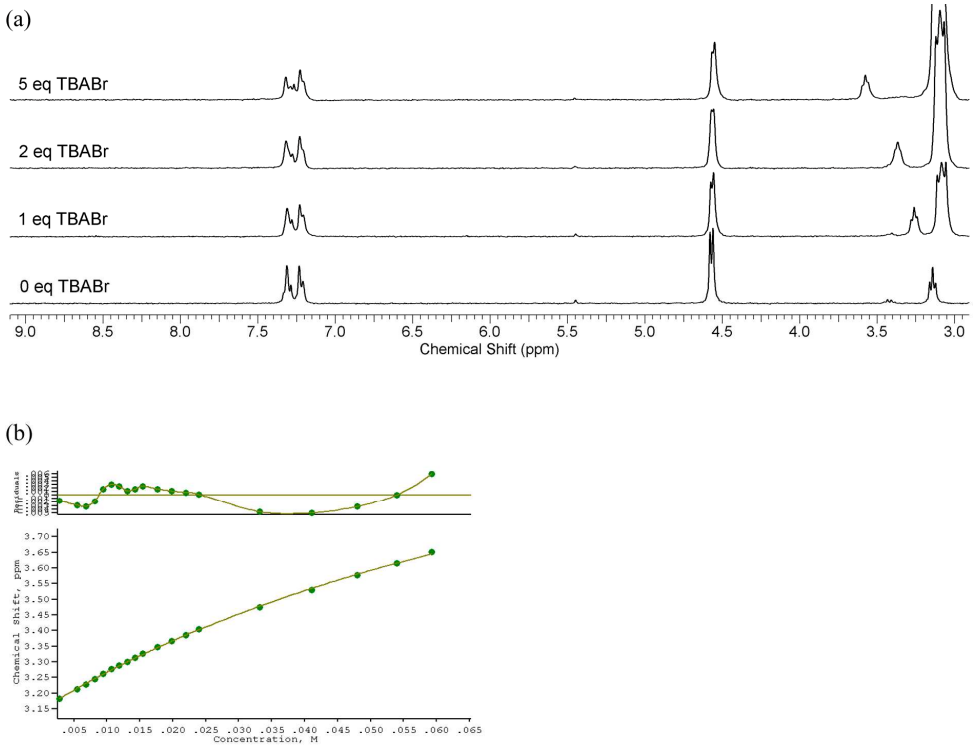

Figure S11. ^{1}H NMR titration of compound **2** with TBABr in CD_3CN at 298 K. Fit plots show chemical shift (ppm) versus anion concentration (M). (a) Stack plot. (b) Fit plot for OH proton at δ = 3.14 ppm. K_a = 11 M^{-1} (error 6%).

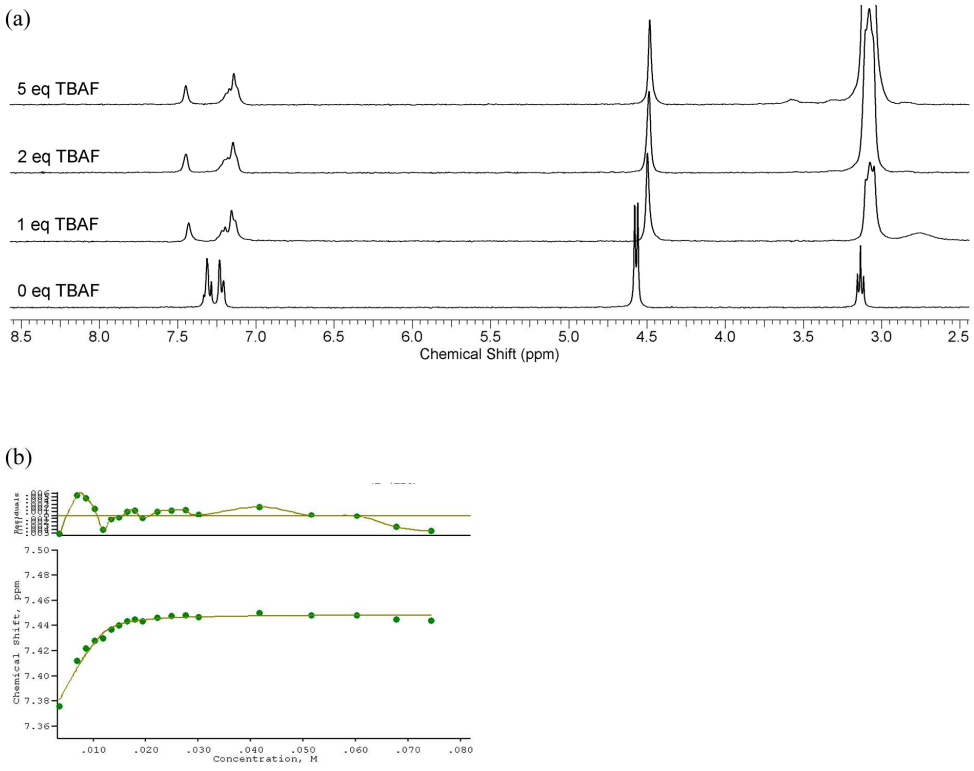

Figure S12. ^{1}H NMR titration of compound **2** with TBAF·$3H_2O$ in CD_3CN at 298 K. Fit plots show chemical shift (ppm) versus anion concentration (M). (a) Stack plot. (b) Fit plot for CH proton at δ = 7.31 ppm. K_a = 2234 M^{-1} (error 1%).

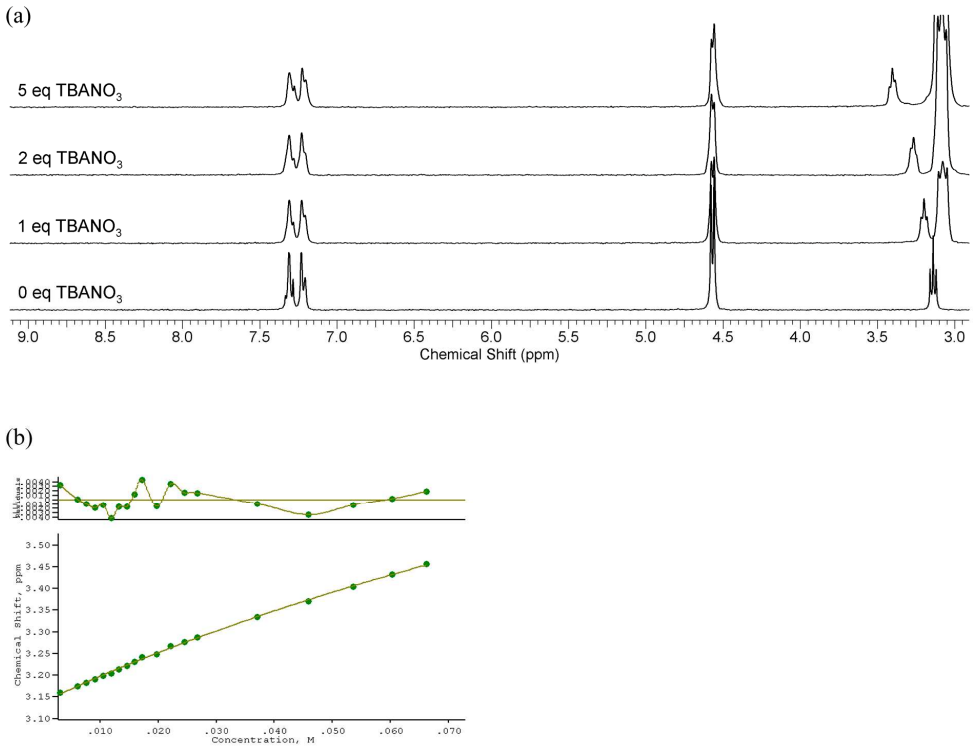

Figure S13. ^{1}H NMR titration of compound **2** with $TBANO_3$ in CD_3CN at 298 K. Fit plots show chemical shift (ppm) versus anion concentration (M). (a) Stack plot. (b) Fit plot for OH proton at δ = 3.14 ppm. K_a = 5 M^{-1} (error 12%).

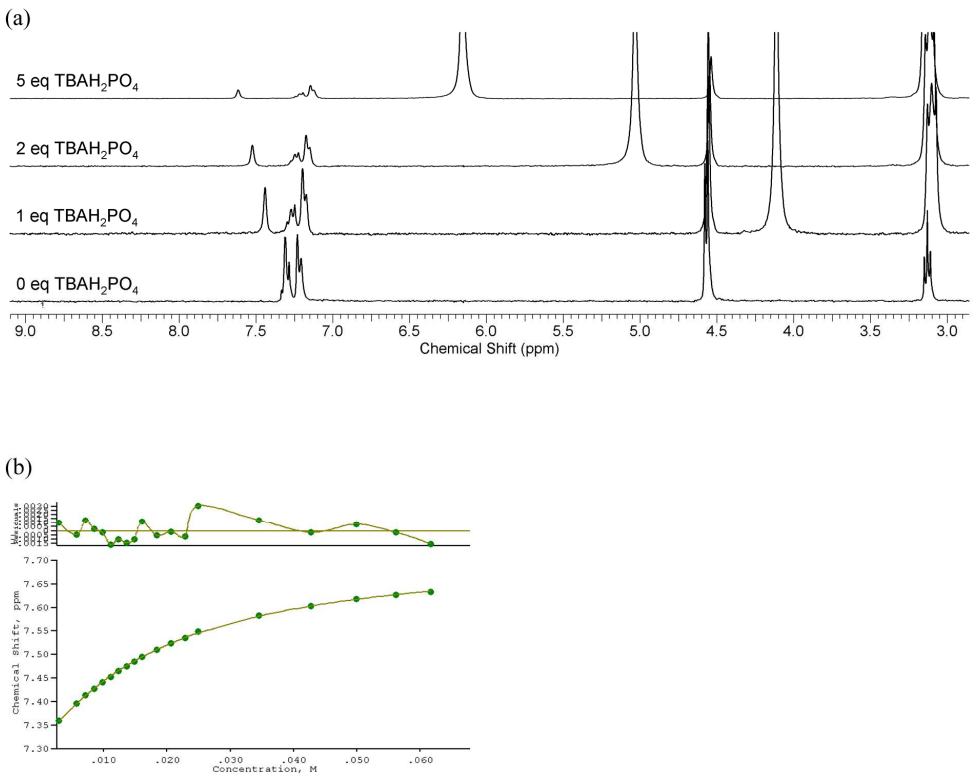

Figure S14. ^{1}H NMR titration of compound **2** with $TBAH_2PO_4$ in CD_3CN at 298 K. Fit plots show chemical shift (ppm) versus anion concentration (M). (a) Stack plot. (b) Fit plot for CH proton at δ = 7.31 ppm. K_a = 661 M^{-1} (error 2%).

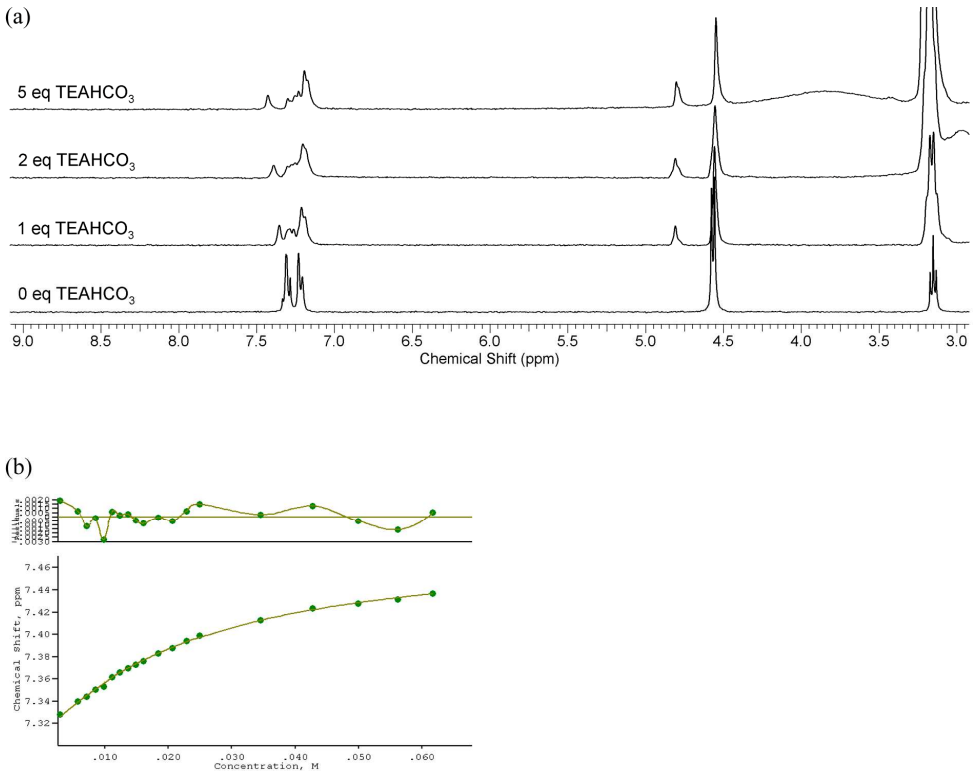

Figure S15. ^{1}H NMR titration of compound **2** with $TEAHCO_3$ in CD_3CN at 298 K. Fit plots show chemical shift (ppm) versus anion concentration (M). (a) Stack plot. (b) Fit plot for CH proton at δ = 7.31 ppm. K_a = 54.6 M^{-1} (error 4%).

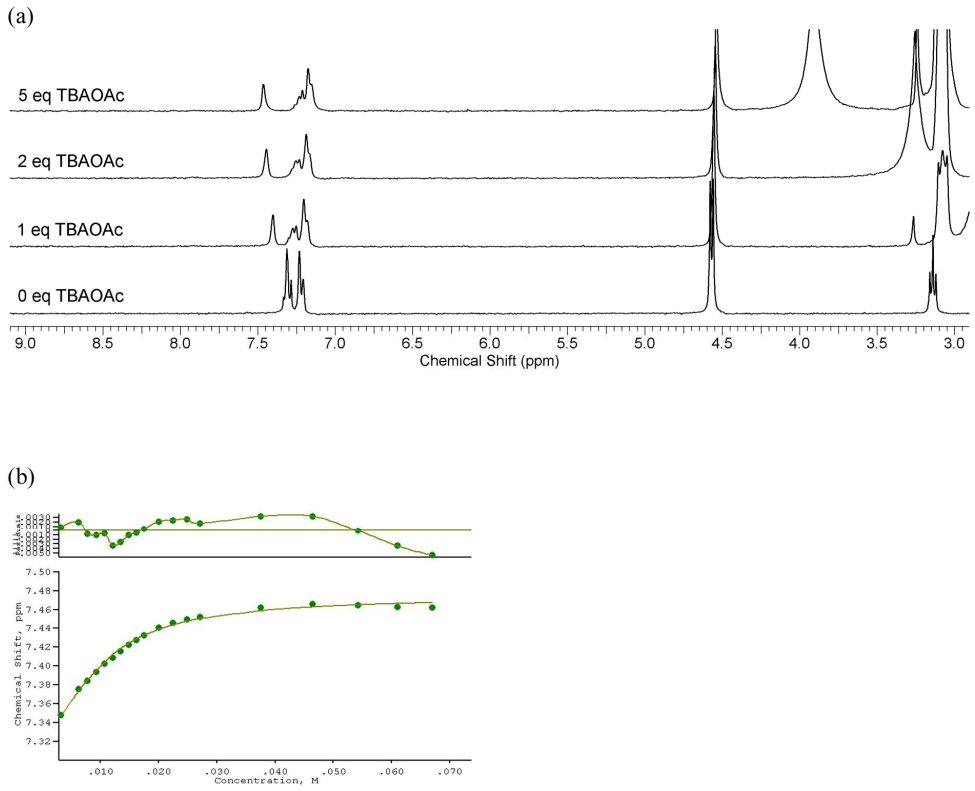

Figure S16. ^{1}H NMR titration of compound **2** with TBAOAc in CD_3CN at 298 K. Fit plots show chemical shift (ppm) versus anion concentration (M). (a) Stack plot. (b) Fit plot for CH proton at δ = 7.31 ppm. K_a =289 M^{-1} (error 5%).

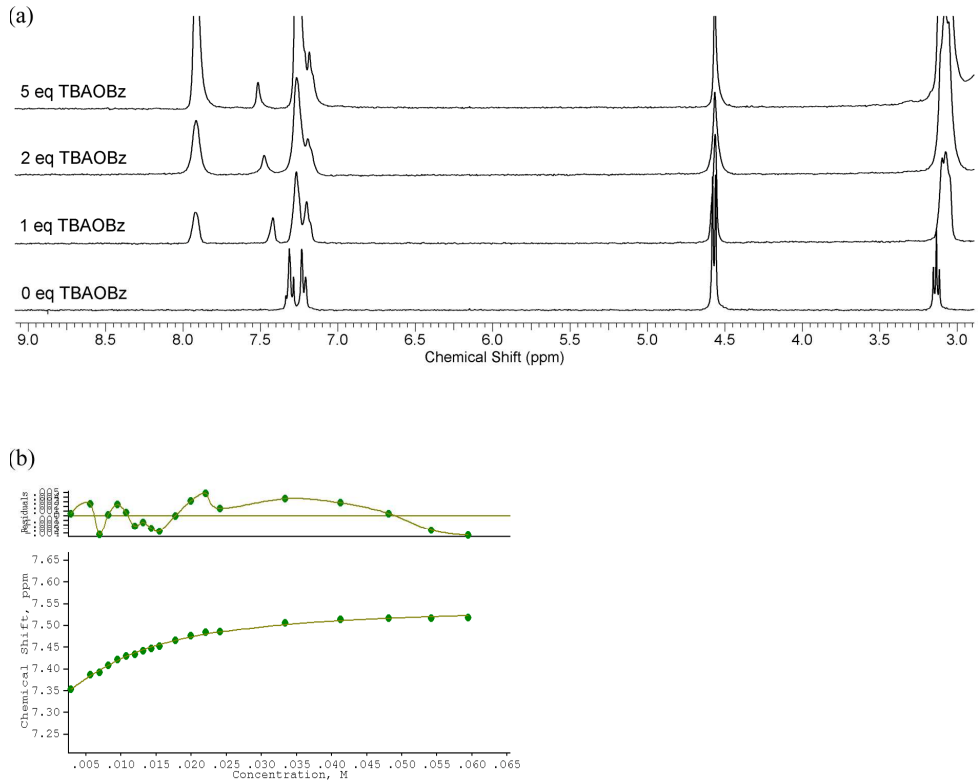

Figure S17. ^{1}H NMR titration of compound **2** with TBAOBz in CD_3CN at 298 K. Fit plots show chemical shift (ppm) versus anion concentration (M). (a) Stack plot. (b) Fit plot for CH proton at δ = 7.31 ppm. K_a = 156 M^{-1} (error 6%).

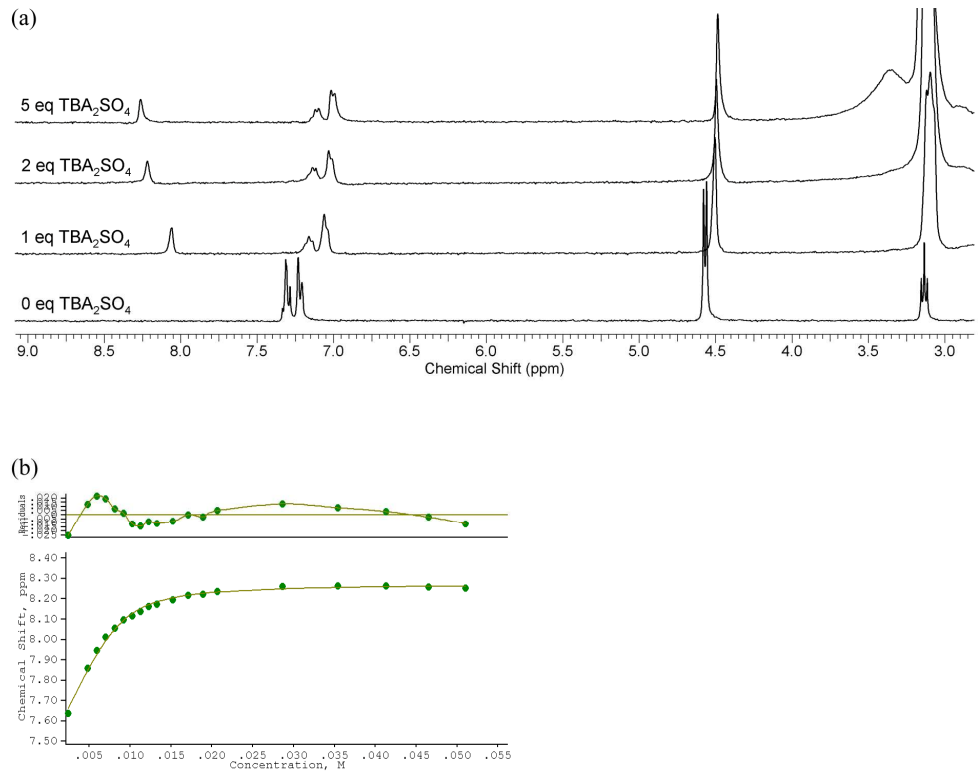

Figure S18. ^{1}H NMR titration of compound **2** with TBA_2SO_4 in CD_3CN at 298 K. Fit plots show chemical shift (ppm) versus anion concentration (M). (a) Stack plot. (b) Fit plot for CH proton at δ = 7.31 ppm. K_a = 1446 M^{-1} (error 11%).

*S3.2.3. Interactions of compound **3** with various anions*

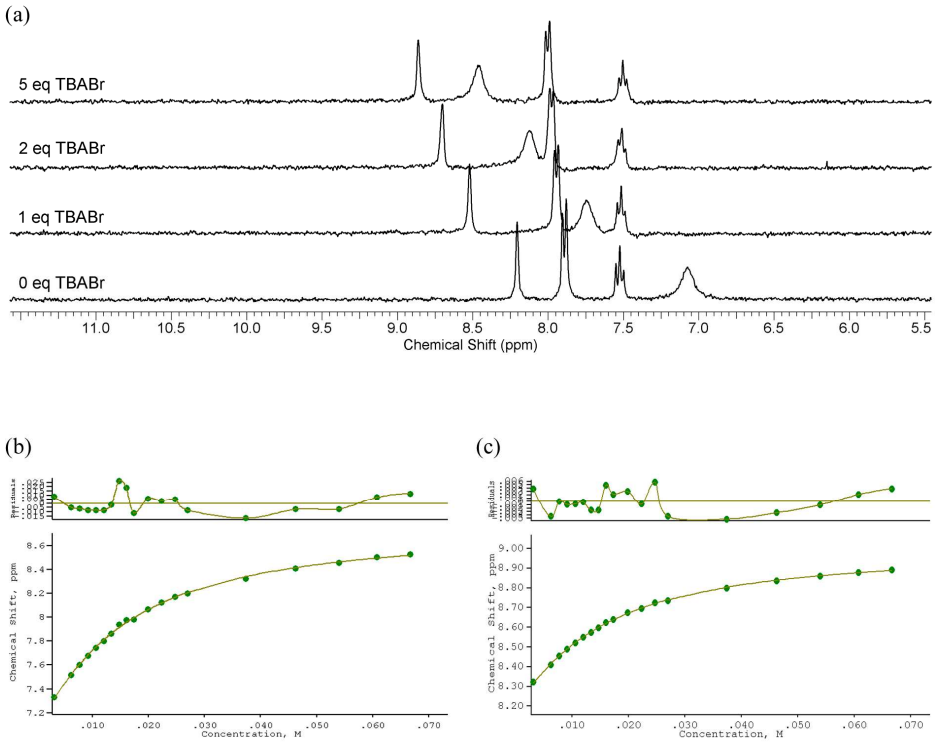

Figure S19. ^{1}H NMR titration of compound **3** with TBABr in CD_3CN at 298 K. Fit plots show chemical shift (ppm) versus anion concentration (M). (a) Stack plot. (b) Fit plot for NH proton at δ = 7.09 ppm. K_a = 96 M^{-1} (error 4%). (c) Fit plot for CH proton at δ = 8.20 ppm. K_a = 95 M^{-1} (error 3%).

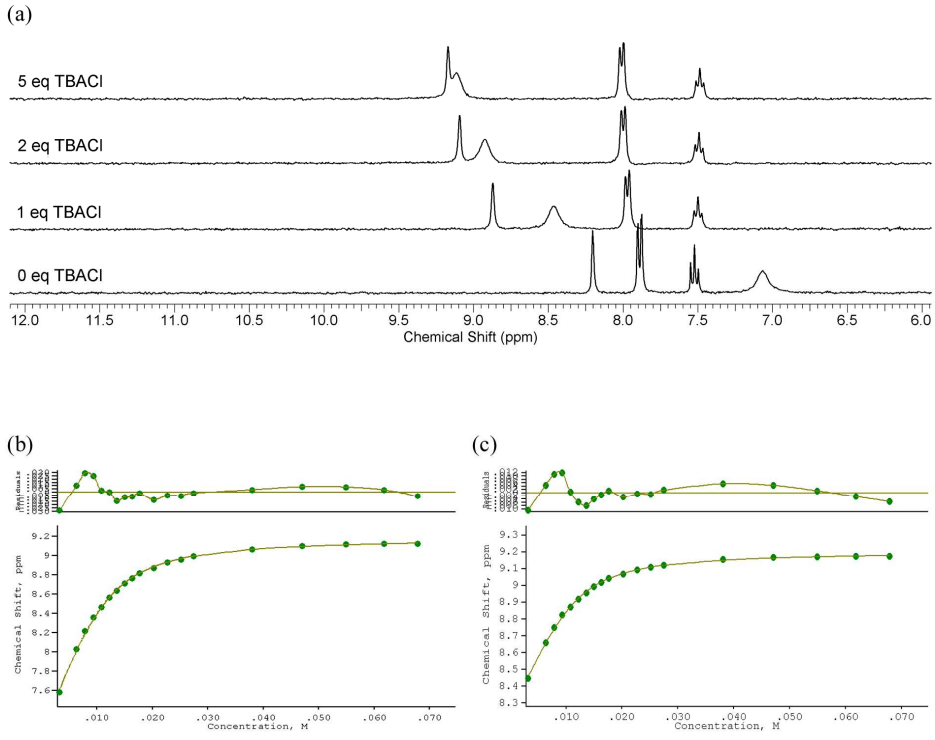

Figure S20. ^{1}H NMR titration of compound **3** with TBACl in CD_3CN at 298 K. Fit plots show chemical shift (ppm) versus anion concentration (M). (a) Stack plot. (b) Fit plot for NH proton at δ = 7.09 ppm. K_a = 545 M^{-1} (error 4%). (c) Fit plot for CH proton at δ = 8.20 ppm. K_a = 619 M^{-1} (error 4%).

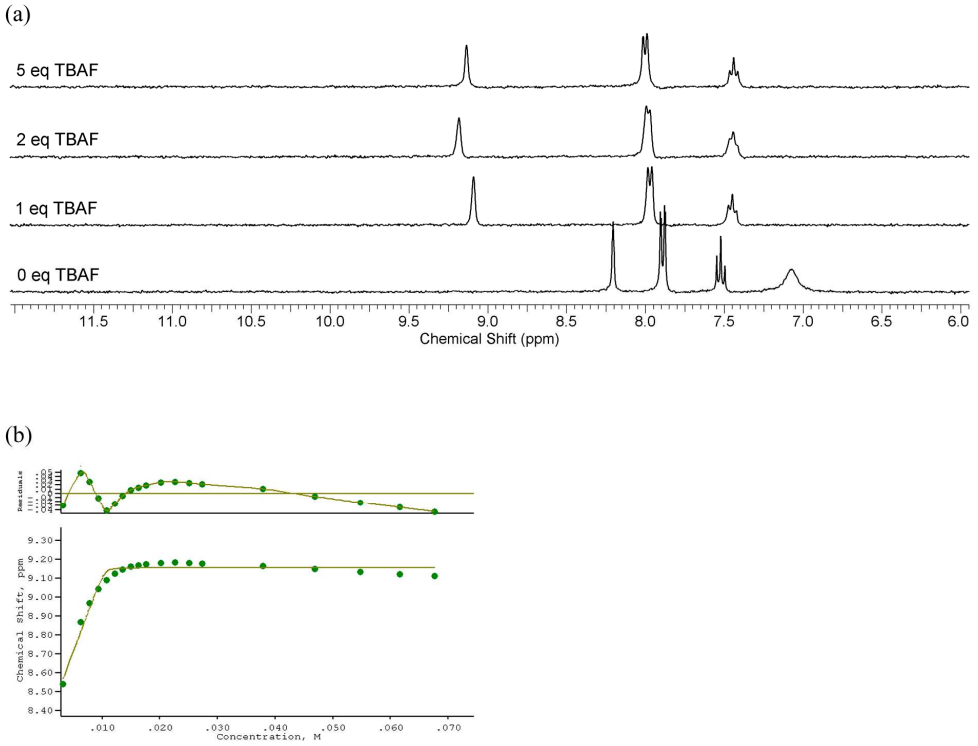

Figure S21. ^{1}H NMR titration of compound **3** with TBAF·3H$_2$O in CD$_3$CN at 298 K. Fit plots show chemical shift (ppm) versus anion concentration (M). (a) Stack plot. (b) Fit plot for CH proton at δ = 8.20 ppm. $K_a > 10^4$ M^{-1}.

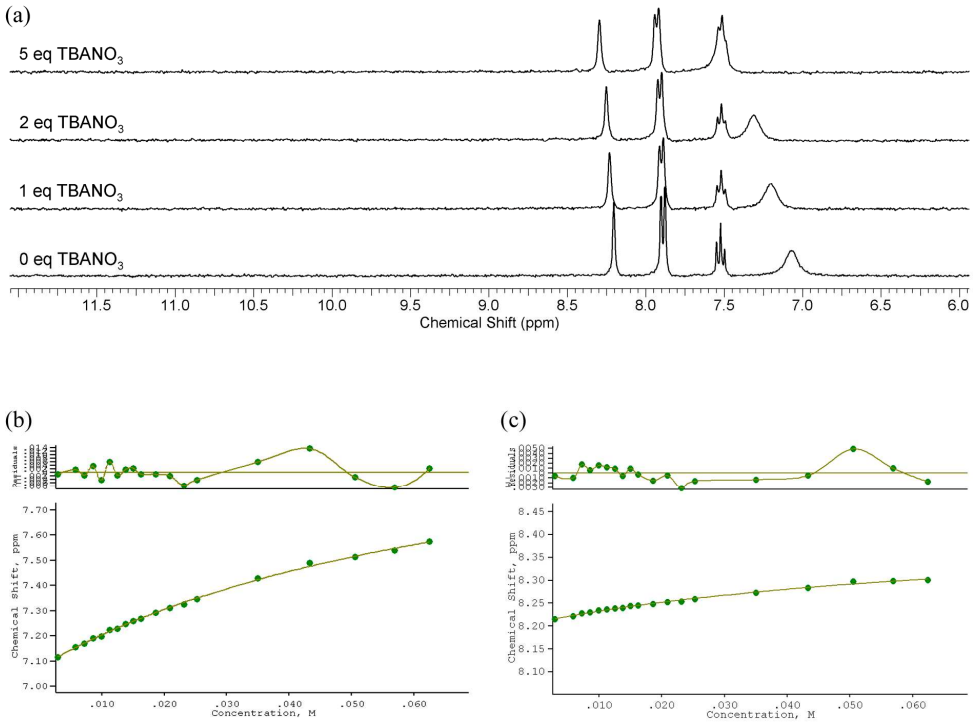

Figure S22. ^{1}H NMR titration of compound **3** with TBANO$_3$ in CD$_3$CN at 298 K. Fit plots show chemical shift (ppm) versus anion concentration (M). (a) Stack plot. (b) Fit plot for NH proton at δ = 7.09 ppm. K_a = 16.2 M^{-1} (error 9%). (c) Fit plot for CH proton at δ = 8.20 ppm. K_a = 15.7 M^{-1} (error 12%).

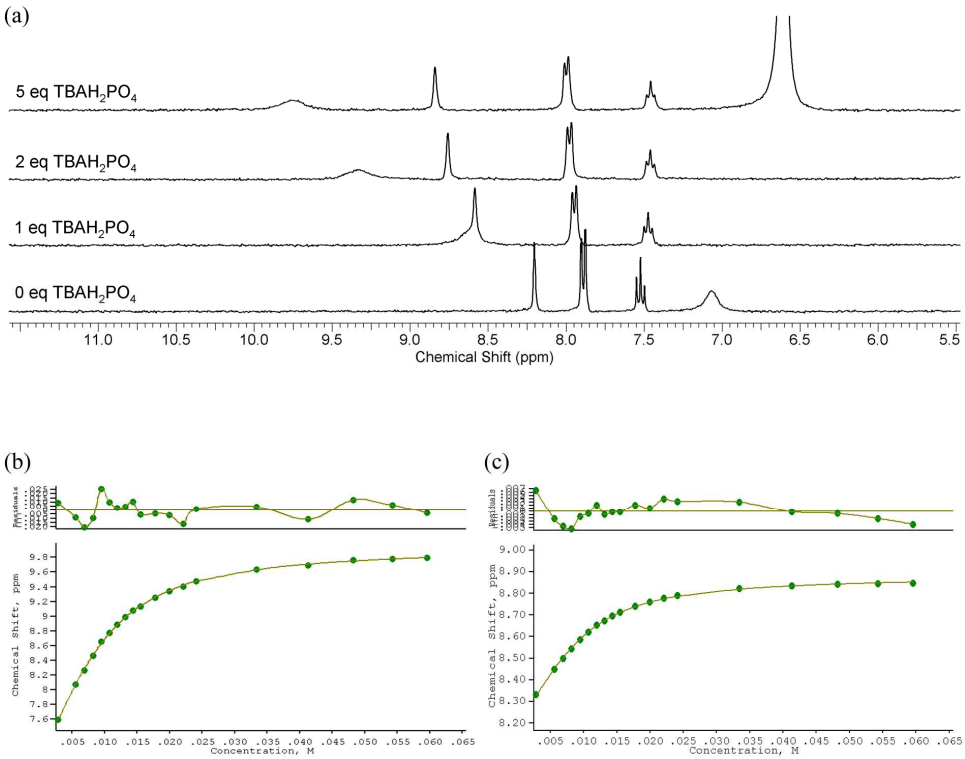

Figure S23. ^{1}H NMR titration of compound **3** with $TBAH_2PO_4$ in CD_3CN at 298 K. Fit plots show chemical shift (ppm) versus anion concentration (M). (a) Stack plot. (b) Fit plot for NH proton at δ = 7.09 ppm. K_a = 320 M^{-1} (error 2%). (b) Fit plot for CH proton at δ = 8.20 ppm. K_a = 397 M^{-1} (error 3%).

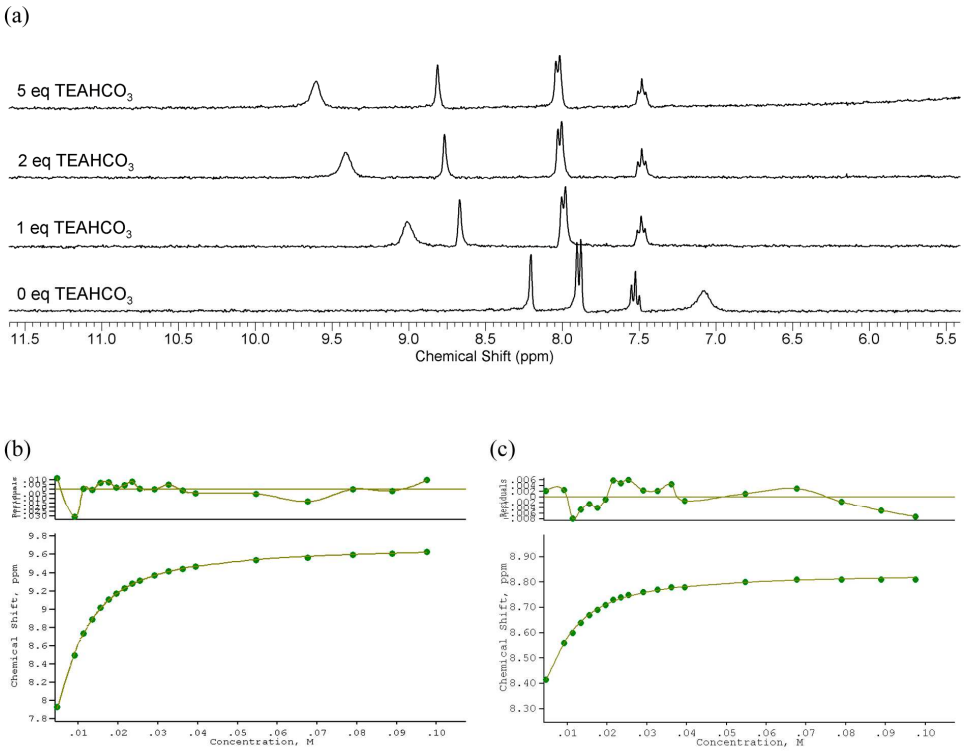

Figure S24. ^{1}H NMR titration of compound **3** with $TEAHCO_3$ in CD_3CN at 298 K. Fit plots show chemical shift (ppm) versus anion concentration (M). (a) Stack plot. (b) Fit plot for NH proton at δ = 7.09 ppm. K_a = 328 M^{-1} (error 2%). (b) Fit plot for CH proton at δ = 8.20 ppm. K_a = 330 M^{-1} (error 4%).

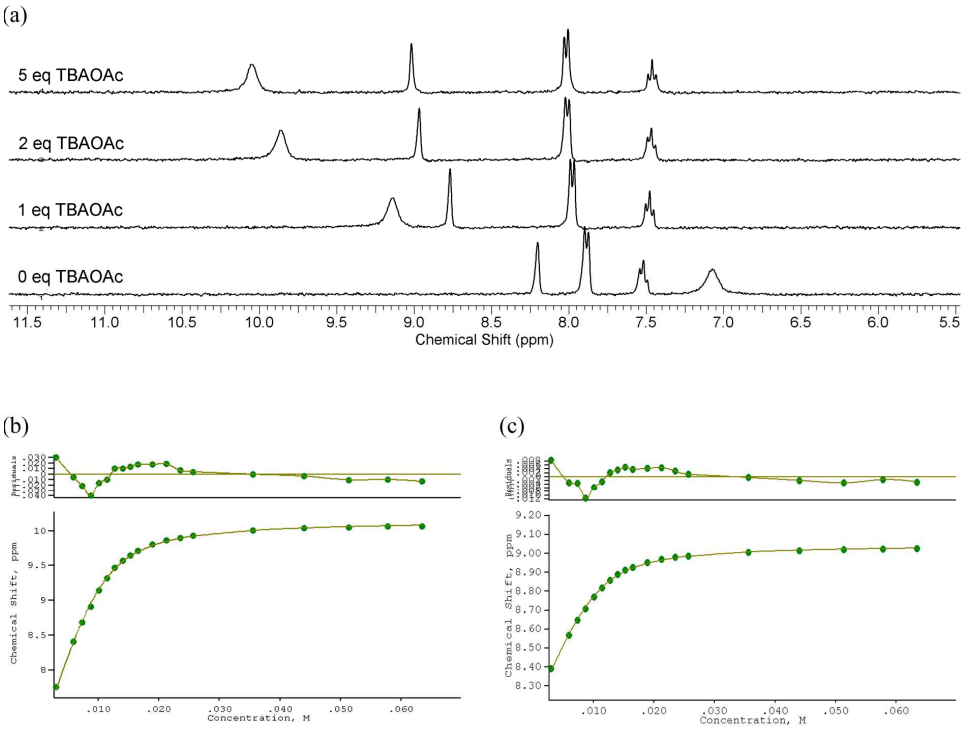

Figure S25. ^{1}H NMR titration of compound **3** with TBAOAc in CD_3CN at 298 K. Fit plots show chemical shift (ppm) versus anion concentration (M). (a) Stack plot. (b) Fit plot for NH proton at δ = 7.09 ppm. K_a = 831 M^{-1} (error 4%). (b) Fit plot for CH proton at δ = 8.20 ppm. K_a = 822 M^{-1} (error 4%).

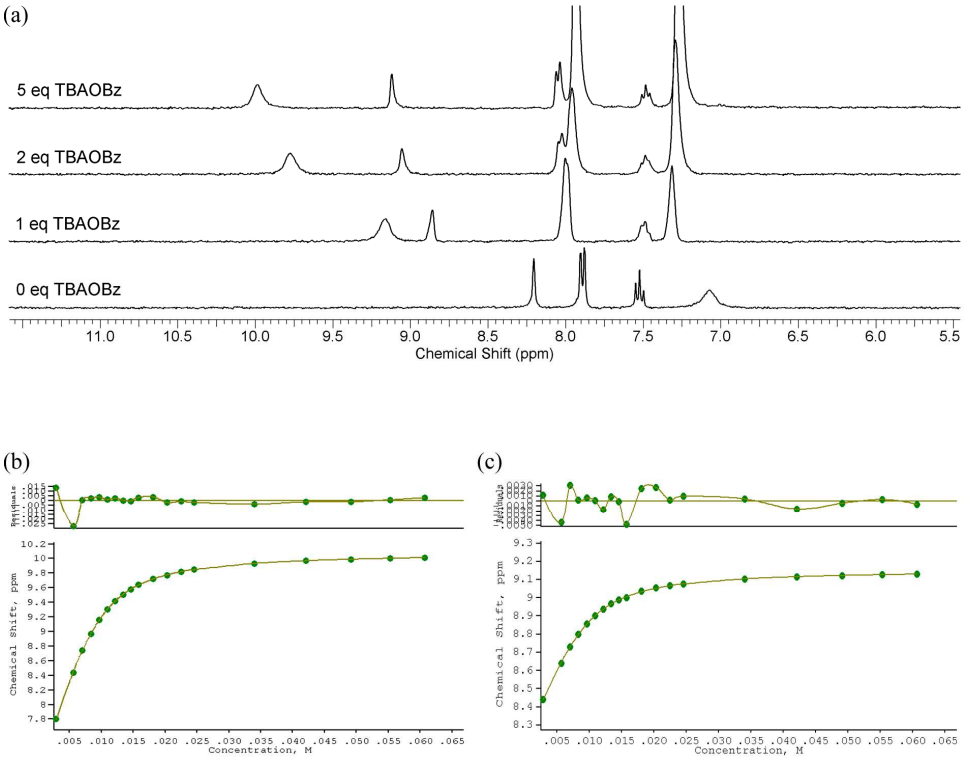

Figure S26. ^{1}H NMR titration of compound **3** with TBAOBz in CD_3CN at 298 K. Fit plots show chemical shift (ppm) versus anion concentration (M). (a) Stack plot. (b) Fit plot for NH proton at δ = 7.09 ppm. K_a = 746 M^{-1} (error 2%). (c) Fit plot for CH proton at δ = 8.20 ppm. K_a = 690 M^{-1} (error 1%).

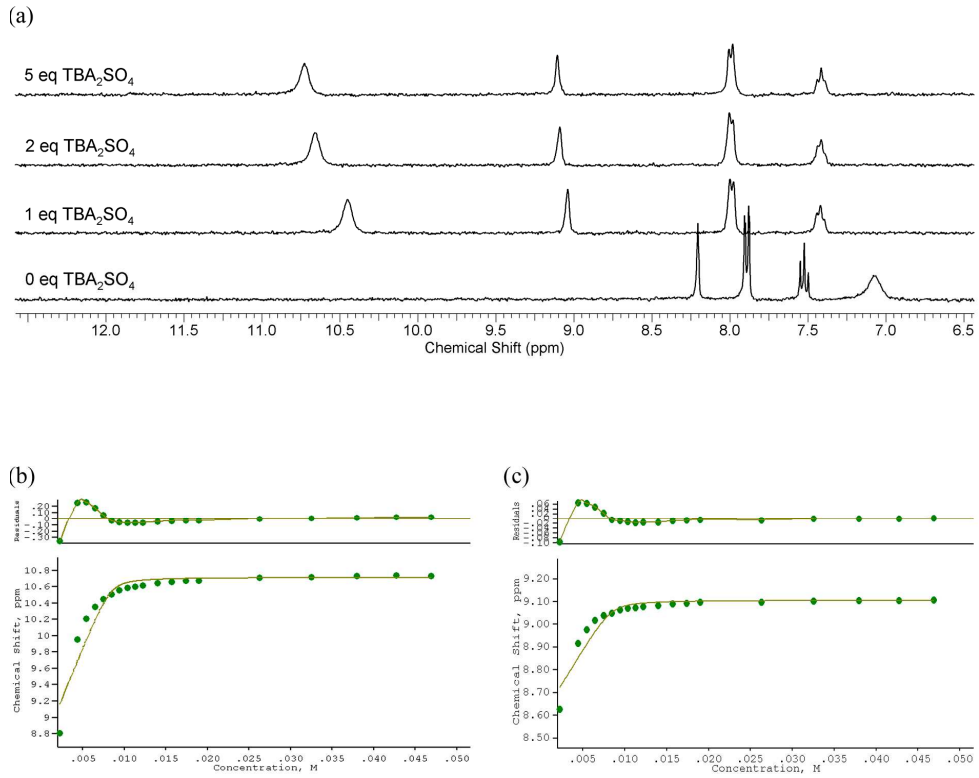

Figure S27. ^{1}H NMR titration of compound **3** with TBA_2SO_4 in CD_3CN at 298 K. Fit plots show chemical shift (ppm) versus anion concentration (M). (a) Stack plot. (b) Fit plot for NH proton at δ = 7.09 ppm. (c) Fit plot for CH proton at δ = 8.20 ppm. (b) and (c) show that the fit to a 1:1 model gives large errors and the association constant could not be calculated.

*S3.2.4. Interactions of compound **4** with various anions*

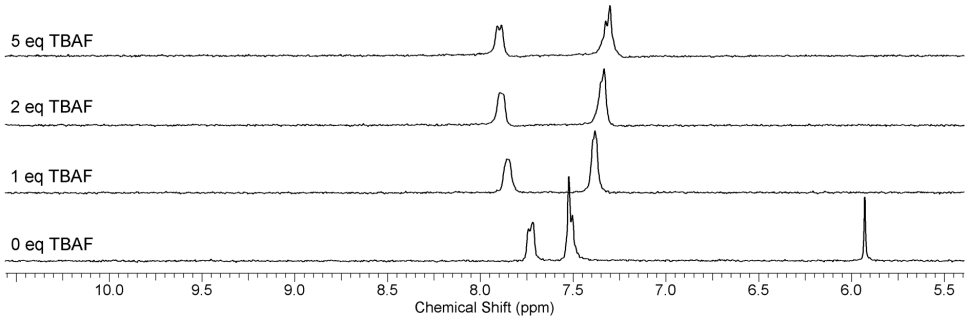

Figure S28. Stack plot of the ^{1}H NMR titration of compound **4** with $TBAF\cdot 3H_2O$ in CD_3CN at 298 K. Deprotonation of receptor occurred (see section S3.3).

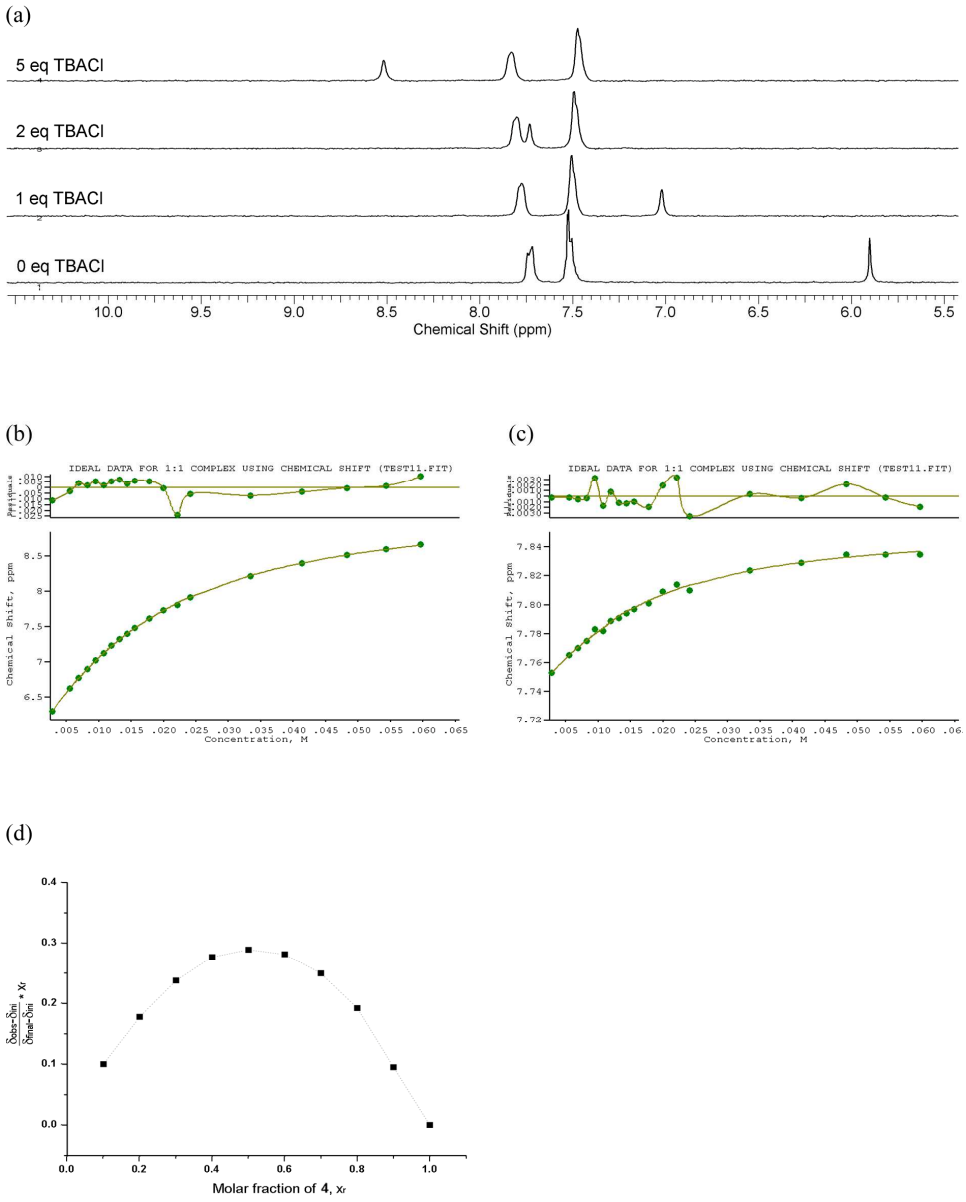

Figure S29. ^{1}H NMR titration of compound **4** with TBACl in CD_3CN at 298 K. Fit plots show chemical shift (ppm) versus anion concentration (M). (a) Stack plot. (b) Fit plot for OH proton at δ = 5.90 ppm. K_a = 84 M^{-1} (error 2%). (c) Fit plot for CH proton at δ = 7.73 ppm. K_a = 108 M^{-1} (error 4%). (d) Job plot for OH proton at δ = 5.90 ppm.

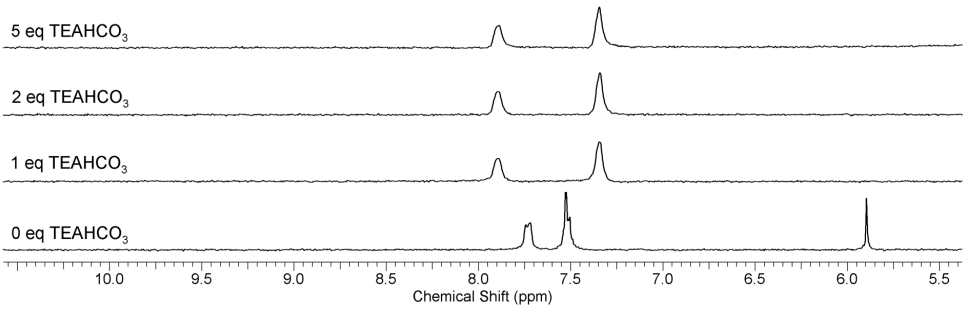

Figure S30. Stack plot of the ^{1}H NMR titration of compound **4** with $TEAHCO_3$ in CD_3CN at 298 K. Deprotonation of receptor occurred (see section S3.3).

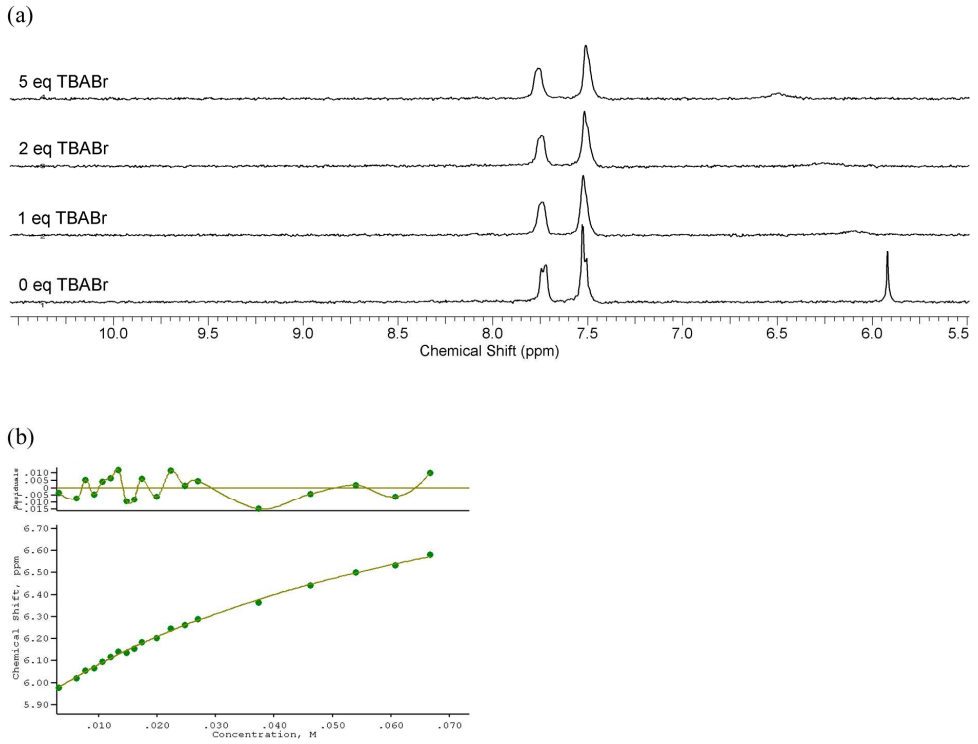

Figure S31. ^{1}H NMR titration of compound **4** with TBABr in CD_3CN at 298 K. Fit plots show chemical shift (ppm) versus anion concentration (M). (a) Stack plot. (b) Fit plot for OH proton at δ = 5.90 ppm. K_a = 14.5 M^{-1} (error 11%).

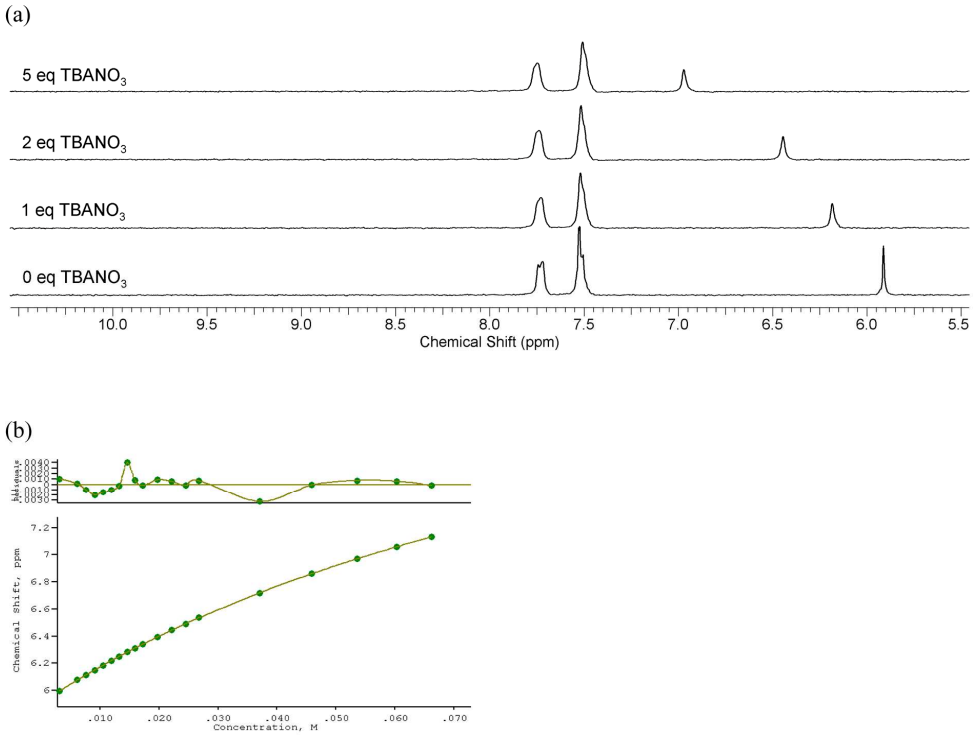

Figure S32. ^{1}H NMR titration of compound **4** with $TBANO_3$ in CD_3CN at 298 K. Fit plots show chemical shift (ppm) versus anion concentration (M). (a) Stack plot. (b) Fit plot for OH proton at δ = 5.90 ppm. K_a = 9.7 M^{-1} (error 1%).

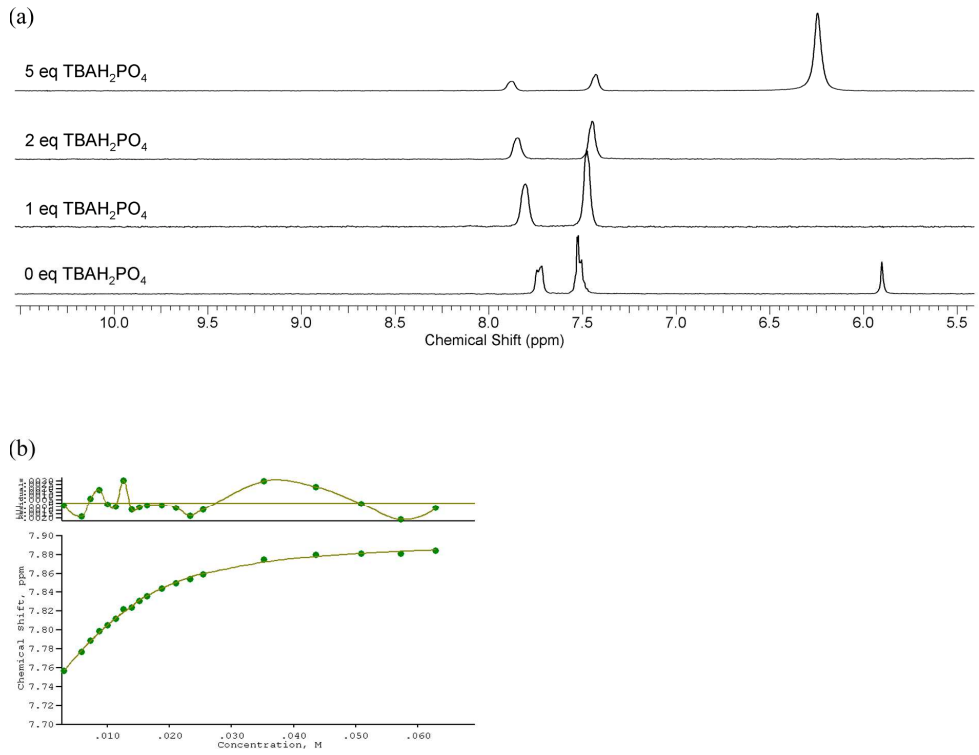

Figure S33. ^{1}H NMR titration of compound **4** with $TBAH_2PO_4$ in CD_3CN at 298 K. Fit plots show chemical shift (ppm) versus anion concentration (M). (a) Stack plot. (b) Fit plot for CH proton at δ = 7.73 ppm. K_a = 241 M^{-1} (error 6%).

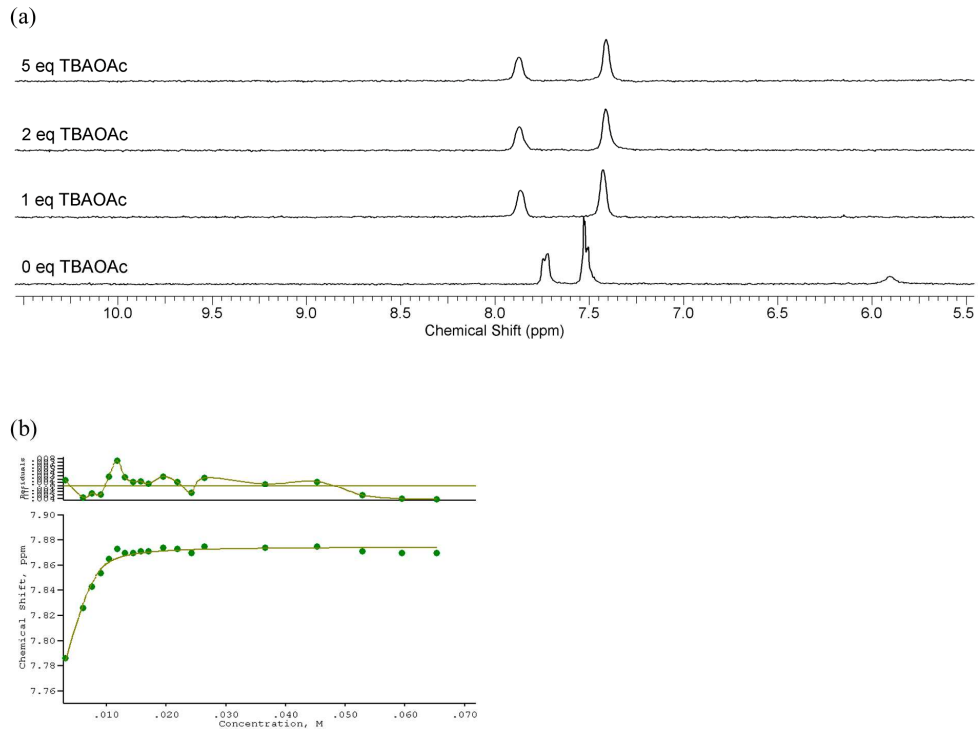

Figure S34. ^{1}H NMR titration of compound **4** with TBAOAc in CD_3CN at 298 K. Fit plots show chemical shift (ppm) versus anion concentration (M). (a) Stack plot. (b) Fit plot for CH proton at δ = 7.73 ppm. K_a = 3088 M^{-1} (error 16%).

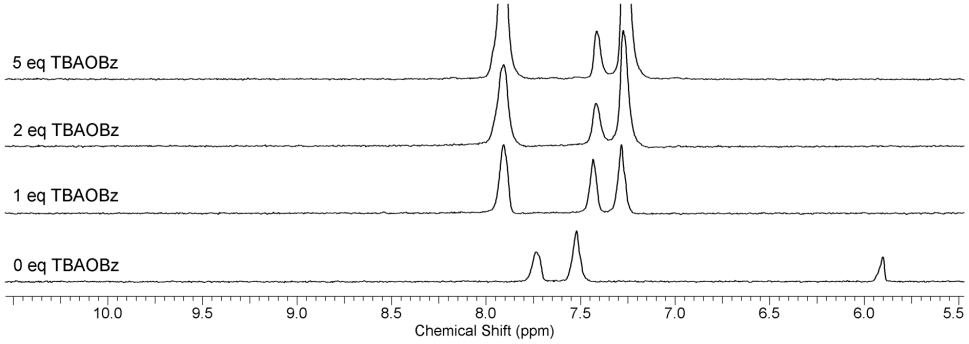

Figure S35. Stack plot of the ^{1}H NMR titration of compound **4** with TBAOBz in CD_3CN at 298 K. Overlap with the signals corresponding to benzoate prevented calculation of association constants.

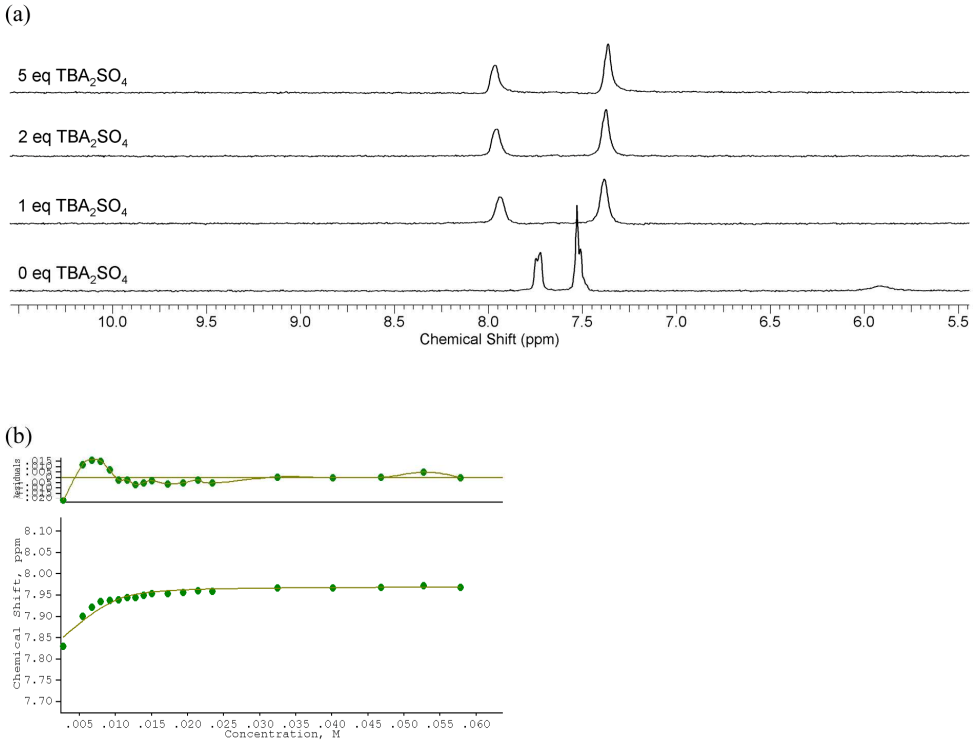

Figure S36. ^{1}H NMR titration of compound **4** with TBA_2SO_4 in CD_3CN at 298 K. Fit plots show chemical shift (ppm) versus anion concentration (M). (a) Stack plot. (b) Fit plot for OH proton at δ = 7.73 ppm. K_a = 1810 M^{-1} (error 4%).

*S3.2.5. Interactions of compound **5** with various anions*

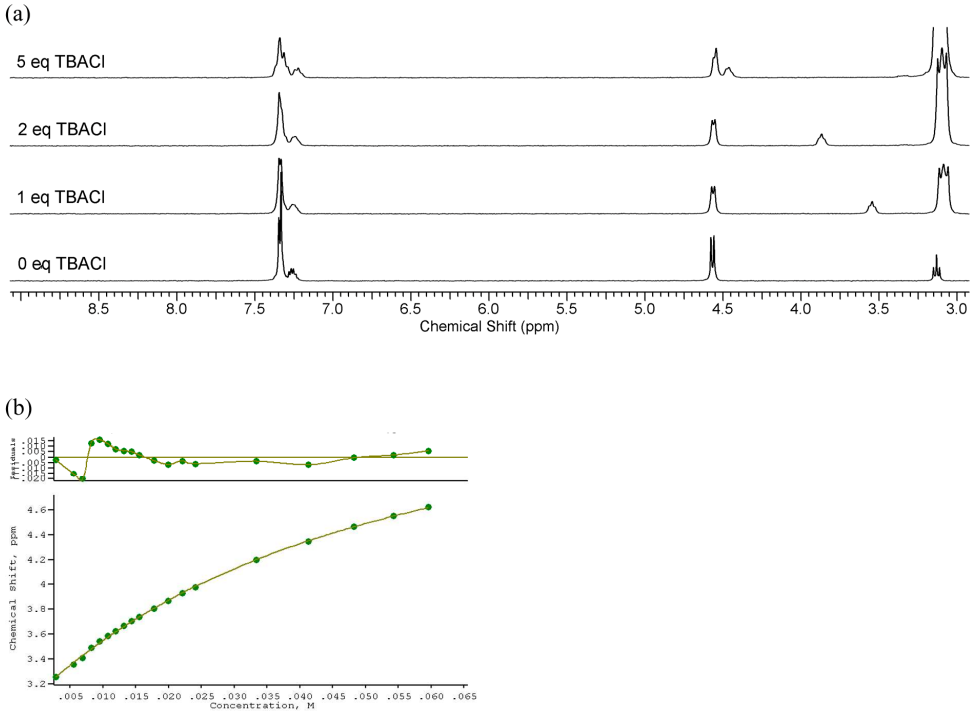

Figure S37. ^{1}H NMR titration of compound **5** with TBABr in CD_3CN at 298 K. Fit plots show chemical shift (ppm) versus anion concentration (M). (a) Stack plot. (b) Fit plot for OH proton at δ = 3.14 ppm. K_a = 7.6 M^{-1} (error 6%).

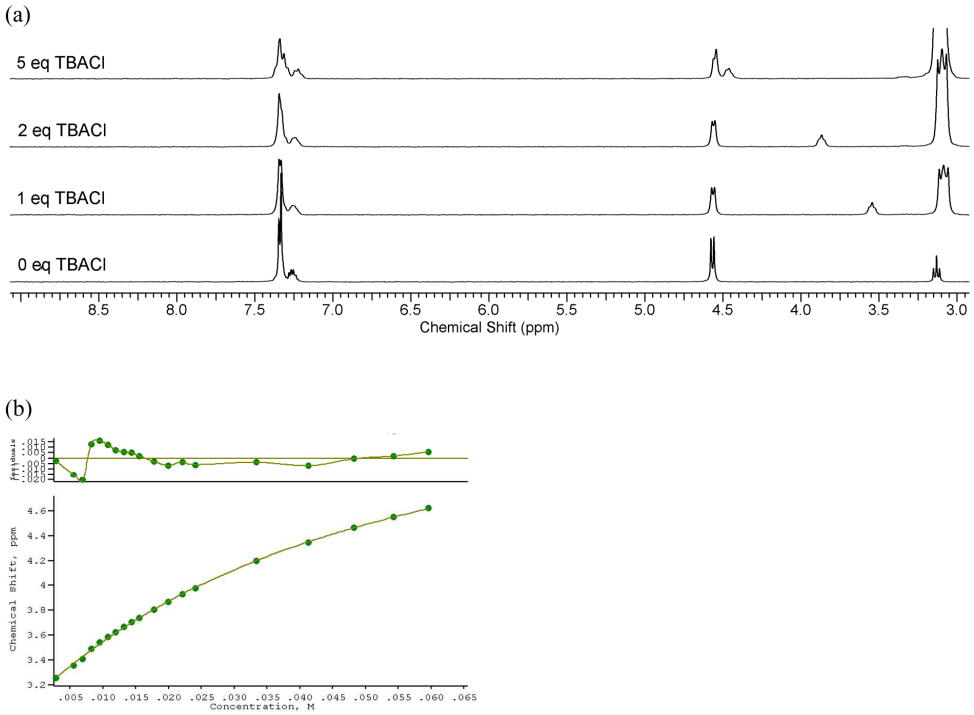

Figure S38. ^{1}H NMR titration of compound **5** with TBACl in CD_3CN at 298 K. Fit plots show chemical shift (ppm) versus anion concentration (M). (a) Stack plot. (b) Fit plot for OH proton at δ = 3.14 ppm. K_a = 24.1 M^{-1} (error 5%).

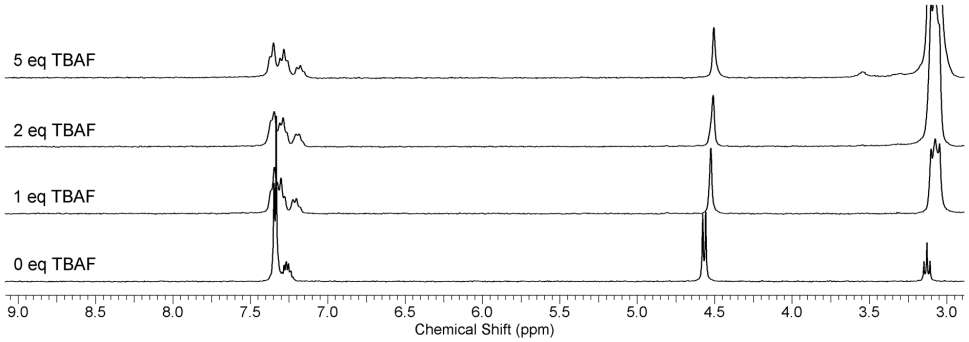

Figure S39. Stack plot of the ^{1}H NMR titration of compound **5** with TBAF·3H_2O in CD_3CN at 298 K. Changes in chemical shift are too small (< 0.1 ppm) to allow accurate determination of association constants.

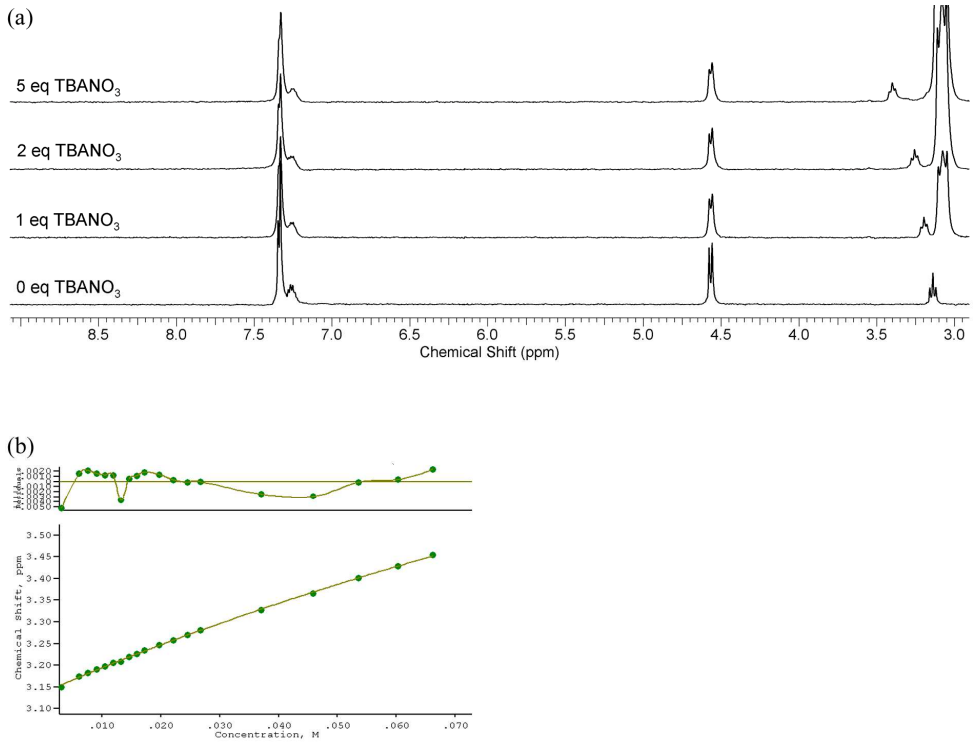

Figure S40. ^{1}H NMR titration of compound **5** with $TBANO_3$ in CD_3CN at 298 K. Fit plots show chemical shift (ppm) versus anion concentration (M). (a) Stack plot. (b) Fit plot for OH proton at δ = 3.14 ppm. K_a = 3.9 M^{-1} (error 13%).

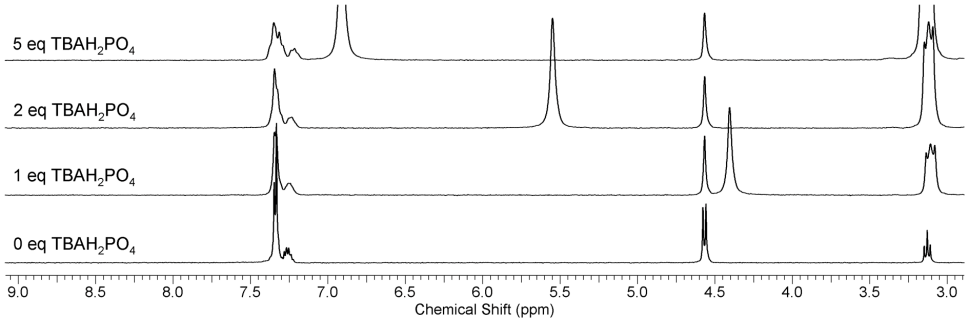

Figure S41. Stack plot of the ^{1}H NMR titration of compound **5** with $TBAH_2PO_4$ in CD_3CN at 298 K. Changes in chemical shift are too small (< 0.1 ppm) to allow accurate determination of association constants.

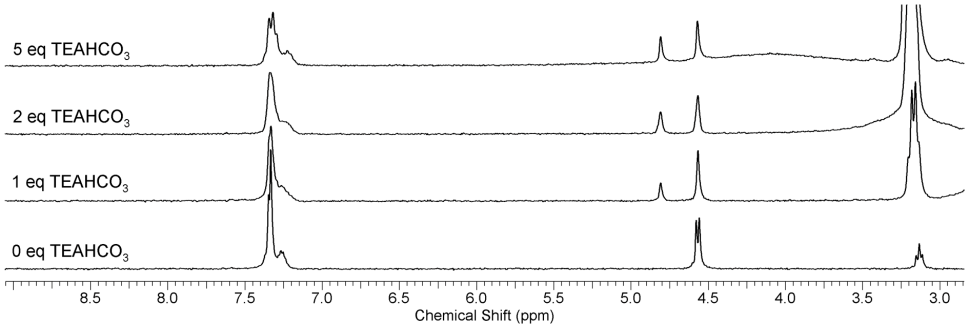

Figure S42. Stack plot of the ^{1}H NMR titration of compound **5** with $TEAHCO_3$ in CD_3CN at 298 K. Changes in chemical shift are too small (< 0.1 ppm) to allow accurate determination of association constants.

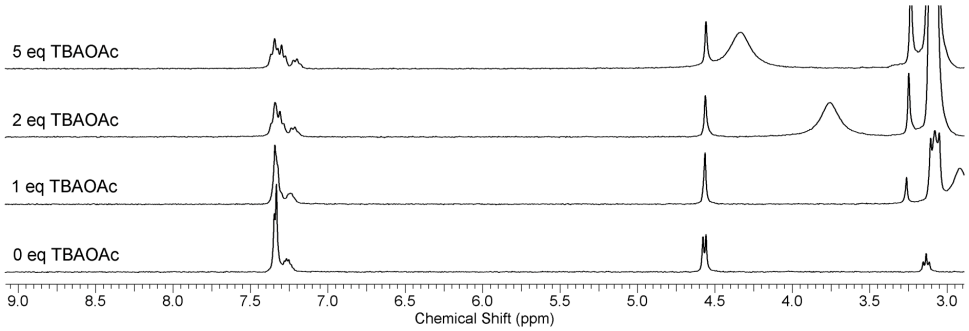

Figure S43. Stack plot of the ^{1}H NMR titration of compound **5** with TBAOAc in CD_3CN at 298 K. Changes in chemical shift are too small (< 0.1 ppm) to allow accurate determination of association constants.

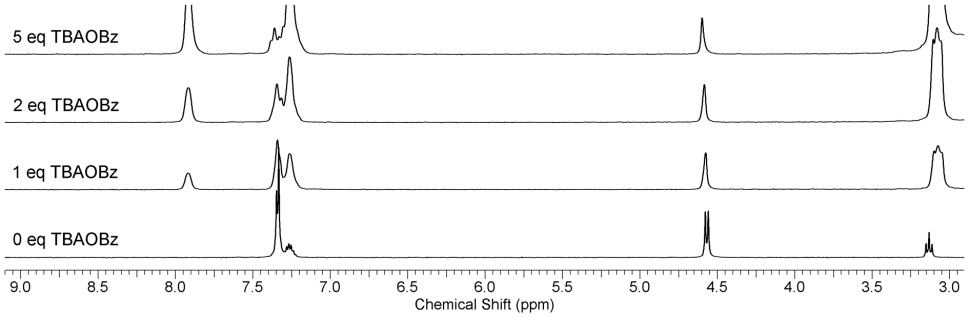

Figure S44. Stack plot of the ^{1}H NMR titration of compound **5** with TBAOBz in CD_3CN at 298 K. Changes in chemical shift are too small (< 0.1 ppm) to allow accurate determination of association constants.

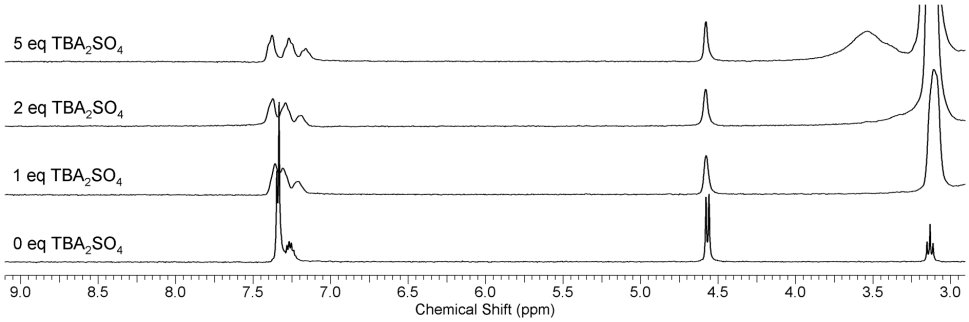

Figure S45. Stack plot of the ^{1}H NMR titration of compound **5** with TBA_2SO_4 in CD_3CN at 298 K. Changes in chemical shift are too small (< 0.1 ppm) to allow accurate determination of association constants.

*S3.2.6. Interactions of compound **6** with various anions*

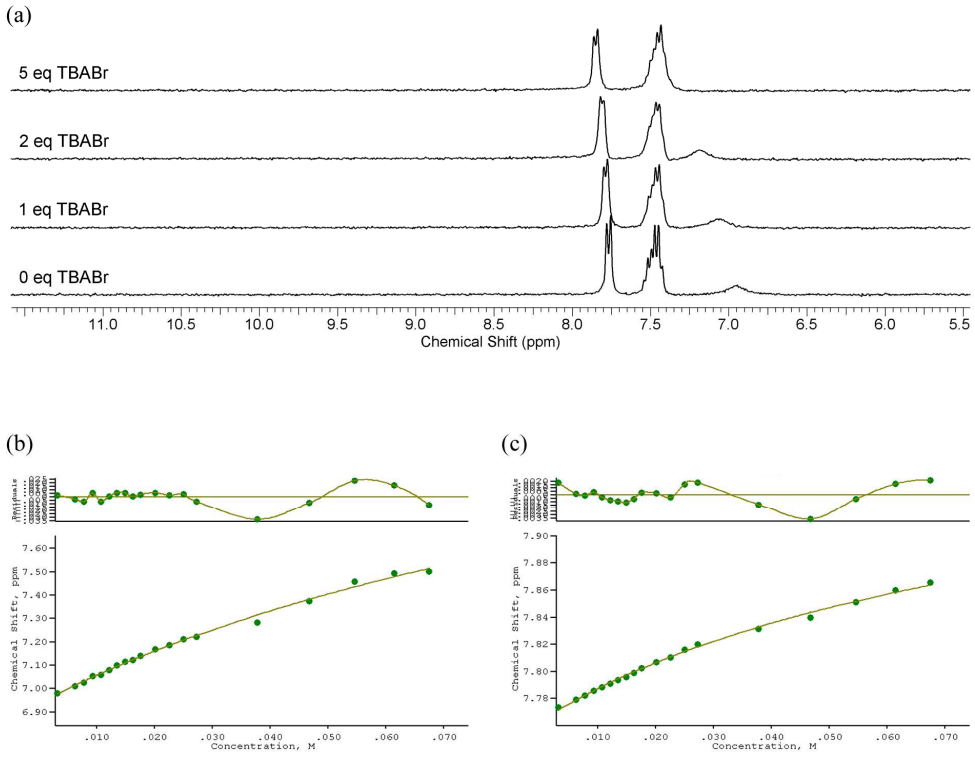

Figure S46. ^{1}H NMR titration of compound **6** with TBABr in CD_3CN at 298 K. Fit plots show chemical shift (ppm) versus anion concentration (M). (a) Stack plot. (b) Fit plot for NH proton at δ = 6.95 ppm. K_a = 8.3 M^{-1} (error 20%). (c) Fit plot for CH proton at δ = 7.77 ppm. K_a = 13.3 M^{-1} (error 11%).

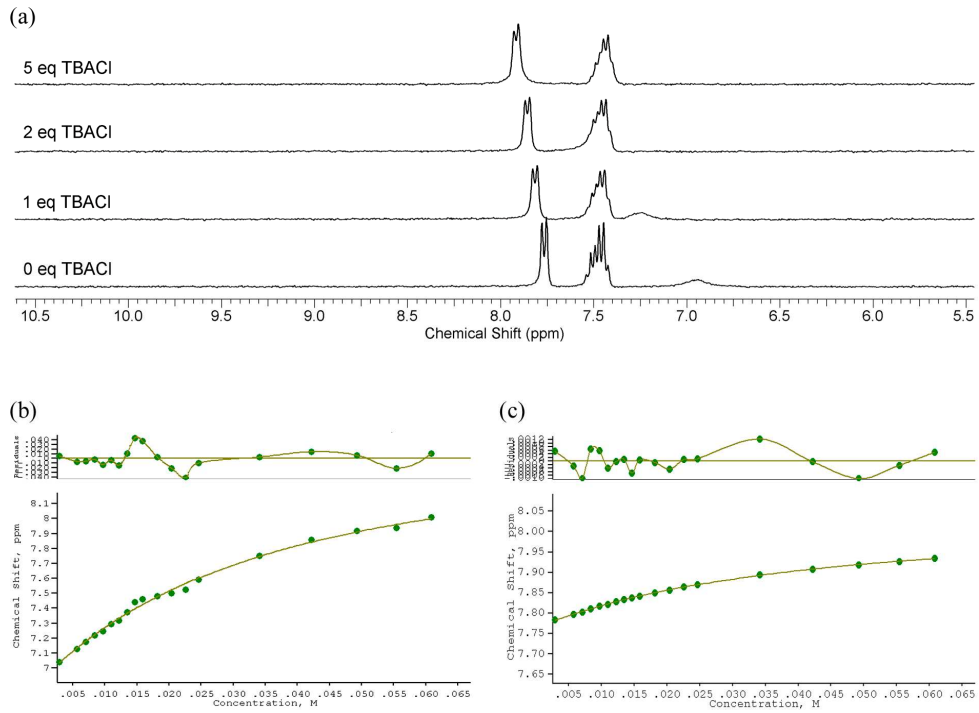

Figure S47. ^{1}H NMR titration of compound **6** with TBACl in CD_3CN at 298 K. Fit plots show chemical shift (ppm) versus anion concentration (M). (a) Stack plot. (b) Fit plot for NH proton at δ = 6.95 ppm. K_a = 36 M^{-1} (error 13%). (c) Fit plot for CH proton at δ = 7.77 ppm. K_a = 32 M^{-1} (error 4%).

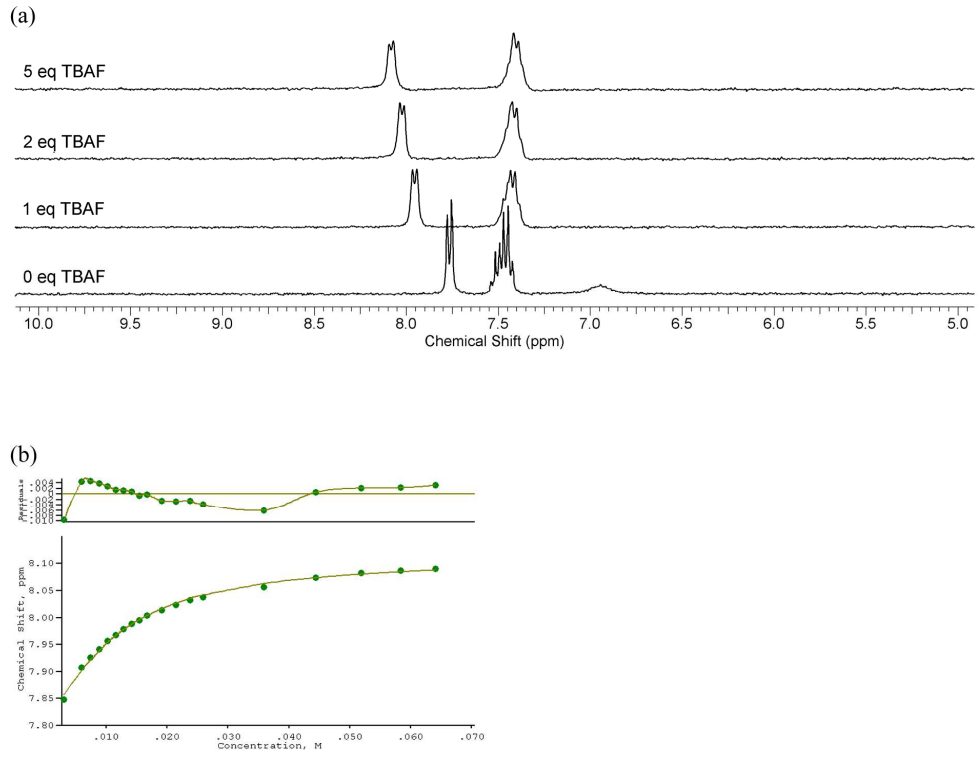

Figure S48. ^{1}H NMR titration of compound **6** with TBAF·$3H_2O$ in CD_3CN at 298 K. Fit plots show chemical shift (ppm) versus anion concentration (M). (a) Stack plot. (b) Fit plot for CH proton at δ = 7.77 ppm. K_a = 171 M^{-1} (error 6%).

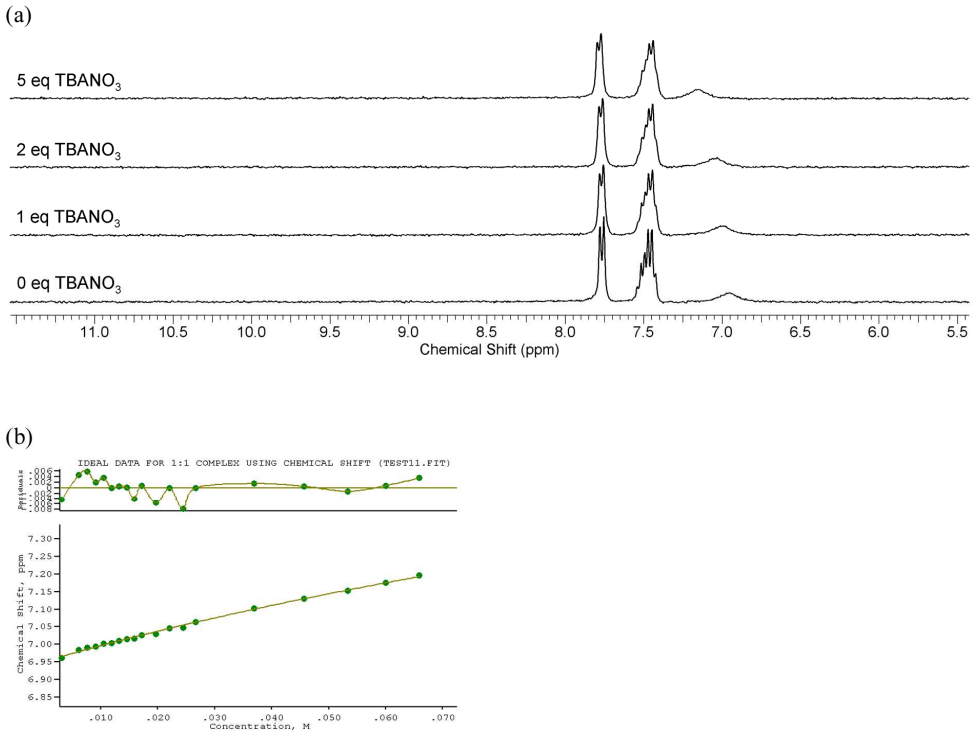

Figure S49. ^{1}H NMR titration of compound **6** with $TBANO_3$ in CD_3CN at 298 K. Fit plots show chemical shift (ppm) versus anion concentration (M). (a) Stack plot. (b) Fit plot for NH proton at δ = 6.95 ppm. K_a = 4.4 M^{-1} (error 25%).

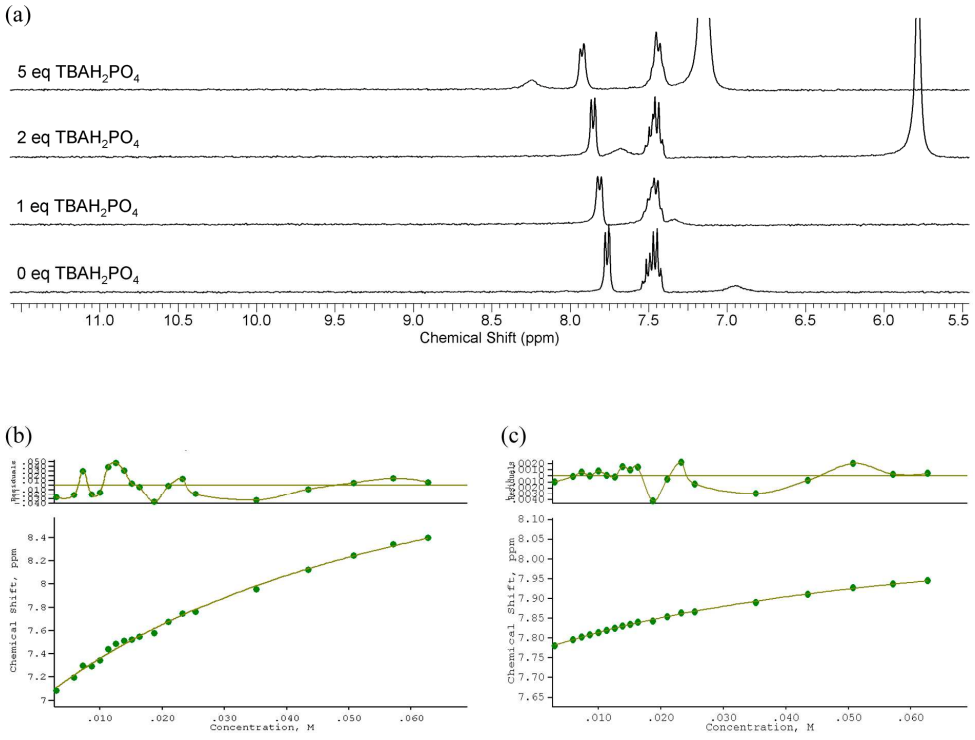

Figure S50. ^{1}H NMR titration of compound **6** with $TBAH_2PO_4$ in CD_3CN at 298 K. Fit plots show chemical shift (ppm) versus anion concentration (M). (a) Stack plot. (b) Fit plot for NH proton at δ = 6.95 ppm. K_a = 18.5 M^{-1} (error 16%). (b) Fit plot for CH proton at δ = 7.77 ppm. K_a = 18.7 M^{-1} (error 7%).

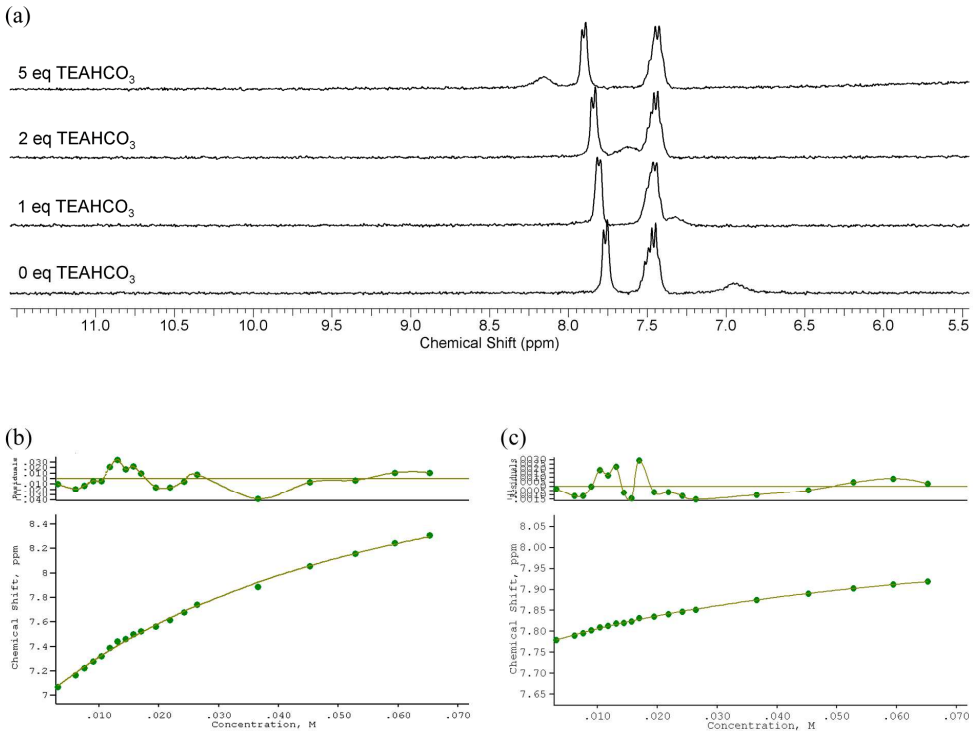

Figure S51. ^{1}H NMR titration of compound **6** with $TEAHCO_3$ in CD_3CN at 298 K. Fit plots show chemical shift (ppm) versus anion concentration (M). (a) Stack plot. (b) Fit plot for NH proton at δ = 6.95 ppm. K_a = 19.8 M^{-1} (error 11%). (b) Fit plot for CH proton at δ = 7.77 ppm. K_a = 18.1 M^{-1} (error 7%).

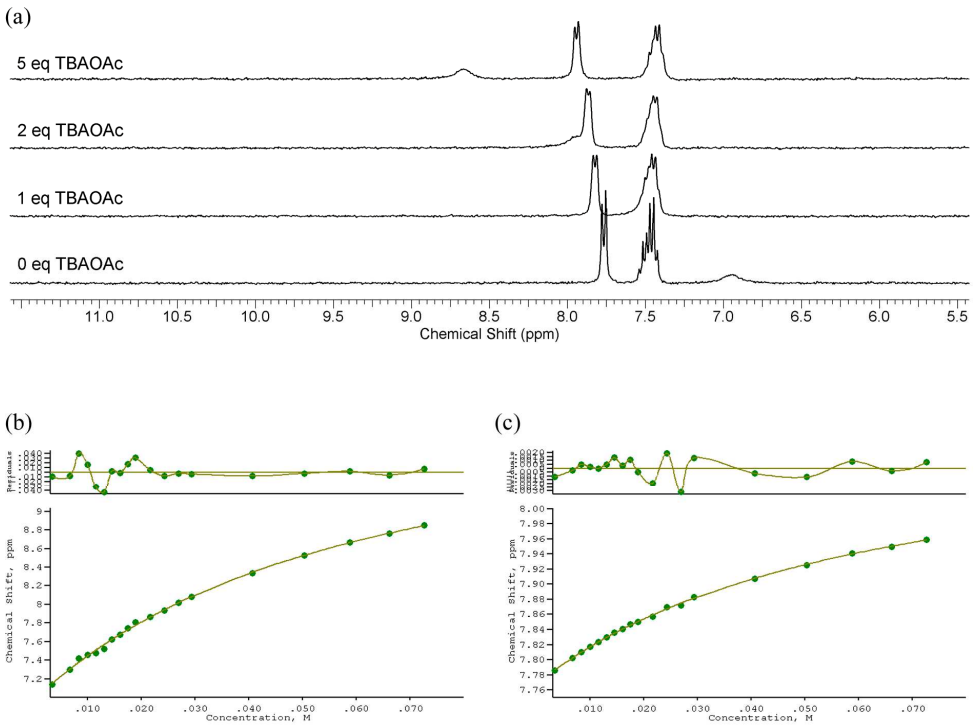

Figure S52. ^{1}H NMR titration of compound **6** with TBAOAc in CD_3CN at 298 K. Fit plots show chemical shift (ppm) versus anion concentration (M). (a) Stack plot. (b) Fit plot for NH proton at δ = 6.95 ppm. K_a = 197 M^{-1} (error 8%). (b) Fit plot for CH proton at δ = 7.77 ppm. K_a = 197 M^{-1} (error 5%).

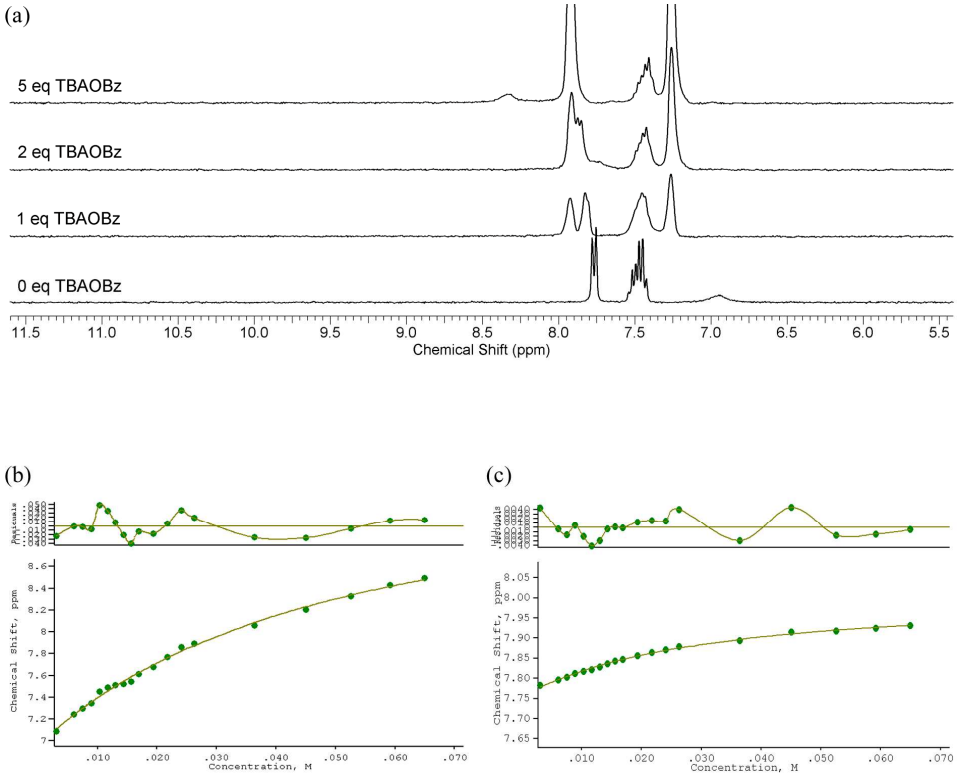

Figure S53. ^{1}H NMR titration of compound **6** with TBAOBz in CD_3CN at 298 K. Fit plots show chemical shift (ppm) versus anion concentration (M). (a) Stack plot. (b) Fit plot for NH proton at δ = 6.95 ppm. K_a =24.3 M^{-1} (error 12%). (c) Fit plot for CH proton at δ = 7.77 ppm. K_a = 44.7 M^{-1} (error 7%).

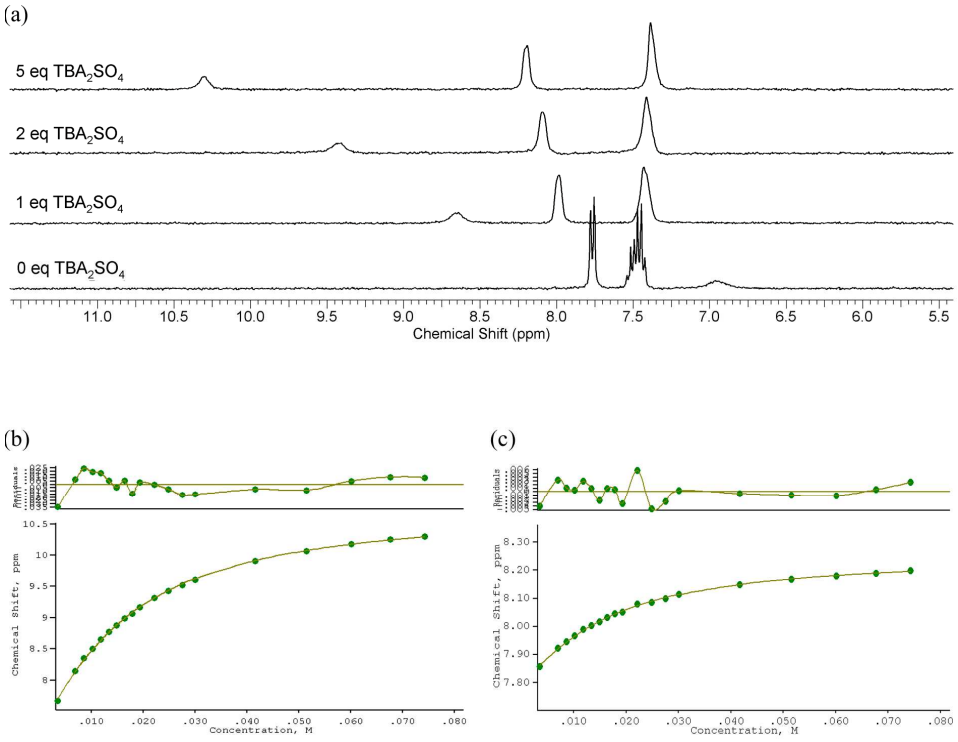

Figure S54. ^{1}H NMR titration of compound **6** with TBA_2SO_4 in CD_3CN at 298 K. Fit plots show chemical shift (ppm) versus anion concentration (M). (a) Stack plot. (b) Fit plot for NH proton at δ = 6.95 ppm. K_a =91 M^{-1} (error 3%). (c) Fit plot for CH proton at δ = 7.77 ppm. K_a = 99 M^{-1} (error 4%).

S3.3. Comparison with TBAOH – deprotonation or anion binding

Initially, to determine whether the addition of anions leads to deprotonation of the receptor or to anion binding, ^{1}H NMR titration with the strong base TBAOH were performed by the addition of aliquots of a 1M TBAOH solution in methanol to a 10 mM CD_3CN solution of the receptor. Aliquots were added to obtain 0, 0.5, 1, 1.5, 2, 3 and 5 equivalents of TBAOH. The results are shown in the stack plots in Figures S55-S60.

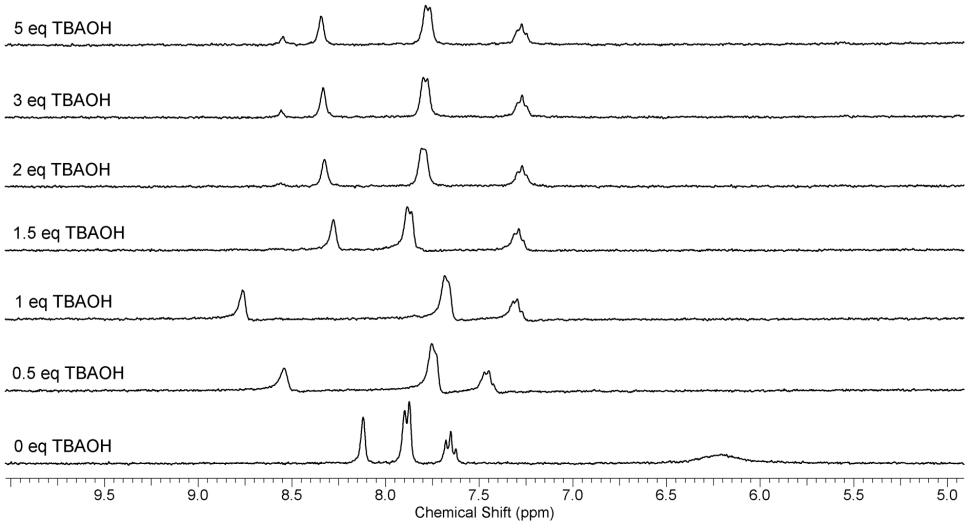

Figure S55. Stack plot of the ^{1}H NMR titration of compound **1** with TBAOH (1M in MeOH) in CD_3CN at 298 K.

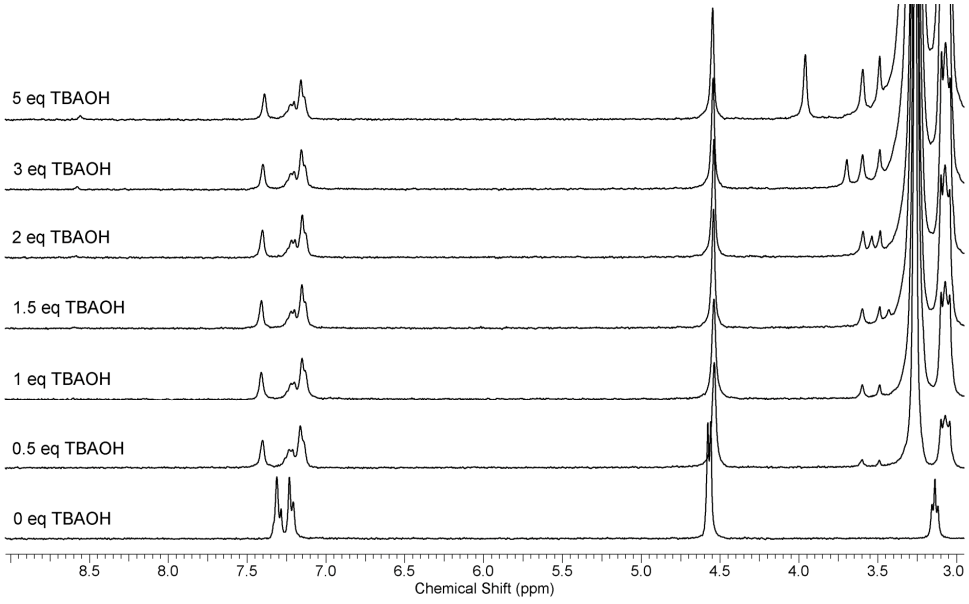

Figure S56. Stack plot of the ^{1}H NMR titration of compound **2** with TBAOH (1M in MeOH) in CD_3CN at 298 K.

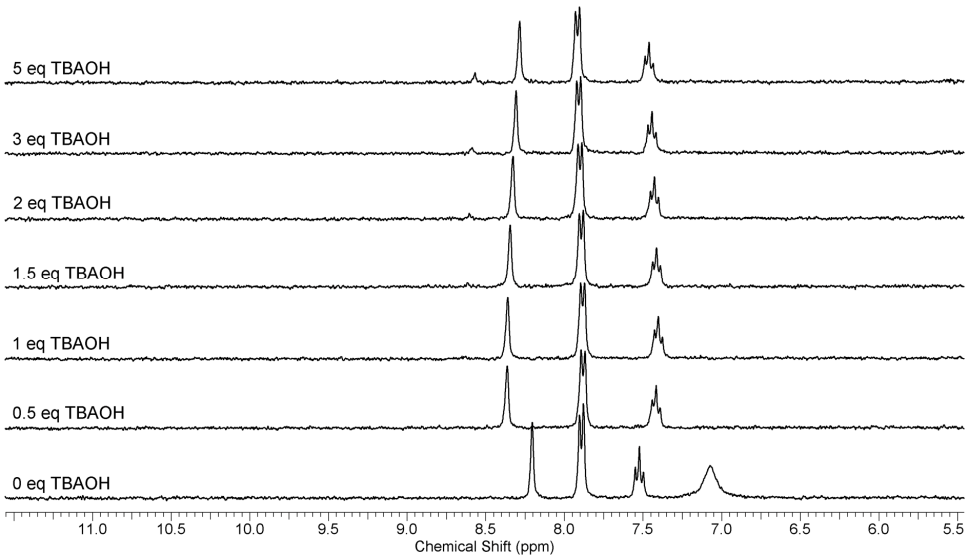

Figure S57. Stack plot of the ^{1}H NMR titration of compound **3** with TBAOH (1M in MeOH) in CD_3CN at 298 K.

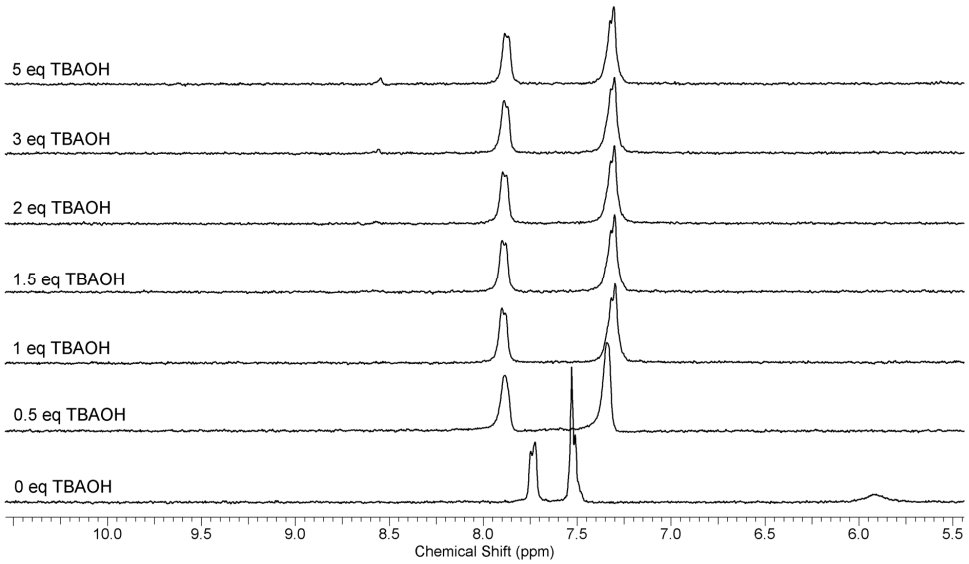

Figure S58. Stack plot of the ^{1}H NMR titration of compound **4** with TBAOH (1M in MeOH) in CD_3CN at 298 K.

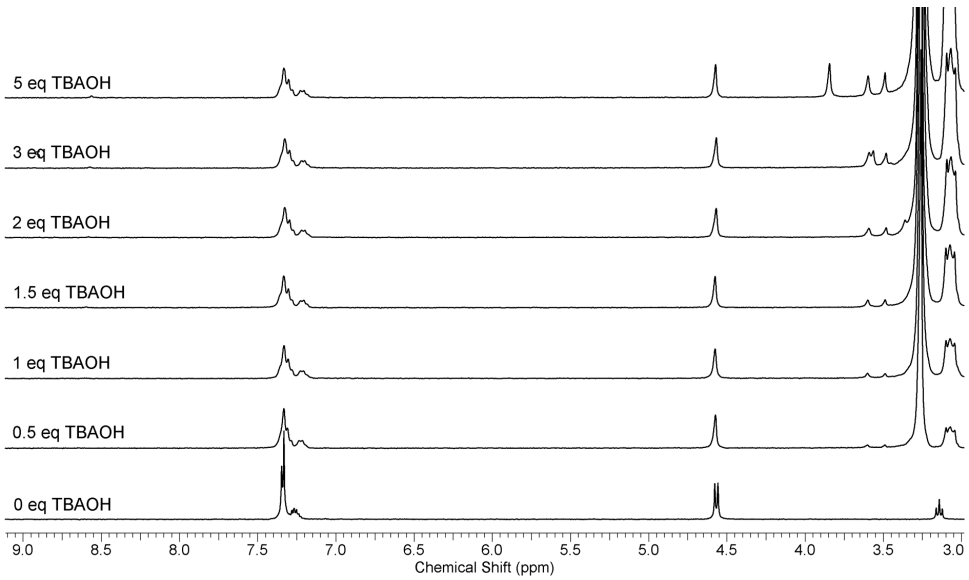

Figure S59. Stack plot of the ^{1}H NMR titration of compound **5** with TBAOH (1M in MeOH) in CD_3CN at 298 K.

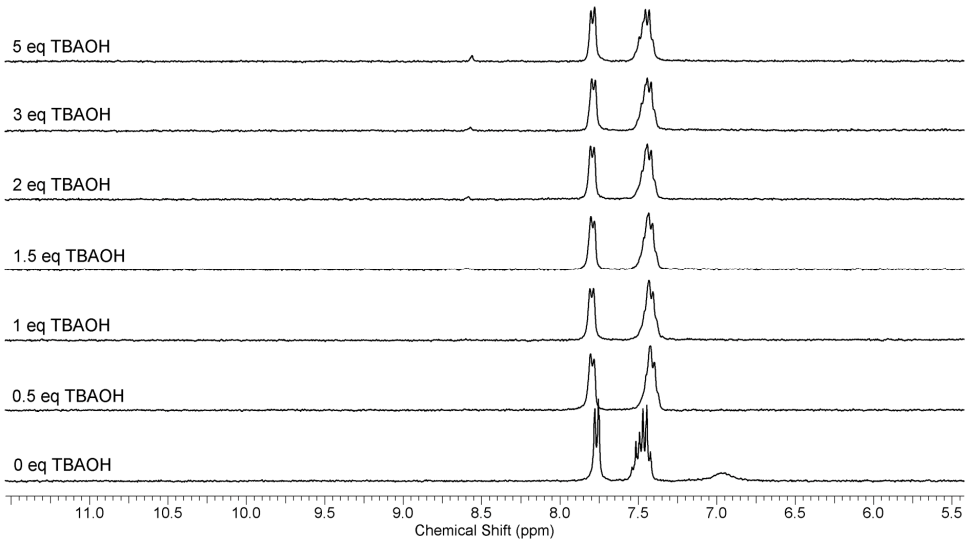

Figure S60. Stack plot of the ^{1}H NMR titration of compound **6** with TBAOH (1M in MeOH) in CD_3CN at 298 K.

An initial visual comparison between the ^{1}H NMR spectra obtained during the addition TBA salts and TBAOH was obtained by preparing stacked plots (Figures S61-S66). These indicate that TBAF and $TEAHCO_3$ can deprotonate the fluorinated alcohols **1** and **4**, but no deprotonation is expected for any other combination of anion salt/receptor.

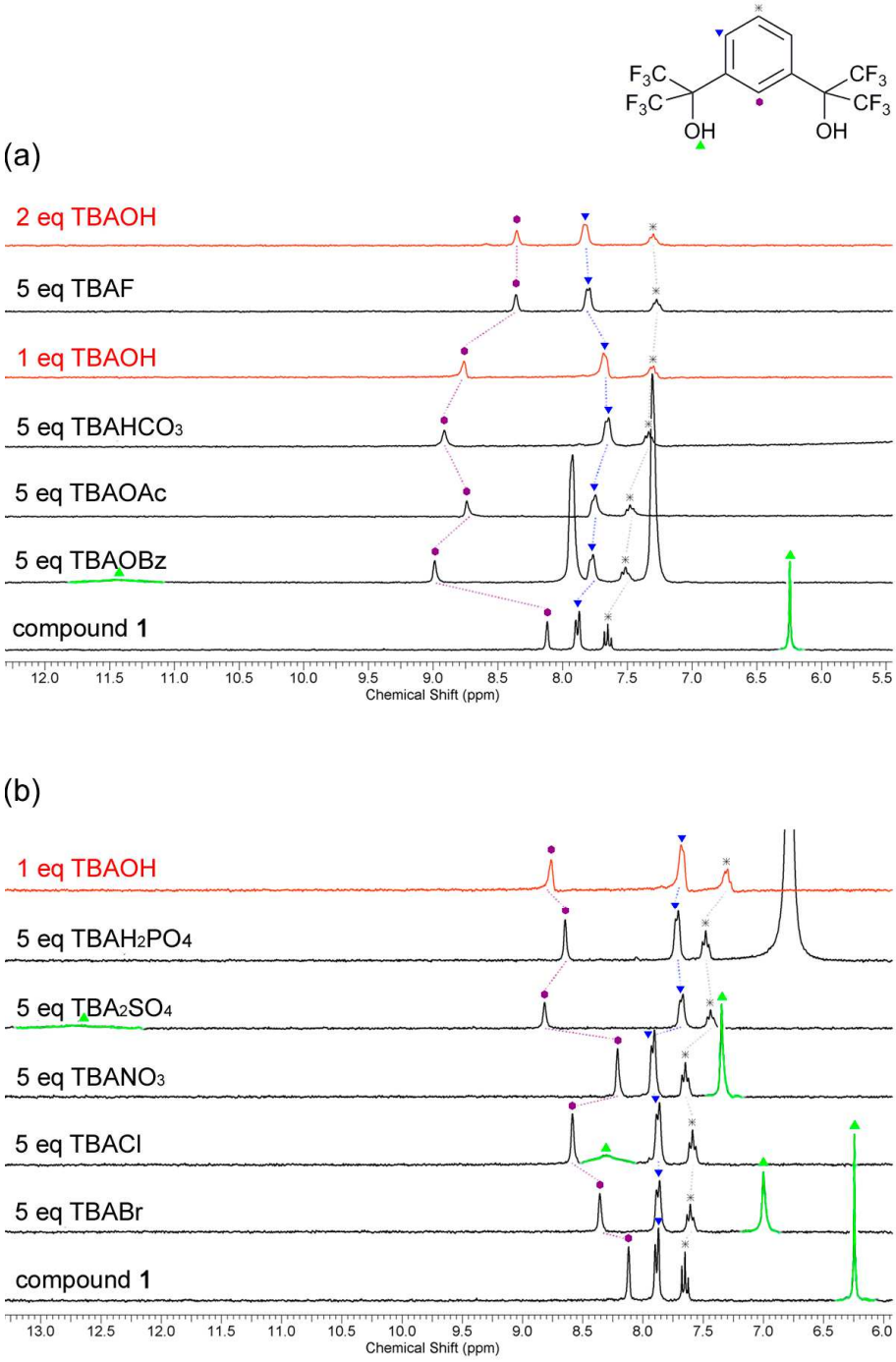

Figure S61. Comparison between the changes in chemical shifts of receptor **1** upon the addition of excess anion or strong base (TBAOH) in CD_3CN at 298 K. The OH signal is shown in green and all other aromatic CH signals are assigned as shown in the top right corner. (a) Comparison for the strongly basic anions F^-, HCO_3^-, OAc^-, OBz^-; (b) Comparison for the weaker basic anions $H_2PO_4^-$, SO_4^{2-}, NO_3^-, Cl^- and Br^-.

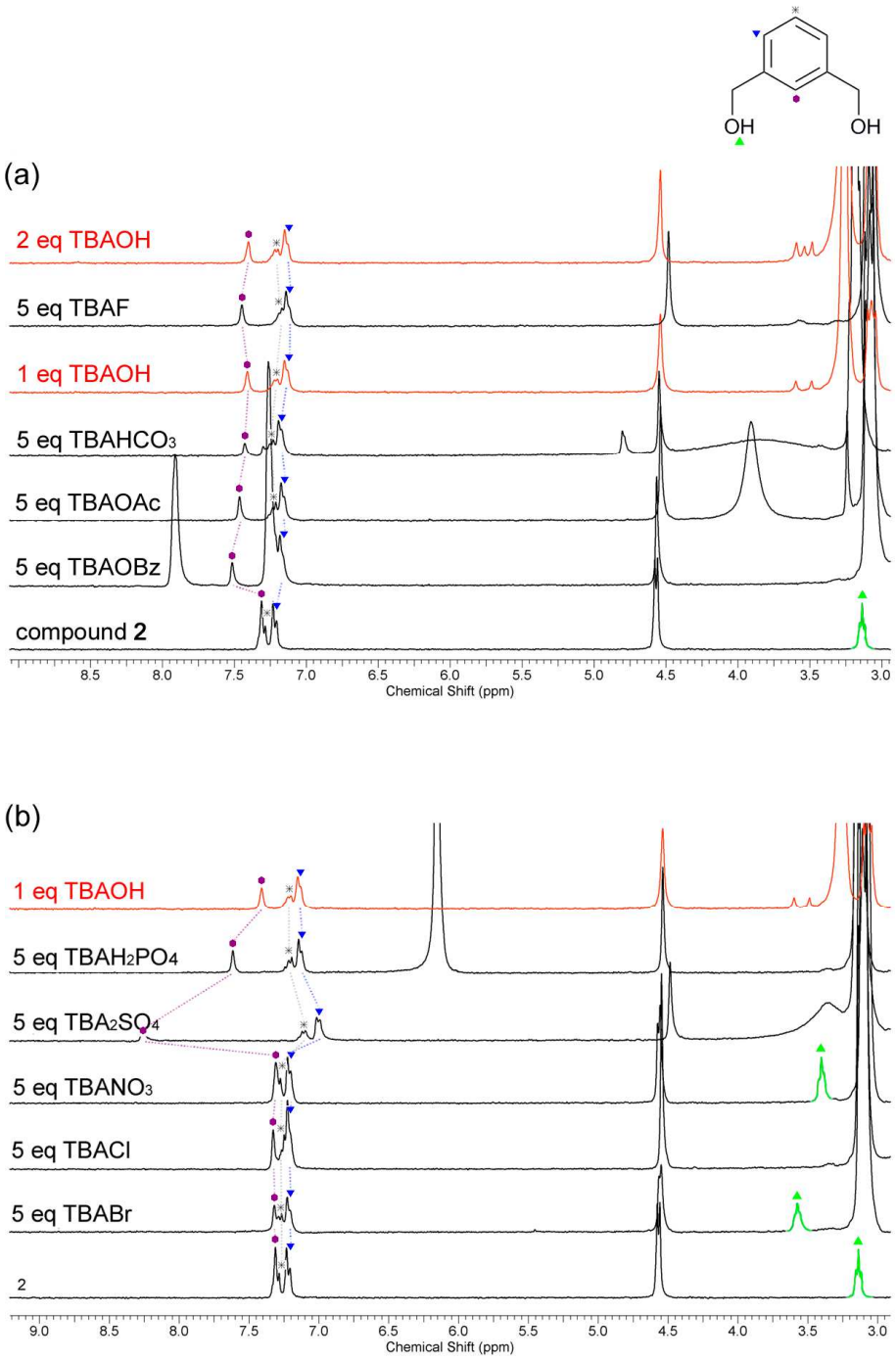

Figure S62. Comparison between the changes in chemical shifts of receptor **2** upon the addition of excess anion or strong base (TBAOH) in CD_3CN at 298 K. The OH signal is shown in green and all other aromatic CH signals are assigned as shown in the top right corner. (a) Comparison for the strongly basic anions F^-, HCO_3^-, OAc^-, OBz^-; (b) Comparison for the weaker basic anions $H_2PO_4^-$, SO_4^{2-}, NO_3^-, Cl^- and Br^-.

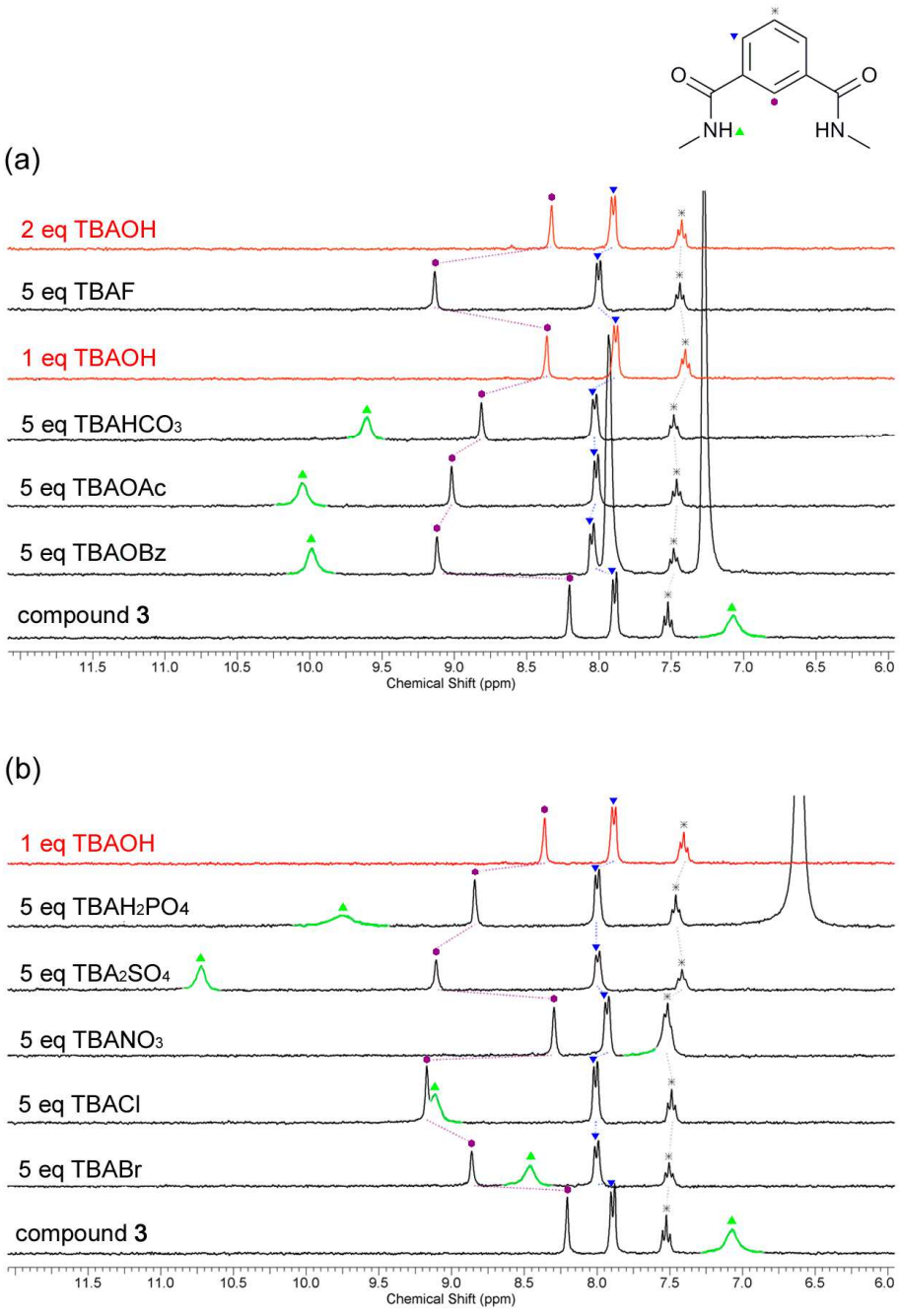

Figure S63. Comparison between the changes in chemical shifts of receptor **3** upon the addition of excess anion or strong base (TBAOH) in CD_3CN at 298 K. The NH signal is shown in green and all other aromatic CH signals are assigned as shown in the top right corner. (a) Comparison for the strongly basic anions F^-, HCO_3^-, OAc^-, OBz^-; (b) Comparison for the weaker basic anions $H_2PO_4^-$, SO_4^{2-}, NO_3^-, Cl^- and Br^-.

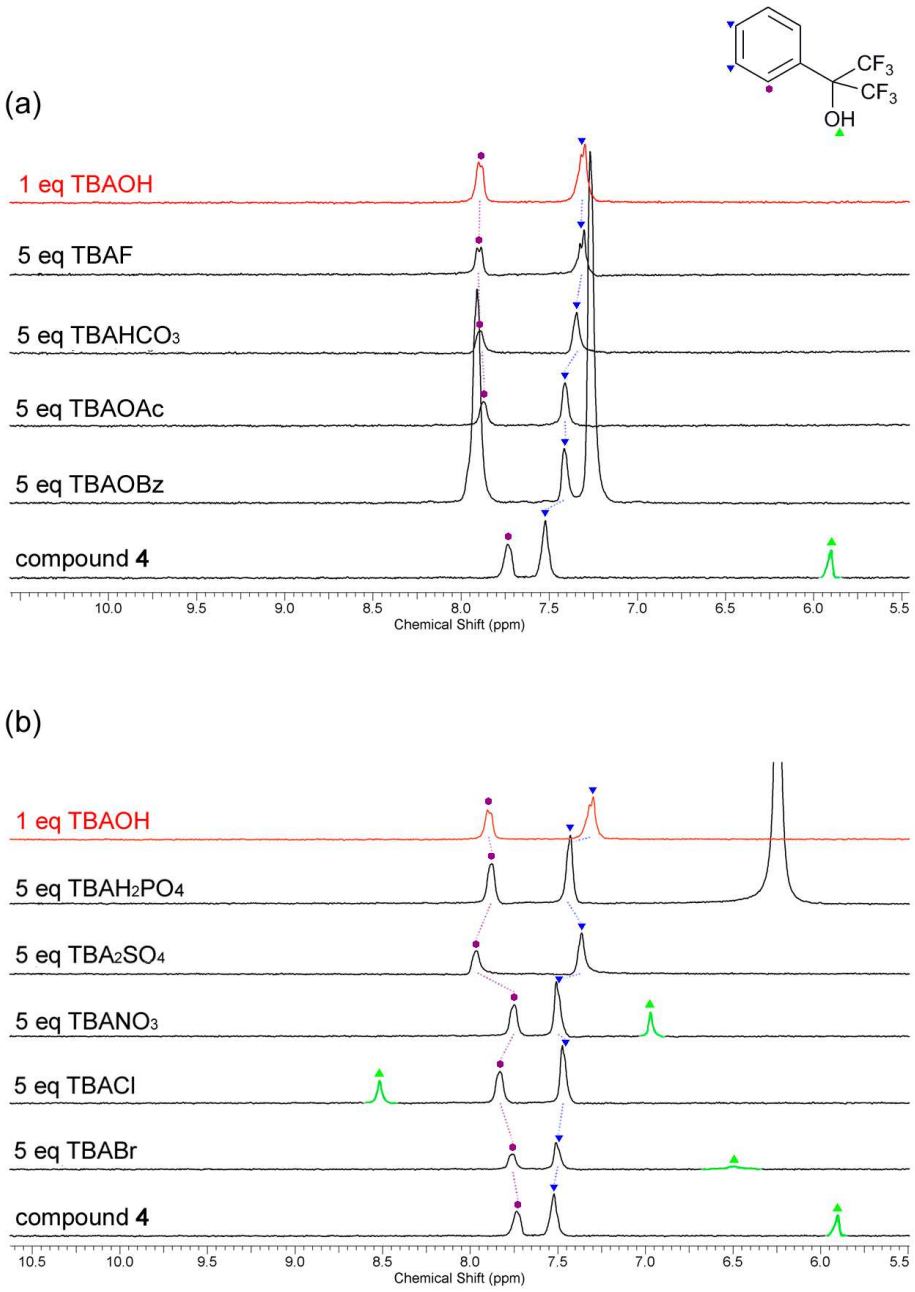

Figure S64. Comparison between the changes in chemical shifts of receptor **4** upon the addition of excess anion or strong base (TBAOH) in CD_3CN at 298 K. The OH signal is shown in green and all other aromatic CH signals are assigned as shown in the top right corner. (a) Comparison for the strongly basic anions F^-, HCO_3^-, OAc^-, OBz^-; (b) Comparison for the weaker basic anions $H_2PO_4^-$, SO_4^{2-}, NO_3^-, Cl^- and Br^-.

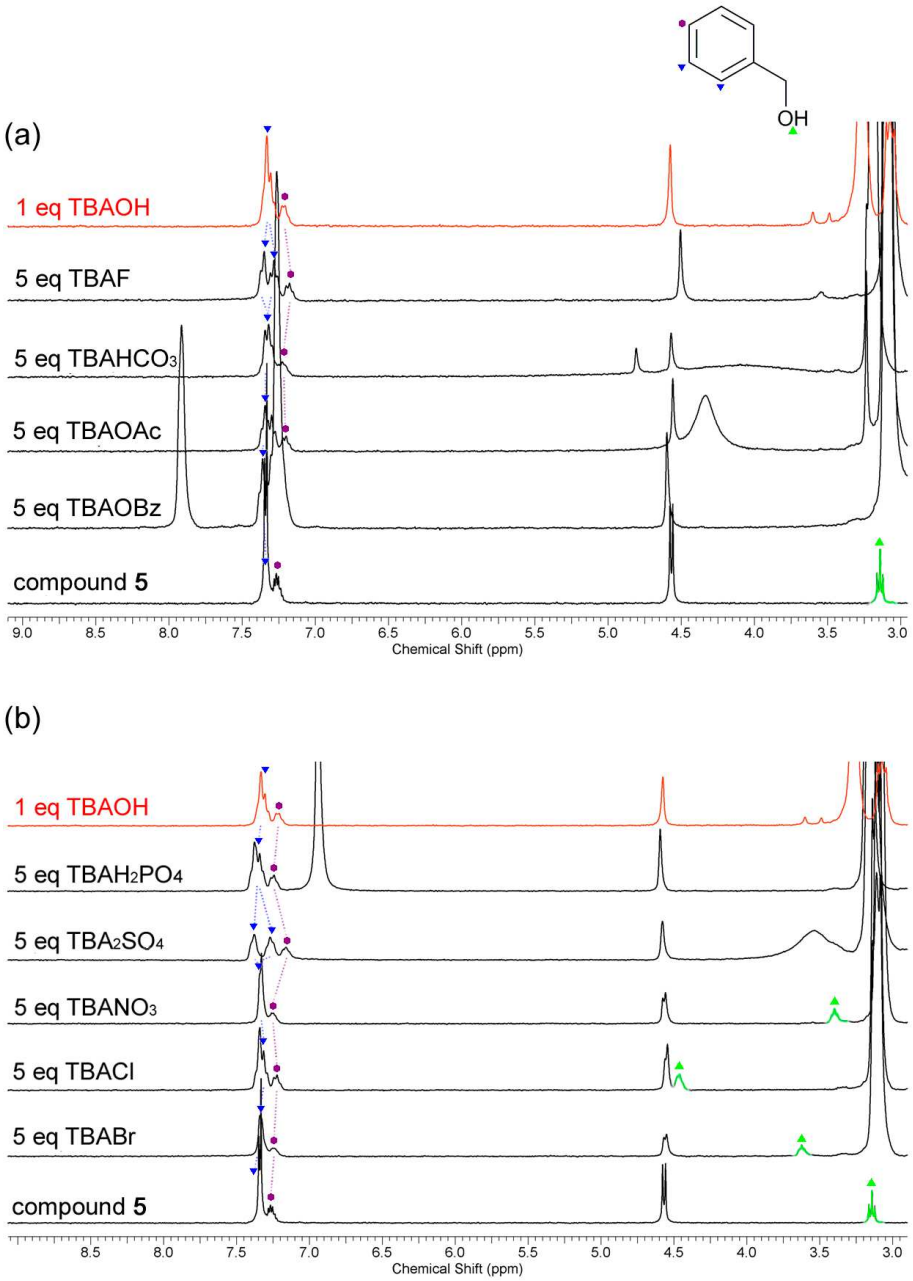

Figure S65. Comparison between the changes in chemical shifts of receptor **5** upon the addition of excess anion or strong base (TBAOH) in CD_3CN at 298 K. The OH signal is shown in green and all other aromatic CH signals are assigned as shown in the top right corner. (a) Comparison for the strongly basic anions F^-, HCO_3^-, OAc^-, OBz^-; (b) Comparison for the weaker basic anions $H_2PO_4^-$, SO_4^{2-}, NO_3^-, Cl^- and Br^-.

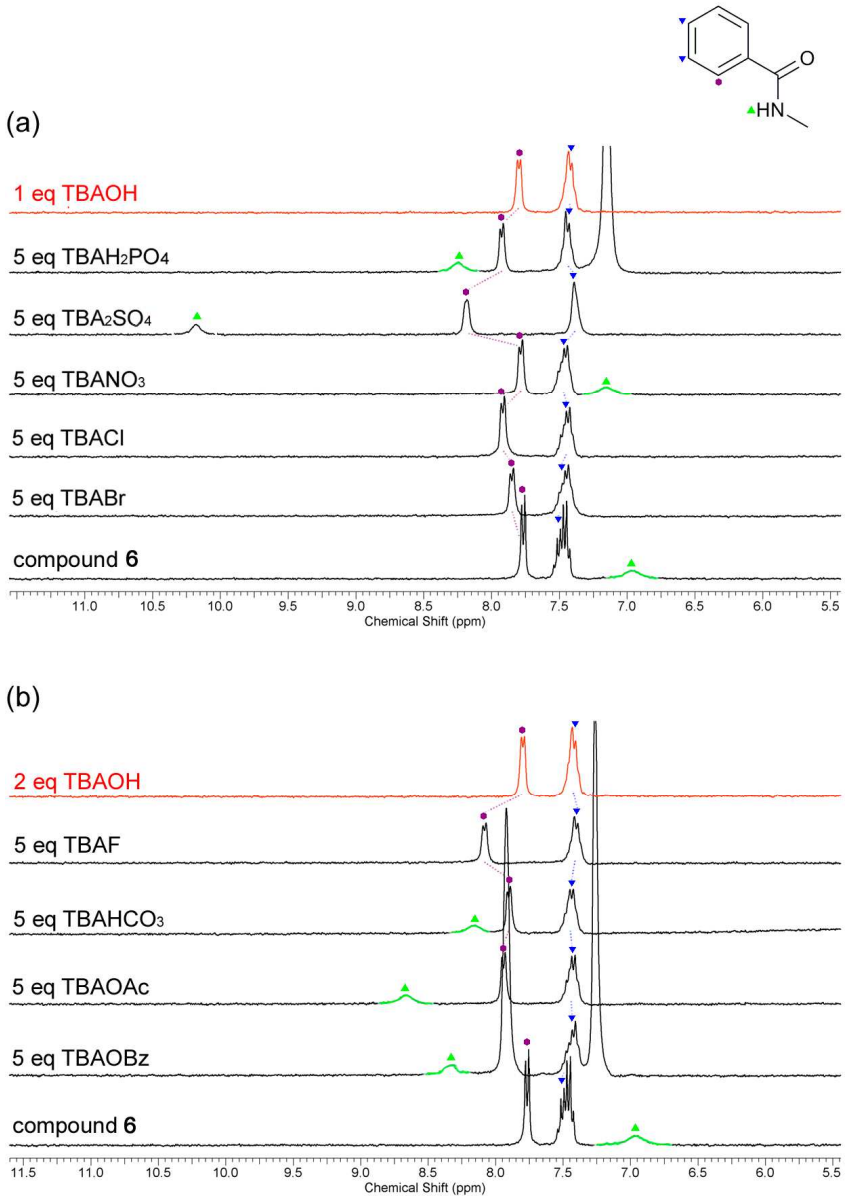

Figure S66. Comparison between the changes in chemical shifts of receptor **6** upon the addition of excess anion or strong base (TBAOH) in CD_3CN at 298 K. The NH signal is shown in green and all other CH peaks have been assigned as shown in the top right corner. (a) Comparison for the strongly basic anions F^-, HCO_3^-, OAc^-, OBz^-; (b) Comparison for the weaker basic anions $H_2PO_4^-$, SO_4^{2-}, NO_3^-, Cl^- and Br^-.

In order to be more certain whether some anion deprotonate the receptors or not, plots were made showing the change in chemical shift upon the addition of anion or TBAOH for each CH signal in the ^{1}H NMR spectra. Deprotonation is the most likely event if two requirements are met: (1) complete dissapearance of the OH or NH signal upon the addition of anion; (2) the changes in chemical shift of all CH signals are similar for the addition of anion and base (TBAOH). An overview is given in figures S67-S72 and confirm that receptor **1** is deprotonated by TBAF and $TEAHCO_3$, with a double deprotonation of **1** upon the addition of TBAF. Receptor **4** seems to be deprotonated by TBAF (and possibly also $TEAHCO_3$).

(a)

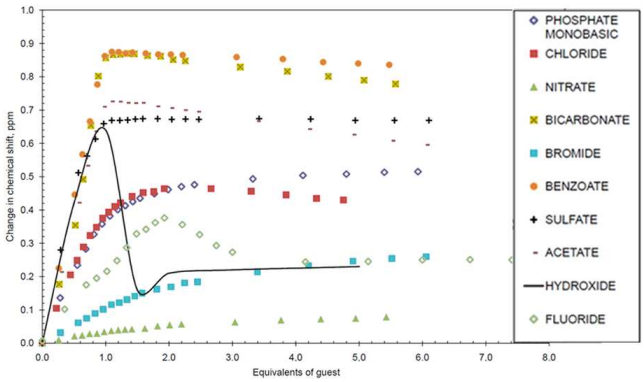

(b)

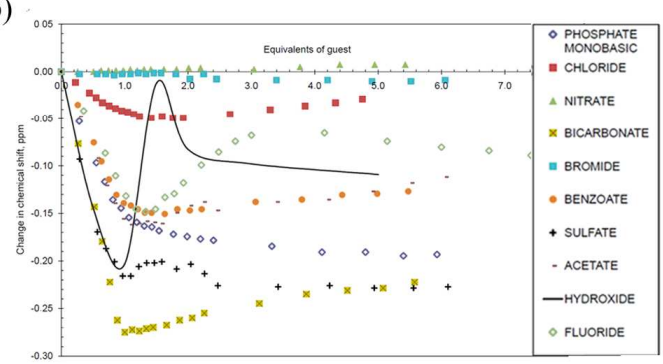

(c)

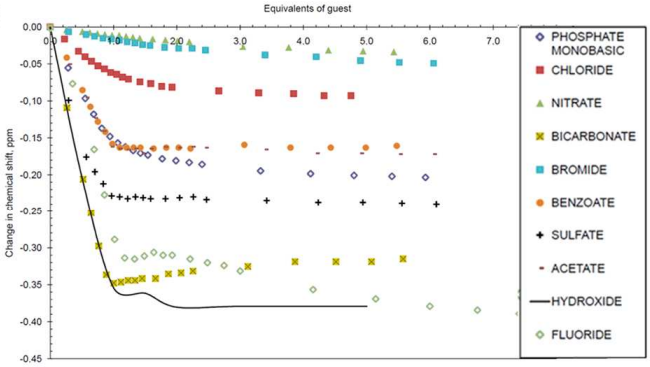

(d)

Anion	NH/OH disappears	CH1 same anion/base	CH2 same anion/base	CH3 same anion/base	Conclusion
F^-	✓	✓	?	✓	Deprotonation
Cl^-	×	×	×	×	Binding
Br^-	×	×	×	×	Binding
NO_3^-	×	×	×	×	Binding
$H_2PO_4^-$	✓	×	?	×	Binding
HCO_3^-	✓	?	?	✓	Deprotonation
OAc^-	✓	✓	?	×	Binding
OBz^-	×	×	?	×	Binding
SO_4^{2-}	×	✓	?	×	Binding

Figure S67. Comparison of the change in chemical shift of receptor **1** upon the addition of anion (TBA or TEA salts) and base (TBAOH) in CD_3CN at 298 K. (a) Change in chemical shift for CH proton at δ = 8.11 ppm. (b) Change in chemical shift for CH proton at δ = 7.87 ppm. (c) Change in chemical shift for CH proton at δ = 7.65 ppm. (d) Overview of the comparison between anion binding and deprotonation, including whether the OH signal disappears or not and whether the change in chemical shift for the CH signal is similar for the addition of anion and base.

(a)

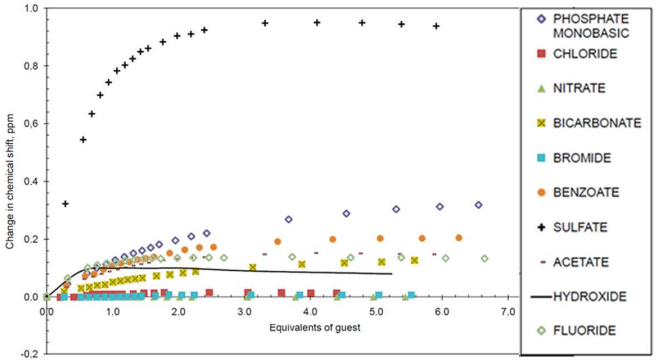

(b)

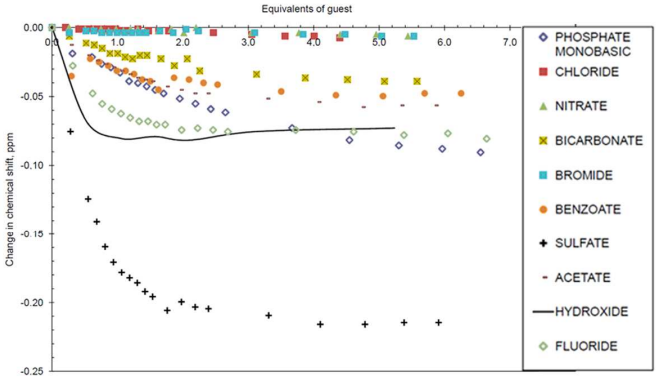

(c)

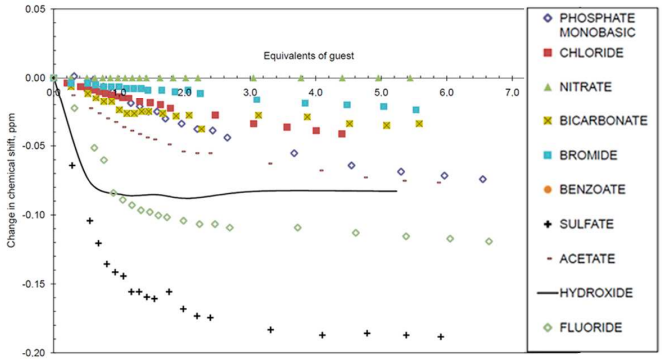

(d)

Anion	NH/OH disappears	CH1 same anion/base	CH2 same anion/base	CH3 same anion/base	Conclusion
F^-	✓	?	?	×	Binding
Cl^-	✓	×	×	×	Binding
Br^-	×	×	×	×	Binding
NO_3^-	×	×	×	×	Binding
$H_2PO_4^-$	✓	×	×	×	Binding
HCO_3^-	✓	?	×	×	Binding
OAc^-	✓	?	×	?	Binding
OBz^-	✓	×	×	overlap	Binding
SO_4^{2-}	✓	×	×	×	Binding

Figure S68. Comparison of the change in chemical shift of receptor **2** upon the addition of anion (TBA or TEA salts) and base (TBAOH) in CD_3CN at 298 K. (a) Change in chemical shift for CH proton at δ = 7.31 ppm. (b) Change in chemical shift for CH proton at δ = 7.23 ppm. (c) Change in chemical shift for CH proton at δ = 7.28 ppm. (d) Overview of the comparison between anion binding and deprotonation, including whether the OH signal disappears or not and whether the change in chemical shift for the CH signal is similar for the addition of anion and base.

(a)

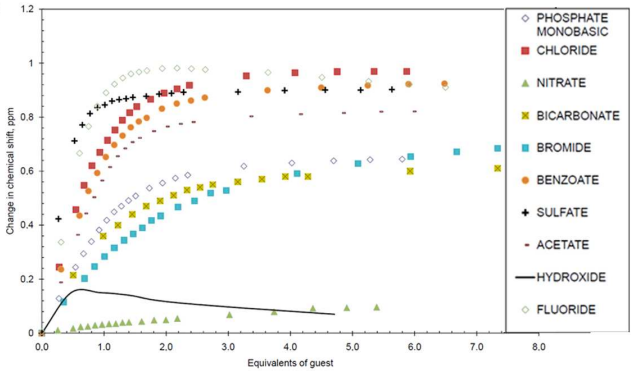

(b)

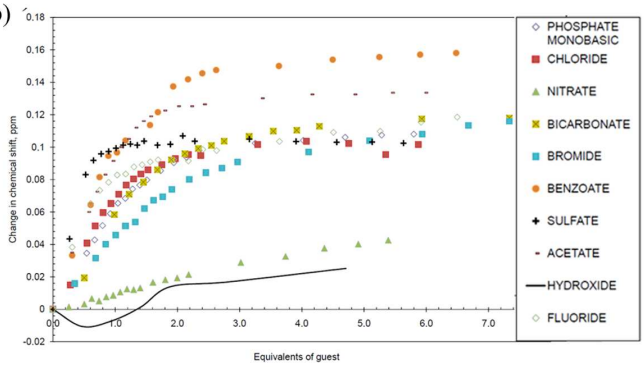

(c)

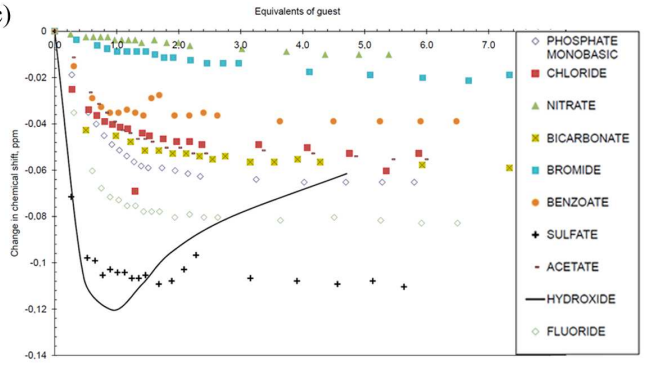

(d)

Anion	NH/OH disappears	CH1 same anion/base	CH2 same anion/base	CH3 same anion/base	Conclusion
F^-	✓	×	×	×	Binding
Cl^-	×	×	×	×	Binding
Br^-	×	×	×	×	Binding
NO_3^-	×	×	×	×	Binding
$H_2PO_4^-$	×	×	×	×	Binding
HCO_3^-	×	×	×	×	Binding
OAc^-	×	×	×	×	Binding
OBz^-	×	×	×	×	Binding
SO_4^{2-}	×	×	×	?	Binding

Figure S69. Comparison of the change in chemical shift of receptor **3** upon the addition of anion (TBA or TEA salts) and base (TBAOH) in CD_3CN at 298 K. (a) Change in chemical shift for CH proton at δ = 8.20 ppm. (b) Change in chemical shift for CH proton at δ = 7.89 ppm. (c) Change in chemical shift for CH proton at δ = 7.52 ppm. (d) Overview of the comparison between anion binding and deprotonation, including whether the OH signal disappears or not and whether the change in chemical shift for the CH signal is similar for the addition of anion and base.

(a)

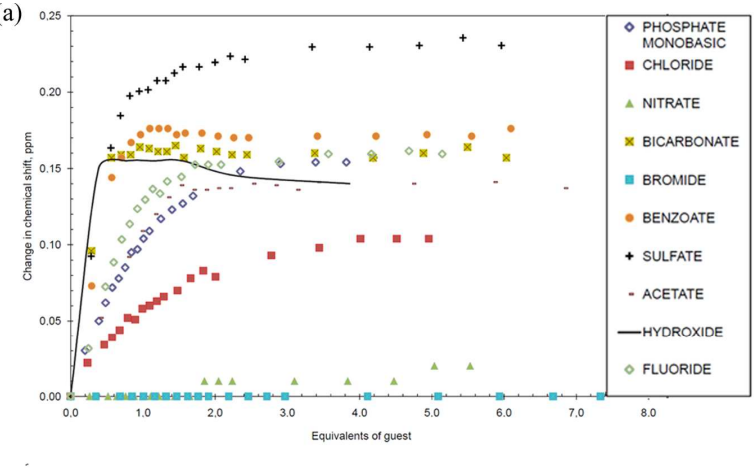

(b)

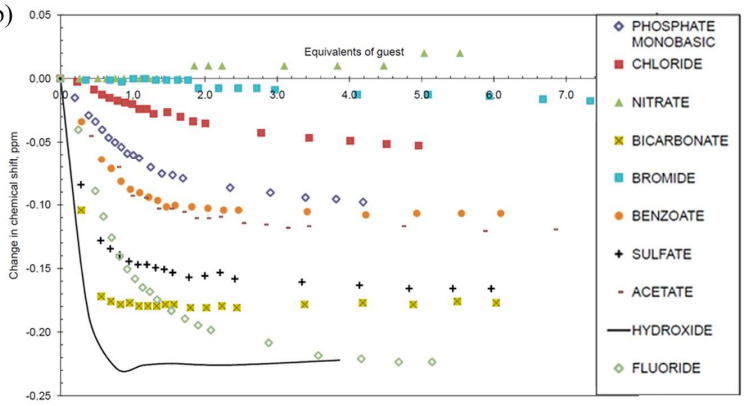

(c)

Anion	NH/OH disappears	CH1 same anion/base	CH2 same anion/base	Conclusion
F^-	✓	✓	✓	Deprotonation
Cl^-	×	×	×	Binding
Br^-	×	×	×	Binding
NO_3^-	×	×	×	Binding
$H_2PO_4^-$	✓	✓	×	Binding
HCO_3^-	✓	✓	×	Binding?
OAc^-	✓	✓	×	Binding
OBz^-	✓	✓	×	Binding
SO_4^{2-}	✓	×	×	Binding

Figure S70. Comparison of the change in chemical shift of receptor **4** upon the addition of anion (TBA or TEA salts) and base (TBAOH) in CD_3CN at 298 K. (a) Change in chemical shift for CH proton at δ = 7.73 ppm. (b) Change in chemical shift for CH proton at δ = 7.52 ppm. (c) Overview of the comparison between anion binding and deprotonation, including whether the OH signal disappears or not and whether the change in chemical shift for the CH signal is similar for the addition of anion and base.

(a)

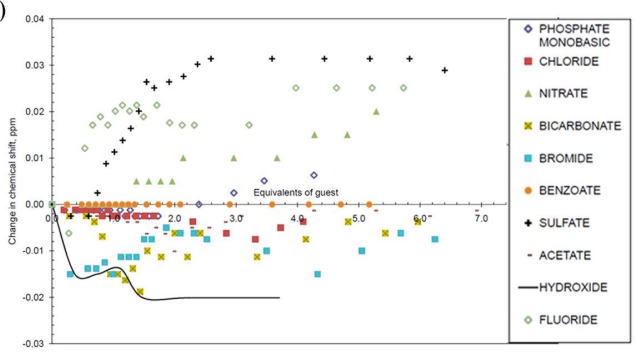

(b)

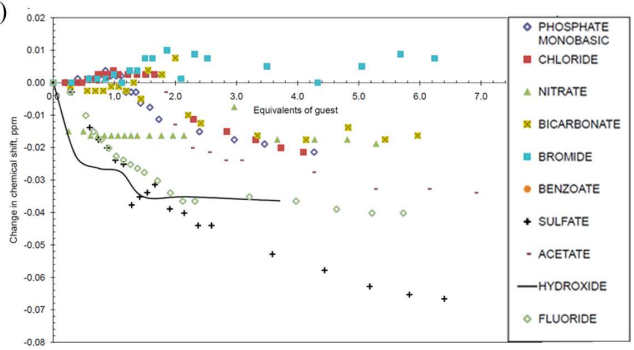

(c)

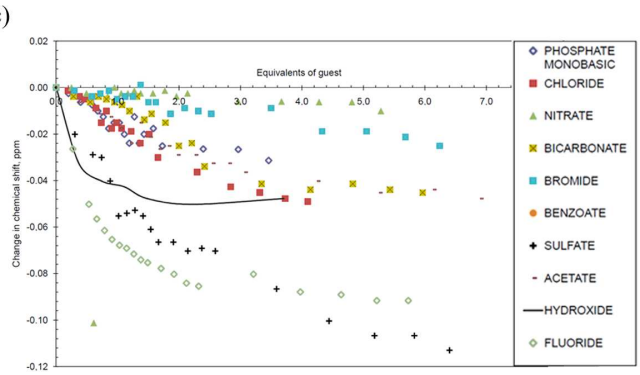

(d)

Anion	NH/OH disappears	CH1 same anion/base	CH2 same anion/base	CH3 same anion/base	Conclusion
F^-	✓	×	×	?	Binding
Cl^-	×	×	×	×	Binding
Br^-	×	?	×	×	Binding
NO_3^-	×	×	×	×	Binding
$H_2PO_4^-$	✓	×	×	×	Binding
HCO_3^-	✓	?	?	×	Binding
OAc^-	✓	×	?	×	Binding
OBz^-	✓	overlap	overlap	overlap	/
SO_4^{2-}	✓	×	×	×	Binding

Figure S71. Comparison of the change in chemical shift of receptor **5** upon the addition of anion (TBA or TEA salts) and base (TBAOH) in CD_3CN at 298 K. (a) Change in chemical shift for CH proton at δ = 7.35 ppm. (b) Change in chemical shift for CH proton at δ = 7.33 ppm. (c) Change in chemical shift for CH proton at δ = 7.27 ppm. (d) Overview of the comparison between anion binding and deprotonation, including whether the OH signal disappears or not and whether the change in chemical shift for the CH signal is similar for the addition of anion and base.

(a)

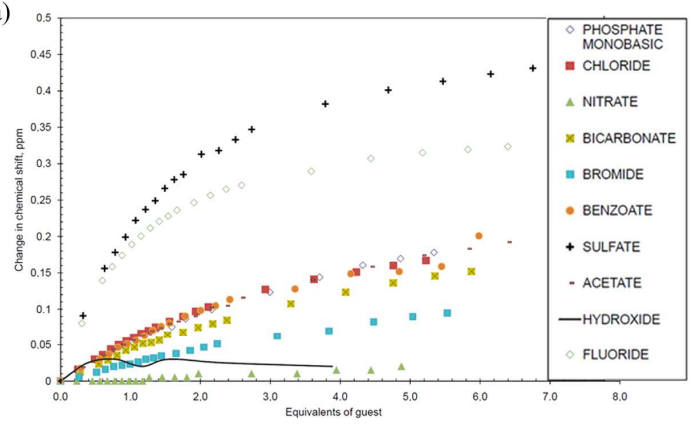

(b)

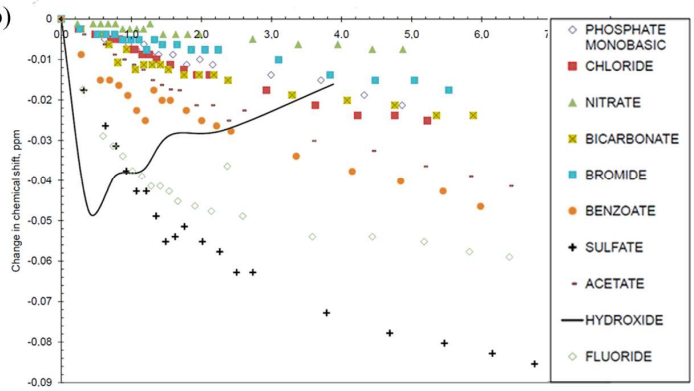

(c)

Anion	NH/OH disappears	CH1 same anion/base	CH2 same anion/base	Conclusion
F^-	✓	×	×	Binding
Cl^-	×	×	×	Binding
Br^-	×	×	×	Binding
NO_3^-	×	×	×	Binding
$H_2PO_4^-$	×	×	×	Binding
HCO_3^-	×	×	×	Binding
OAc^-	×	×	×	Binding
OBz^-	×	×	×	Binding
SO_4^{2-}	×	×	×	Binding

Figure S72. Comparison of the change in chemical shift of receptor **6** upon the addition of anion (TBA or TEA salts) and base (TBAOH) in CD_3CN at 298 K. (a) Change in chemical shift for CH proton at δ = 7.77 ppm. (b) Change in chemical shift for CH proton at δ = 7.47 ppm. (c) Overview of the comparison between anion binding and deprotonation, including whether the OH signal disappears or not and whether the change in chemical shift for the CH signal is similar for the addition of anion and base.

S4. MASS SPECTROSCOPY BINDING STUDY

Samples were prepared by dissolving receptor **1** in HPLC-grade acetonitrile (10 ug/mL), followed by the addition of 5 equivalents of TBA chloride or TBA fluoride. Samples were analysed using a MaXis (Bruker Daltonics, Bremen, Germany) mass spectrometer equipped with a Time of Flight (TOF) analyser. High resolution mass spectra were recorded using negative ion electrospray ionisation. The results are shown in Figure S73 for TBA fluoride (showing deprotonation by fluoride and no complex formation) and Figure S74 for TBA chloride (showing both 1:1 and 2:2 complex formation).

Acquisition Parameter					
Source Type	ESI	Ion Polarity	Negative	Set Nebulizer	2.0 Bar
Focus	Not active	Set Capillary	2000 V	Set Dry Heater	200 °C
Scan Begin	120 m/z	Set End Plate Offset	-500 V	Set Dry Gas	8.0 l/min
Scan End	1500 m/z	Set Collision Cell RF	300.0 Vpp	Set Divert Valve	Waste

-MS, 0.6-0.7min #(37-39)

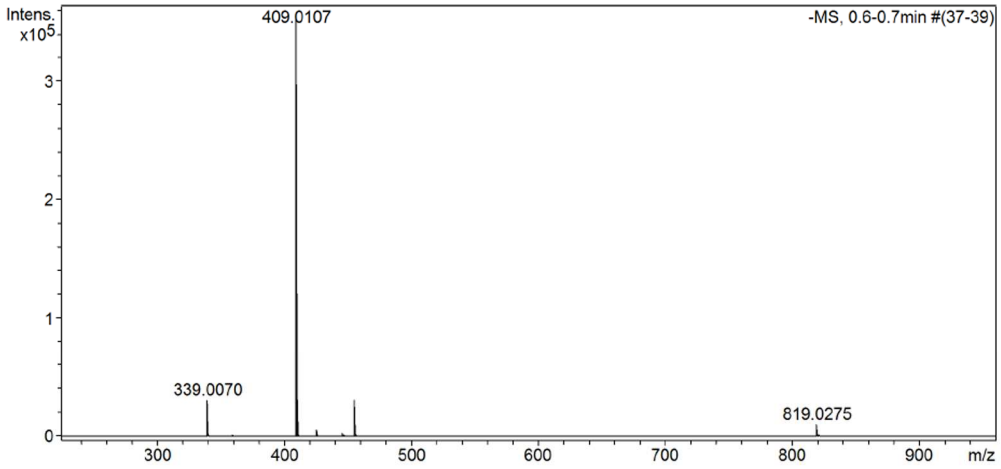

Meas. m/z	Formula	m/z	err [ppm]	err [mDa]	# Sigma	mSigma	rdb	e⁻ Conf	N-Rule
409.0107	C 12 H 5 F 12 O 2	409.0103	-1.0	-0.4	1	14.9	4.5	even	ok
455.0160	C 13 H 7 F 12 O 4	455.0158	-0.3	-0.2	1	24.3	4.5	even	ok
	C 14 H 3 F 12 N 4	455.0172	2.6	1.2	2	37.7	9.5	even	ok
819.0275	C 24 H 11 F 24 O 4	819.0280	0.6	0.5	1	43.4	7.5	even	ok
	C 25 H 7 F 24 N 4	819.0293	2.2	1.8	2	56.0	12.5	even	ok

Figure S73. ESI- mass spectroscopy spectra obtained from a sample of receptor **1** + 5 eq TBAF in acetonitrile. The peak at *m/z* = 409.0107 corresponds to deprotonated receptor **1** $[M\text{-}H]^-$, the peak at *m/z* = 819.0275 corresponds to deprotonated receptor **1** $[M+M\text{-}H]^-$.

Acquisition Parameter					
Source Type	ESI	Ion Polarity	Negative	Set Nebulizer	2.0 Bar
Focus	Not active	Set Capillary	2000 V	Set Dry Heater	200 °C
Scan Begin	120 m/z	Set End Plate Offset	-500 V	Set Dry Gas	8.0 l/min
Scan End	1500 m/z	Set Collision Cell RF	300.0 Vpp	Set Divert Valve	Waste

-MS, 0.7-0.8min #(41-47)

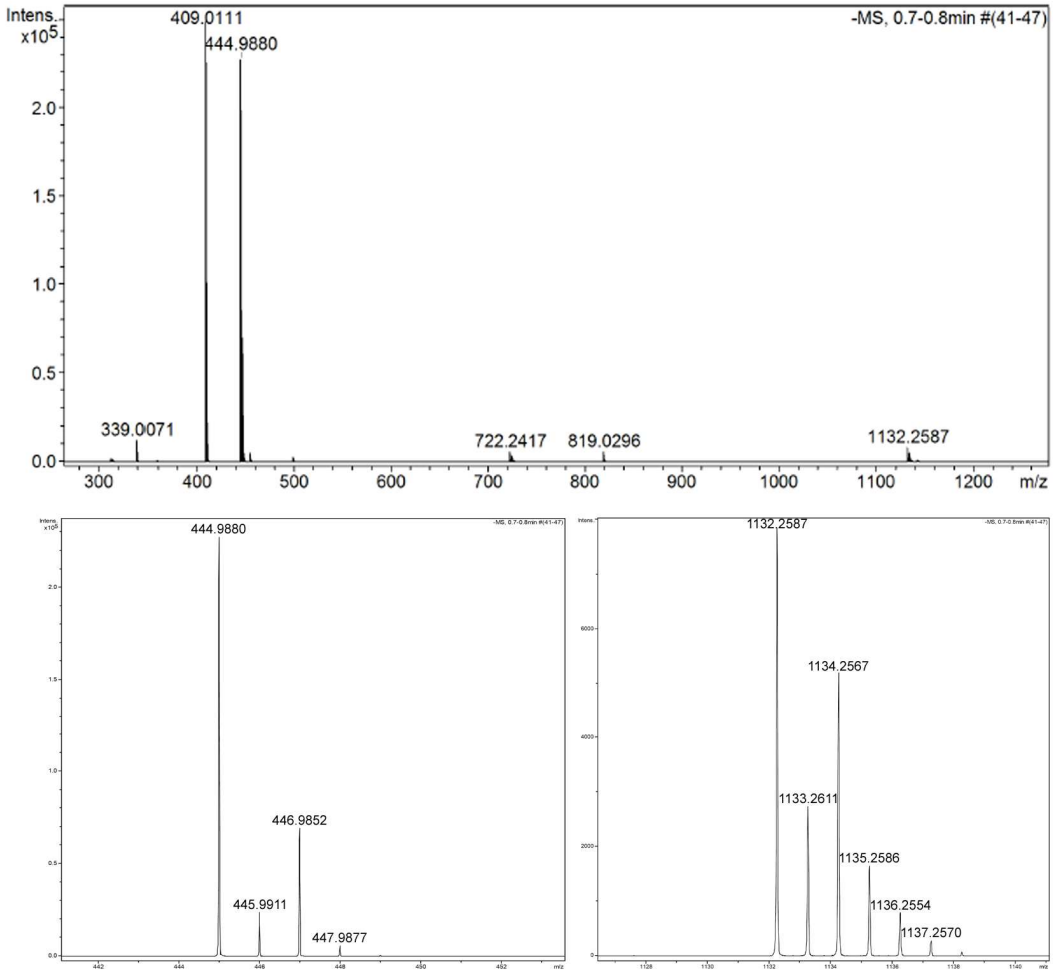

Meas. m/z	Formula	m/z	err [ppm]	err [mDa]	# Sigma	mSigma	rdb	e⁻ Conf	N-Rule
409.0111	C 12 H 5 F 12 O 2	409.0103	-1.9	-0.8	1	17.6	4.5	even	ok
444.9880	C 12 H 6 Cl F 12 O 2	444.9870	-2.2	-1.0	1	19.8	3.5	even	ok
	C 18 H F 12	444.9892	2.7	1.2	2	174.8	12.5	even	ok
722.2417	C 28 H 42 Cl 2 F 12 N O 2	722.2406	-1.4	-1.0	1	47.8	1.5	even	ok
	C 34 H 37 Cl F 12 N	722.2428	1.6	1.2	2	120.2	10.5	even	ok
	C 19 H 33 Cl F 12 N 13 O	722.2433	2.3	1.7	3	127.2	3.5	even	ok
	C 35 H 32 F 12 N 3	722.2410	-0.9	-0.7	4	286.9	15.5	even	ok
	C 23 H 36 F 12 N 5 O 7	722.2429	1.6	1.2	5	291.4	2.5	even	ok
	C 19 H 32 F 12 N 11 O 5	722.2402	-2.1	-1.5	6	333.1	3.5	even	ok
	C 20 H 28 F 12 N 15 O	722.2415	-0.2	-0.2	7	336.3	8.5	even	ok
819.0296	C 13 H 11 F 24 N 6 O 7	819.0311	1.9	1.6	1	22.3	-0.5	even	ok
	C 24 H 11 F 24 O 4	819.0280	-2.0	-1.6	2	46.1	7.5	even	ok
	C 25 H 7 F 24 N 4	819.0293	-0.3	-0.3	3	59.0	12.5	even	ok
	C 24 H 12 Cl F 24 N 2	819.0311	1.9	1.6	4	166.4	7.5	even	ok
1132.2587	C 26 H 40 Cl 2 F 24 N 17 O	1132.2601	1.2	1.4	1	20.4	2.5	even	ok
	C 40 H 48 Cl 2 F 24 N O 4	1132.2583	-0.4	-0.4	2	63.6	4.5	even	ok
	C 41 H 44 Cl 2 F 24 N 5	1132.2596	0.8	0.9	3	72.9	9.5	even	ok

Figure S74. ESI- mass spectroscopy spectra obtained from a sample of receptor **1** + 5 eq TBACl in acetonitrile. The peak at *m/z* = 409.0107 corresponds to deprotonated receptor **1** $[M-H]^-$, the peak at *m/z* = 444.9880 corresponds to a 1:1 complex of receptor **1** with chloride $[M+Cl]^-$, the peak at *m/z* = 1132.2587 corresponds to a 2:2 complex of receptor **1** with chloride (with one TBA counterion to obtain an overall single negative charge) $[M+M+Cl+Cl+TBA]^-$,

S5. pKa CALCULATIONS

pK_a values were calculated using ACD I-Labs 2.0 (algorithm v5.0.0.184 (ACD1 pK_a) and algorithm v12.1.0.50374 (ACD2 pK_a))[4] and Chemicalize[5]. The average pK_a value was subsequently calculated, as well as the standard deviation (SD). The results are given in Table 3.

Table S3. pKa values calculated using ACD I-Labs 2.0 (algorithm 1 and 2) and chemicalize, as well as the average pK_a value with standard deviation (SD).

Compound	pK_a	Chemicalize	ACD1	ACD2	Average pK_a	SD
1	$pK_{a,1}$	7.09	6.8	8.61	7.5	0.8
	$pK_{a,2}$	7.71	7.9	9.32	8.3	0.7
2	$pK_{a,1}$	14.68	14.5	13.98	14.4	0.3
	$pK_{a,2}$	15.31	15.5	14.74	15.2	0.3
3	$pK_{a,1}$	14.02	14.3	14.20	14.2	0.1
	$pK_{a,2}$	15.11	15.5	15.11	15.2	0.2
4	pK_a	7.42	7.7	9.20	8.1	0.8
5	pK_a	15.02	14.9	14.36	14.8	0.3
6	pK_a	14.93	14.8	15.00	14.9	0.1

S6. SINGLE CRYSTAL X-RAY DIFFRACTION

S5.1 General

Data were collected on a *Rigaku AFC12* goniometer equipped with an enhanced sensitivity (HG) *Saturn724+* detector mounted at the window of an *FR-E+ Super-Bright* molybdenum rotating anode generator with VHF *Varimax* optics (70 µm focus) and cell determination, data collection, data reduction and cell refinement and absorption correction were performed using CrystalClear-SM Expert 2.0 r7 (Rigaku, 2011). The structures were solved using SHELXS-97 and refined on *F2* by the full-matrix least-squares technique using the SHELXL-97 program package.[6,7] Graphics are generated using ORTEP-III, MERCURY 3.0 or ViewerLite and Pov-Ray. In all cases the non-hydrogen atoms are refined anisotropically till convergence. Hydrogen atoms were stereochemically fixed at idealized positions and then refined isotropically, unless otherwise stated. Hydrogen bonds are calculated using the HTAB command in SHELXL-97. Structures were deposited with the Cambridge Crystallographic Database Centre (CCDC).

S5.2 X-ray data for complex of 1 with TBACl, CCDC 962267

Single crystals suitable for X-ray diffraction were obtained via the slow evaporation at room temperature of a MeCN solution containing compound **1** and 15 equivalents of TBACl. Crystal data for ((**1**)·$(TBA)^+$·Cl^-). $C_{28}H_{42}F_{12}NO_2Cl$, M_r = 688.08 g/mol, crystal size = 0.37 x 0.11 x 0.08 mm³, colourless block, triclinic, space group *P-1*, a = 10.867(9) Å, b = 12.175(8) Å, c = 14.662(12) Å, α = 111.01(4) º, β = 102.34(7) º, γ= 101.96(5) º, V = 1681(2) Å^3, Z = 2, ρ_c = 1.359 g cm^{-3}, μ = 0.206 mm^{-1}, radiation and wavelength = MoK\a (0.71075), T = 100(2) K, θ_{max} = 25.02, reflections collected: 12684, independent reflections: 5895 (R_{int} = 0.0474), 405 parameters, R indices (all data): R_1 = 0.0553, wR_2 = 0.0989, final R indices [$I > 2\sigma I$]: R_1 = 0.0420, wR_2 = 0.0931, *GOOF* = 0.933, largest diff. peak and hole = 0.296 and -0.280 e Å³.

Table S4. Hydrogen bond properties for ((**1**)·$(TBA)^+$·Cl^-).

Donor--H···Acceptor	D-H (Å)	H···A (Å)	D···A (Å)	D-H···A (°)
O1--H100···Cl1	0.92(3)	2.05(3)	2.929(3)	160(2)
O2--H101···Cl1	0.92(2)	2.06(2)	2.954(2)	163(2)

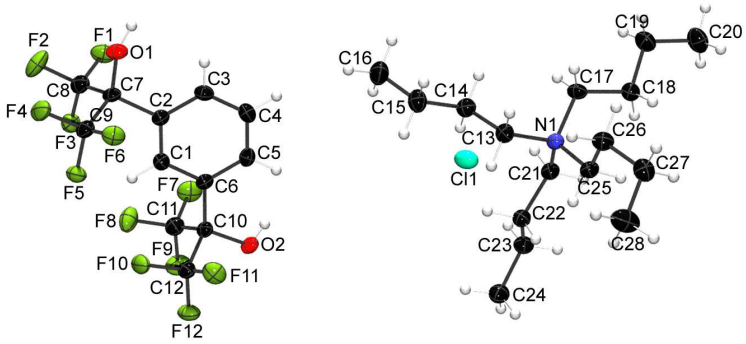

Figure S75. ORTEP diagram of the asymmetric unit of ((**1**)·(TBA)$^{+}$·Cl^{-}) with atom numbering, showing 50 % probability factor for the thermal ellipsoids.

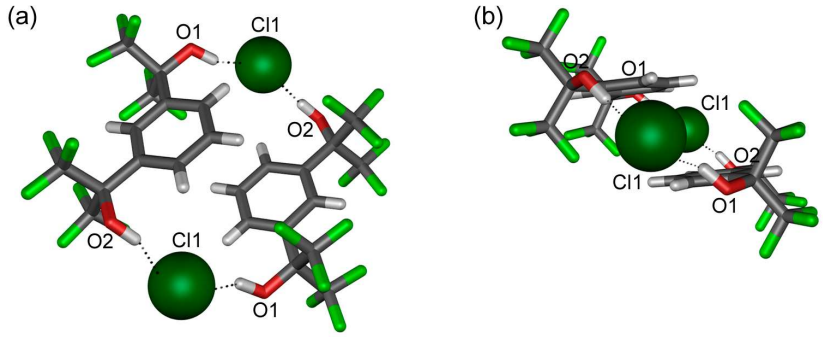

Figure S76. Two views (a and b) of the intermolecular hydrogen bonds in the crystal of ((**1**)•(TBA)$^{+}$•Cl^{-}). For clarity, the TBA counterions are omitted and only heteroatoms involved in hydrogen bonding are labelled. Hydrogen bonds are represented by dashed lines.

S5.3 X-ray data for complex of 1 with TBAF, CCDC 962265

Single crystals suitable for X-ray diffraction were obtained via the slow evaporation at room temperature of a MeCN solution containing compound **1** and 15 equivalents of TBAF. Crystal data for ((**1**)·(TBA)$^{+}$·F^{-}). $C_{28}H_{42}F_{13}NO_2$, M_r = 671.63 g/mol, crystal size = 0.18 x 0.08 x 0.03 mm³, colourless fragment, triclinic, space group *P-1*, a = 12.13(2) Å, b = 12.30(2) Å, c = 13.15(2) Å, α = 111.064(3) º, β = 102.557(11) º, γ = 111.48(3) º, V = 1559(5) Å^3, Z = 2, ρ_c = 1.430 g cm^{-3}, μ = 0.141 mm^{-1}, radiation and wavelength = MoK\a (0.71073), T = 100(2) K, θ_{max} = 25.025, reflections collected: 14351, independent reflections: 5487 (R_{int} = 0.0838), 452 parameters, 318 restraints, R indices (all data): R_1 = 0.1735, wR_2 = 0.3890, final R indices [$I > 2\sigma I$]: R_1 = 0.1271, wR_2 = 0.3357, *GOOF* = 1.176, largest diff. peak and hole = 0.462 and -0.602 e Å³. The crystal is pseudo merohedrally twinned [0 1 0 1 0 0 -1 -1 -1, BASF 0.196]. The TBA cation is disordered across two positions – geometrical similarity restraints and thermal parameter restrains/constraints were applied.

Table S5. Hydrogen bond properties for ((**1**)·(TBA)$^+$·F$^-$).

Donor--H···Acceptor	D-H (Å)	H···A (Å)	D···A (Å)	D-H···A (°)
O1--H1···F1	0.84	1.62	2.429(8)	161.2
O2--H2···F1	0.84	1.62	2.421(8)	157.4

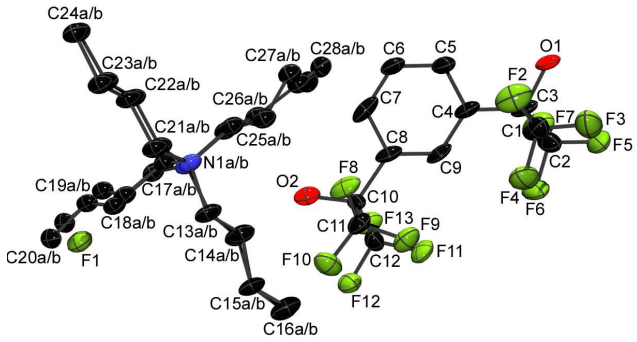

Figure S77. ORTEP diagram of the asymmetric unit of ((**1**)·(TBA)$^+$·F$^-$) with atom numbering, showing 50% probability factor for the thermal ellipsoids. Hydrogen atoms are omitted for clarity due to disorder in TBA counterion.

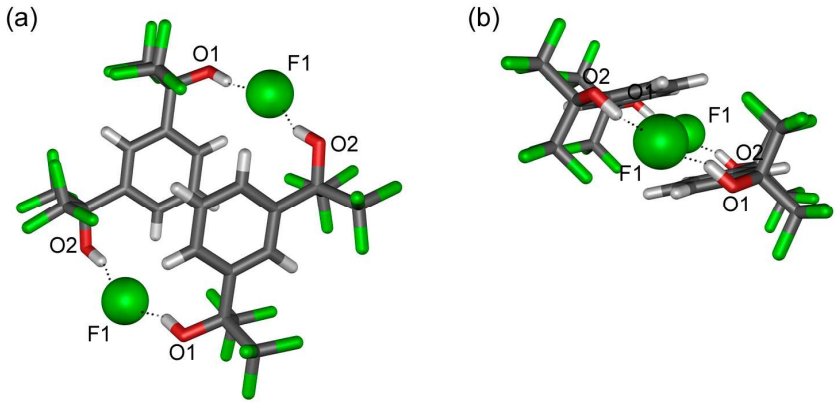

Figure S78. Two views (a and b) of the intermolecular hydrogen bonds in the crystal of ((**1**)·(TBA)$^+$·F$^-$). For clarity, the TBA counterions are omitted and only heteroatoms involved in hydrogen bonding are labelled. Hydrogen bonds are represented by dashed lines.

S5.4 X-ray data for complex of 1 with $TEAHCO_3$, CCDC 962266

Single crystals suitable for X-ray diffraction were obtained via the slow evaporation at room temperature of a MeCN solution containing compound **1** and 15 equivalents of $TEAHCO_3$. The obtained structure does not contain the bicarbonate atom (presumably removed from solution as CO_2), but only deprotonated receptor and a TEA^+ counterion. Crystal data for ((**1**-H)$^-$·(TEA)$^+$).

$C_{20}H_{25}F_{12}NO_2$, M_r = 539.41 g/mol, crystal size = 0.28 x 0.08 x 0.06 mm³, colourless block, monoclinic, space group $P2_1/m$, a = 7.7525(6) Å, b = 14.2782(10) Å, c = 10.7005(8) Å, α = 90 º, β = 107.110(7) º, γ = 90 º, V = 1132.03(15) Å^3, Z = 2, ρ_c = 1.582 g cm^{-3}, μ = 0.168 mm^{-1}, radiation and wave-length = MoK\a (0.71075), T = 100(2) K, θ_{max} = 27.48, reflections collected: 5314, independent reflections: 2669 (R_{int} = 0.0208), 203 parameters, 179 restraints, R indices (all data): R_1 = 0.0333, wR_2 = 0.0778, final R indices [$I > 2\sigma I$]: R_1 = 0.0293, wR_2 = 0.0751, $GOOF$ = 1.077, largest diff. peak and hole = 0.421 and -0.256 e Å³. Only one of two hydroxyl groups of **1** is deprotonated, but due to symmetry it could not be determined which one. Hydrogen atoms with 50% occupancies were used to overcome this problem.

Table S6. Hydrogen bond properties for ((**1**-H)$^-$·(TEA)$^+$).

Donor--H···Acceptor	D-H (Å)	H···A (Å)	D···A (Å)	D-H···A (°)
O1--H1···O1	0.84	1.62	2.4530(14)	172.3

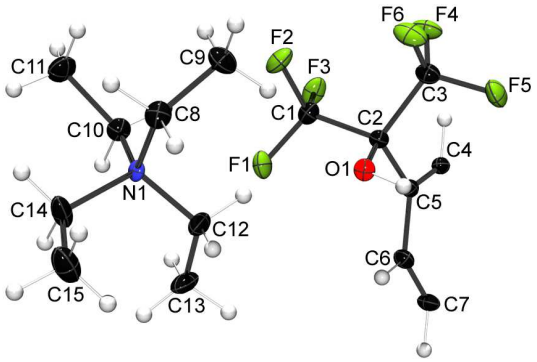

Figure S79. ORTEP diagram of the asymmetric unit of ((**1**-H)$^-$·(TBA)$^+$) with atom numbering, showing 50% probability factor for the thermal ellipsoids.

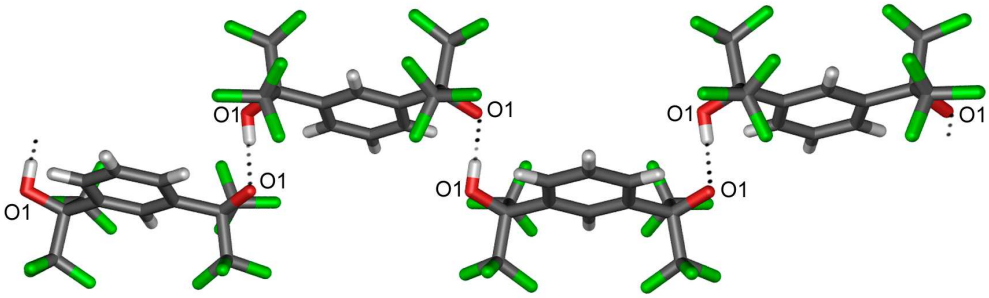

Figure S80. Schematic representation of the intermolecular hydrogen bonds in the crystal of ((**1**-H)$^-$·(TEA)$^+$). For clarity, the TEA counterions are omitted and only heteroatoms involved in hydrogen bonding are labelled. Hydrogen bonds are represented by dashed lines.

S7. REFERENCES AND NOTES

(1) H. Adams, C. A. Hunter, K. R. Lawson, J. Perkins, S. E. Spey, C. J. Urch and J. M. Sanderson, *Chem. Eur. J.*, 2001, **7**, 4863-4877.

(2) S. Hanada, T. Ishida, Y. Motoyama and H. Nagashima, *J. Org. Chem.*, 2007, **72**, 7551-7559.

(3) Hynes, M. J. *J. Chem. Soc., Dalton Trans.* **1993**, 311.

(4) *ACD/I-Lab 2.0*; https://ilab.acdlabs.com/iLab2/ (accessed September 22, 2013); ACD/Labs 2010-2013.

(5) *Chemicalize*; http://www.chemicalize.org/ (accessed September 22, 2013); ChemAxon.

(6) G. Sheldrick, *Acta Crystallogr., Sect. A*, 2008, **64**, 112-122.

(7) Sheldrick, G. M. University of Göttingen, Germany, **1997**.